PSFC/JA-97-22

ION DYNAMICS IN MULTIPLE ELECTROSTATIC WAVES IN A MAGNETIZED PLASMA

D. Benisti, A. K. Ram, and A. Bers

October 1997

Plasma Science and Fusion Center
Massachusetts Institute of Technology
Cambridge, Massachusetts 02139 USA

This work was supported by NSF Grant No. ATM-94-24282 and by DOE Grant No. DE-FG02-91ER-54109. Reproduction, translation, publication, use and disposal, in whole or part, by or for the United States Government is permitted.

To be submitted to *Physics of Plasmas*.

ION DYNAMICS
IN MULTIPLE ELECTROSTATIC WAVES
IN A MAGNETIZED PLASMA

D. Benisti, A. K. Ram, and A. Bers

TABLE OF CONTENTS

Ion Dynamics in Multiple Electrostatic Waves in a Magnetized Plasma

D. Bénisti [1], A.K. Ram and A. Bers,
Plasma Science and Fusion Center, Massachusetts Institute of Technology, Cambridge MA 02139.

Abstract: A general theoretical study of the dynamics of ions interacting with multiple electrostatic waves, propagating perpendicularly to a uniform magnetic field, is performed. For appropriately chosen frequencies and wavenumbers we discover a new nonlinear phenomenon of coherent acceleration (or deceleration) which energizes (or extracts energy from) ions. Ions whose initial energies are below the lower bound of the chaotic part of phase space can be energized by the nonlinear, coherent phenomenon. We also show that the maximum energy the ions can reach is much higher in the case of several waves than in the case of one wave. The mechanism by which the ions reach these high energies is also mostly coherent.

1. Introduction

In this paper we study the dynamics of ions interacting with a discrete spectrum of electrostatic waves propagating perpendicularly to a uniform magnetic field. As shown in[1,2], such a study is also applicable when the direction of propagation of the waves departs by a small angle from perpendicular propagation. In the case when the ions interact with a single electrostatic wave it has been shown[1–4] that the ions gain energy, on the average, only if their motion is chaotic. This occurs for electric field amplitudes above a threshold value.[1–4] In a weakly nonuniform magnetic field the threshold for chaotic dynamics may even be reduced.[5] The energization of ions, in the chaotic phase space of a single wave, was found to be applicable in explaining the generation of energetic ion tails in lower-hybrid heating experiments in tokamaks.[6,7] Experiments have also demonstrated the chaotic energization of plasma ions by single intense electrostatic waves and, furthermore, verified some of the details of the theoretical results for ion dynamics in a single wave. [8] The threshold for chaotic ion heating has been observed, and it has been determined that electrostatic ion Bernstein waves are responsible for rapid changes in the ion distribution function for wave amplitudes above threshold.[8] In this paper we present a general theory of the dynamics of ions in a discrete, multi-wave spectrum propagating across a uniform magnetic field. The results of this study can serve as a basis for new means of energizing, or extracting energy from, ions in a plasma. A forthcoming paper [9] will be dedicated to the application of these results to the particular case of transverse energization of ions in the ionosphere observed to occur in lower hybrid solitary structures,[10] but here we will not discuss any of the possible applications.

The main topic of this paper is to determine the energy an ion can gain from multiple waves, and the nature of the dynamics of the ion while it is being energized. In the case of one wave whose frequency is above the ion-cyclotron frequency, the ion acceleration occurs only in the bounded region of chaotic phase space. This entails a lower bound in the wave amplitude, as well as in the initial ion energy,[1,11] for the ion to be accelerated; it also implies

[1]Present address : Consorzio RFX, Corso Stati Uniti, 4, 35127 Padova, Italy

that the maximum energy an ion can achieve corresponds to the upper limit of the chaotic domain in phase space.

In the case of more than one wave above the ion-cyclotron frequency, we show that, depending on the parameters of the wave spectrum, there can be coherent acceleration.[12] Consequently, an ion may be accelerated regardless of its initial energy, and, in particular, it may be accelerated even if its initial energy corresponds to a region of phase space which is below the chaotic domain of phase space. This coherent acceleration of an ion below the chaotic region is described in detail, using a perturbation analysis carried out to second order in the waves amplitudes. The dependence of the ion energization on the wave spectrum characteristics is also discussed in detail.

Once an ion has accessed the chaotic domain of phase space, we show that it may reach energies which are much higher than in the case of one wave. This happens when there are at least two on-resonance waves (i.e. waves whose frequencies are an integer multiple of the cyclotron frequency) whose amplitudes are appreciable compared to the amplitudes of the other waves of the spectrum. In this case, although the ion motion cannot be considered as coherent for high energies, it is nevertheless dominated by the orbits found from a first order perturbation analysis. The maximum energy an ion reaches then strongly depends on the extent, in action space, of these orbits and the way that these orbits may connect. We determine the characteristics of these orbits and the dependence of the ion energization on wave parameters.

The paper is organized as follows, in section 2 we derive the equations of motion and the Hamiltonian of the dynamics in action-angle variables of the zero-electric field case. In section 3 we restate the known results in the one-wave case. Section 4 is devoted to the coherent acceleration of the low-energy ions and its dependence on various parameters of the wave spectrum. In section 5, we focus on the maximum energy an ion can gain once it has reached the chaotic domain. We show in particular that the maximum energy is higher in the case of multiple waves than in the case of one wave, and discuss how this maximum energy depends on the parameters of the wave spectrum. The last section summarizes the results.

2. Equations of motion and Hamiltonian formulation:

The motion of an ion of mass m and charge q in a uniform magnetic field $\vec{B} = B_0\hat{z}$, and being perturbed by a spectrum of electrostatic waves $\vec{E} = \hat{x}\sum_{i=1}^{N} E_i \sin(k_i x - \omega_i t + \varphi_i)$, is given by

$$\frac{d^2x}{dt^2} + \Omega^2 x = \frac{q}{m}\sum_{i=1}^{N} E_i \sin(k_i x - \omega_i t + \varphi_i) \tag{1}$$

where $\Omega = qB_0/m$ is the cyclotron angular frequency. We normalize time to Ω^{-1} and length to k_1^{-1}, and define the dimensionless variables $X = k_1 x$, $\tau = \Omega t$. We then switch to the normalized action-angle variables of the linear oscillator. The action is $I = X^2/2 + \dot{X}^2/2$, where $\dot{X} = dX/d\tau$. The angle θ is defined by $X = \rho\sin\theta$, $\dot{X} = \rho\cos\theta$, where $\rho = \sqrt{2I}$ is the normalized Larmor radius. In action-angle variables (I, θ), the Hamiltonian corresponding

to (1) is

$$H = I + \sum_{i=1}^{N} \frac{\varepsilon_i}{\kappa_i} \cos(\kappa_i \rho \sin\theta - \nu_i \tau + \varphi_i) \tag{2}$$

where $\kappa_i = k_i/k_1$, $\nu_i = \omega_i/\Omega$, and $\varepsilon_i = (k_1 q E_i)/(m\Omega^2)$. The Hamiltonian (2) will be the starting point of all the analytical calculations made to describe the dynamics defined by (1).

3. Results of one wave case:

It has been shown in [1–4,13] that an ion can gain energy from one wave whose frequency is above the cyclotron frequency only if the ion dynamics are chaotic. In the single wave-particle interaction, the dynamics is qualitatively different depending on whether the wave frequency is an integer multiple of the ion cyclotron frequency (on-resonance case) or not (off-resonance case).

In the off-resonance case, it has been shown in[1,2] that chaotic dynamics occurs if the wave amplitude exceeds a threshold amplitude:

$$\varepsilon > \varepsilon_{th} \approx \nu^{2/3}/4 \tag{3}$$

For amplitudes above the threshold value, the chaotic phase space is bounded from below and from above in action; the lower bound of the stochastic region is

$$\rho \approx \nu - \sqrt{\varepsilon} \tag{4}$$

while the upper bound of the chaotic domain is estimated to be

$$\rho \approx (4\varepsilon\nu)^{2/3}(2/\pi)^{1/3} \tag{5}$$

Since the acceleration of ions by a single wave can only be stochastic, (4) yields the minimum energy an ion needs to have in order to be accelerated by the off-resonance wave, while (5) yields the maximum energy the ion can reach through the stochastic acceleration (see Fig. 1).

In the case of one on-resonance wave [4,13], there is a web-structure in phase-space that extends up to infinite values of the energy. However, the web becomes increasingly thin at large energies. Also, the web structure has a lower bound in energy.[11] This implies that, in the on-resonance case, the initial energy of an ion needs to be high enough for the ion to be accelerated by the wave. It has been shown that this lower bound tends to lift up to higher energies as the wave amplitude is increased until crossing over with (4).[11] Nevertheless, for high harmonics of the cyclotron frequency, the estimate given in (4) for the lower bound in energy is approximately valid also in the on-resonance case. Moreover, even though, in principle, an ion may gain infinite energy in the on-resonance web, the time needed to go far beyond the estimate in (5) is too long to be of practical interest. So, for high ion-cyclotron harmonics, the estimates (4) and (5) can be considered to apply to the on-resonance case (see Fig. 2).

4. Acceleration of low-energy ions with more than one wave:

In the case of more than one wave, the lower bound (4) for stochastic acceleration remains valid if ν is the minimum of the ν_i's. However, unlike for the case of one wave, the energy of an ion can vary a lot even if its initial Larmor radius is less than the limit (4) (see Fig. 3). Hence, an ion below the stochastic domain can be appreciably accelerated or decelerated. The motion of an ion in this domain of phase space is regular, as can be seen on Fig. 3, and can thus be deduced from an integrable Hamiltonian. This integrable Hamiltonian can be derived from the complete Hamiltonian (2) using perturbation theory. We perform the perturbation analysis only up to second order, using the formalism of the Lie transform. This leads to an integrable Hamiltonian $\tilde{H}$ whose orbits are found by solving $\tilde{H} = const.$ As can be seen in Fig. 4, the orbits of $\tilde{H}$ provide a very accurate description of the actual motion. Hence, the dynamics defined by H will approximately be described by the integrable dynamics given by $\tilde{H}$, whose derivation is detailed in the following subsections.

4.1. Coherent acceleration in the case of two off-resonance waves:

In this subsection we focus on the dynamics defined by (2), in the case of two waves such that neither ν_1 nor ν_2 are integers, and for values of ρ less than $\min(\nu_1, \nu_2)$. As already mentioned before, these dynamics can be accurately described by a perturbation analysis on the Hamiltonian (2) up to second order in the wave amplitudes. The perturbation analysis is performed using the formalism of the Lie transform and is described in Appendix A. The perturbation analysis defines a new set of conjugate coordinates, $(\tilde{I}, \tilde{\theta})$, in which the Hamiltonian (2) is transformed to

$$\begin{aligned}\tilde{H}_2^{(off)} &= \tilde{I} + \varepsilon_1^2 S_1(\tilde{\rho}) + \varepsilon_2^2 S_2(\tilde{\rho}) + \varepsilon_1^2 \delta_1 \cos[2\nu_1(\tilde{\theta} - \tau) + 2\varphi_1] S_3(\tilde{\rho}) \\ &\quad + \varepsilon_2^2 \delta_2 \cos[2\nu_2(\tilde{\theta} - \tau) + 2\varphi_2] S_4(\tilde{\rho}) \\ &\quad + \varepsilon_1 \varepsilon_2 \delta_3 \cos[(\nu_1 + \nu_2)(\tilde{\theta} - \tau) + \varphi_1 + \varphi_2] S_5(\tilde{\rho}) \\ &\quad + \varepsilon_1 \varepsilon_2 \delta_4 \cos[(\nu_1 - \nu_2)(\tilde{\theta} - \tau) + \varphi_1 - \varphi_2] S_6(\tilde{\rho}) \end{aligned} \tag{6}$$

where δ_1, δ_2, δ_3, and δ_4, are unity if $2\nu_1$, $2\nu_2$, $(\nu_1+\nu_2)$, and $(\nu_1-\nu_2)$ are integers, respectively, and 0 otherwise, and the functions S_1 to S_6 are described in Appendix A.

To first order in the wave amplitudes, the original variables (I, θ) are related to the new variables $(\tilde{I}, \tilde{\theta})$ by

$$I = \tilde{I} + \varepsilon_1 \sum_{m=-\infty}^{+\infty} \frac{m J_m(\tilde{\rho}) \cos(m\tilde{\theta} - \nu_1 \tau)}{\nu_1 - m} + \varepsilon_2 \sum_{m=-\infty}^{+\infty} \frac{m J_m(\kappa\tilde{\rho}) \cos(m\tilde{\theta} - \nu_2 \tau)}{\kappa(\nu_2 - m)} \tag{7}$$

$$\theta = \tilde{\theta} - \frac{\varepsilon_1}{\tilde{\rho}} \sum_{m=-\infty}^{+\infty} \frac{J_m'(\tilde{\rho}) \sin(m\tilde{\theta} - \nu_1 \tau)}{\nu_1 - m} - \frac{\varepsilon_2}{\tilde{\rho}} \sum_{m=-\infty}^{+\infty} \frac{J_m'(\kappa\tilde{\rho}) \sin(m\tilde{\theta} - \nu_2 \tau)}{\nu_2 - m} \tag{8}$$

where J_m is the Bessel function of order m, and the prime denotes the derivative with respect to the argument of the function. It is sufficient to calculate the change of variables to first order as the second order terms give negligible contributions. However, we need evaluate the second order contributions to $\tilde{H}_2^{(off)}$, as there are no first order terms in $\tilde{H}_2^{(off)}$.

Motivated by the results reported in, [10] and possible applications to plasma heating by lower-hybrid or Bernstein waves, we now focus on the case when the wave frequencies are

above the ion-cyclotron frequency, i.e. $\nu_1 > 1$ and $\nu_2 > 1$. Then, a Taylor expansion of S_i's to the lowest order in $\tilde{\rho}$ indicate that, when $\tilde{\rho} < \min(\nu_1, \nu_2)$, $S_4(\tilde{\rho})$ and $S_5(\tilde{\rho})$ are negligible in (6). These results are confirmed numerically. Hence, for $\tilde{\rho} < \min(\nu_1, \nu_2)$, $\tilde{H}_2^{(off)}$ can be approximated by

$$\tilde{H}_2^{(off)} = \varepsilon_1^2 S_1(\tilde{\rho}) + \varepsilon_2^2 S_2(\tilde{\rho}) + \delta_4 \varepsilon_1 \varepsilon_2 S_6(\tilde{\rho}) \cos[(\nu_1 - \nu_2)(\theta - \tau) + \varphi_1 - \varphi_2]. \tag{9}$$

We then define a canonical change of variables $(\tilde{I}, \tilde{\theta}) \mapsto (\tilde{J}, \tilde{\Phi})$ using the generating function

$$F = \tilde{J}(\tilde{\theta} - \tau) \tag{10}$$

which yields $\tilde{J} = \tilde{I}$, and $\tilde{\Phi} = \tilde{\theta} - \tau$. In variables $(\tilde{J}, \tilde{\Phi})$, (9) is changed into

$$\tilde{H}^{(off)} = \varepsilon_1^2 S_1(\tilde{\rho}) + \varepsilon_2^2 S_2(\tilde{\rho}) + \delta_4 \varepsilon_1 \varepsilon_2 S_6(\tilde{\rho}) \cos[(\nu_1 - \nu_2)\tilde{\Phi} + \varphi_1 - \varphi_2]. \tag{11}$$

The Hamiltonian (11) is integrable and the ion orbits are obtained by solving $\tilde{H}^{(off)} = const.$ If $\delta_4 = 0$, i.e. if $(\nu_1 - \nu_2)$ is not an integer, then solving $\tilde{H}^{(off)} = const$ yields $\tilde{\rho} = const.$ In such a case the original action I only fluctuates by an amount of order ε_1 or ε_2, and behaves as in the case of one wave: there is no acceleration. This is physically clear because when $(\nu_1 - \nu_2)$ is not an integer, the action of the waves only amounts to some rapid perturbations which do not really affect the ion motion. Conversely, when $(\nu_1 - \nu_2)$ is an integer, the non-linear beating of the waves gives rise to a slowly varying force acting on the ion and coherently accelerating it. The third term on the right-hand side of (11) provides this force. The amount of energy an ion gets depends on the relative importance of this term compared to the stabilizing terms $\varepsilon_1^2 S_1(\tilde{\rho}) + \varepsilon_2^2 S_2(\tilde{\rho})$. The study of the competition between the accelerating and stabilizing terms, as a function of the wave amplitudes, wavenumbers, frequencies and initial phases, is the main topic of the remaining of this subsection.

If $(\nu_1 - \nu_2)$ is an integer, there is a large variation in $\tilde{\rho}$ if $\varepsilon_1 \varepsilon_2 S_6(\tilde{\rho})$ is large compared to $\varepsilon_2^2 S_1(\tilde{\rho}) + \varepsilon_2^2 S_2(\tilde{\rho})$. As $(\varepsilon_1 \varepsilon_2)/(\varepsilon_1^2 + \varepsilon_2^2)$ is maximum when $\varepsilon_1 = \varepsilon_2$, the largest acceleration will occur when the two waves have the same amplitude. This is the case we consider from here on.

It is clear from (11) that the initial phases φ_1 and φ_2 play no role in the acceleration mechanism since a translation of the angle $\tilde{\Phi}$ to $\tilde{\Phi} + (\varphi_1 - \varphi_2)/(\nu_1 - \nu_2)$ eliminates any dependence on initial phases. Hence, without loss of generality, we will consider the case when $\varphi_1 = \varphi_2 = 0$. Then for $\varepsilon_1 = \varepsilon_2 = \varepsilon$

$$\tilde{H}^{(off)} = \varepsilon^2 \left\{ S_1(\tilde{\rho}) + S_2(\tilde{\rho}) + S_6(\tilde{\rho}) \right\} \cos\left[(\nu_1 - \nu_2)\tilde{\Phi} \right]. \tag{12}$$

The orbits of $\tilde{H}$, obtained from (12), are independent of the wave amplitudes: dividing each amplitude by the same coefficient will not change the amount of energy an ion can gain from the waves. However, decreasing ε increases the time needed for acceleration; it is clear from the equations of motion derived from (12) that this time is proportional to ε^{-2}.

Let us now study the dependence of the acceleration mechanism on the ratio of the wavenumbers $\kappa = k_2/k_1$, and on the integer difference $(\nu_1 - \nu_2)$. Solving $\tilde{H}^{(off)} = \varepsilon^2 (const.)$ leads to

$$\cos(\nu_1 - \nu_2)\tilde{\Phi} = \frac{(const.) - S_1(\tilde{\rho}) - S_2(\tilde{\rho})}{S_6(\tilde{\rho})} \tag{13}$$

If the initial value of $\tilde{\rho}$ lies between two zeros of $S_6(\tilde{\rho})$, say $\tilde{\rho}_1^*$ and $\tilde{\rho}_2^*$, then it is follows from (13) that $\tilde{\rho}$ will always remain between $\tilde{\rho}_1^*$ and $\tilde{\rho}_2^*$. The zeros of $S_6(\tilde{\rho})$ behave like "barriers" for transport in phase space. So it is important to study the locations, in $(\tilde{\rho})$, of these zeros. To this end we have calculated some approximate expressions of $S_6(\tilde{\rho})$.

When $(\nu_1 - \nu_2) = 1$, we have found numerically that for $\mid \kappa - 1 \mid \geq 0.1$ and for values of $\tilde{\rho}$ larger than the first zero of $S_6(\tilde{\rho})$

$$\nu_1 - \nu_2 = 1;\ S_6(\tilde{\rho}) \simeq \frac{C(\kappa, \nu_1)}{\tilde{\rho}^{0.53}} \sin\left[\frac{2\pi\,(\tilde{\rho} - 3.85/\mid \kappa - 1 \mid)}{6.3/(\kappa - 1)}\right] \tag{14}$$

where $C(\kappa, \nu_1)$ is only a function of κ and ν_1. Note that the positions of the zeros of $S_6(\tilde{\rho})$ do not depend explicitly on ν_1, they only depend on $(\nu_1 - \nu_2)$.

For values of κ such that $\mid \kappa - 1 \mid \leq 0.1$, $S_6(\tilde{\rho})$ is well approximated by a small $\tilde{\rho}$ expansion. A Taylor series expansion to the seventh order in $\tilde{\rho}$ of $S_6(\tilde{\rho})$ enables us to obtain an analytical approximation of the first zero. This approximate value of the first zero, which is very close to the exact zero of $S_6(\tilde{\rho})$, is plotted on Fig. 5 for various values of κ. This figure shows that the first zero of $S_6(\tilde{\rho})$ becomes small for values of κ close to 1.02. This comes from the fact that the first coefficient of the Taylor expansion of $S_6(\tilde{\rho})$ is zero for $\kappa \simeq 1 + 2/\nu_1$. For the parameters of Fig. 5, this corresponds to $\kappa \simeq 1.017$. When the first coefficient of the Taylor expansion of $S_6(\tilde{\rho})$ is zero, then $S_6(\tilde{\rho})$ increases much more slowly with $\tilde{\rho}$ so that it becomes very small compared to S_1 and S_2. In this case the Larmor radius of an ion remains approximately constant; there is no acceleration.

Given the position of the zeros of $S_6(\tilde{\rho})$ obtained from (14), or from Fig. 5, one can have a rough idea of the maximum and minimum values, $\tilde{\rho}_{\max}$ and $\tilde{\rho}_{\min}$ of the Larmor radius of an orbit of $\tilde{H}_2^{(off)}$, given an initial condition $(\tilde{\rho}_0, \tilde{\Phi}_0)$. Indeed, if $\tilde{\rho}_0$ lies between 2 zeros of S_6, $\tilde{\rho}_1^*$ and $\tilde{\rho}_2^*$, then $\tilde{\rho}_1^*$ and $\tilde{\rho}_2^*$ are good approximations of $\tilde{\rho}_{\min}$ and $\tilde{\rho}_{\max}$. Fig. 6 plots $\tilde{\rho}_{\min}$ and $\tilde{\rho}_{\max}$ as found by numerically solving $\tilde{H}_2^{(off)} = const$, versus κ, for an initial condition corresponding to $\tilde{\rho}_0 = 53$, $\tilde{\Phi}_0 = 1.57$. One can see that $\tilde{\rho}_{\min}$ and $\tilde{\rho}_{\max}$ are discontinuous functions of κ. These discontinuities occur when one of the zeros of $S_6(\tilde{\rho})$ equals $\tilde{\rho}_0$. For example, when $\kappa = 0.925$ the first zero, $\tilde{\rho}_0^*$, of $S_6(\tilde{\rho})$ is just slightly above $\tilde{\rho}_0 = 53$. In this case, the ion Larmor radius cannot increase much, as it has to remain less than $\tilde{\rho}_0^*$. Nevertheless, nothing prevents *a priori* the ion Larmor radius to go down to 0, and one can see in Fig. 6 that the minimum value of the Larmor radius is indeed very close to 0 in this case. Thus, when $\kappa = 0.925$, the ion is decelerated. On the contrary, when $\kappa = 0.924$, the first zero of $S_6(\tilde{\rho})$ is slightly below $\tilde{\rho}_0$ so that the ion's Larmor radius cannot decrease much, because it has to remain larger that $\tilde{\rho}_0^*$. However, it can increase up to the value of the second zero of $S_6(\tilde{\rho})$. In this case the ion gets a finite acceleration, and its Larmor radius increases up to $\tilde{\rho}_{\max} \simeq 75$.

When $\kappa \simeq 1.02$, both $\tilde{\rho}_{\min}$ and $\tilde{\rho}_{\max}$ are very close to $\tilde{\rho}_0$. This occurs because the first coefficient of the Taylor expansion of $S_6(\tilde{\rho})$ goes through 0 for $\kappa \simeq 1 + 2/\nu_1$, which implies, that for such values of κ, $S_6(\tilde{\rho})$ becomes very small compared to $S_1(\tilde{\rho})$ and $S_2(\tilde{\rho})$.

Finally, one can see in Fig. 6 that for values of κ close to one, there is a peak of large acceleration. This peak is actually not at $\kappa = 1$ but near a value of κ less than 1. For values of κ corresponding to this peak, $\tilde{\rho}_{\max}$ becomes very close to ν_1. Actually, for large enough values of ε, the lower bound of the stochastic region, as estimated from (4), can actually be

lower than the value of $\tilde{\rho}_{\max}$ predicted from perturbation theory. For such values of ε, an ion can access the stochastic domain where it rapidly gains a lot of energy.

If the initial condition corresponds to a very low value of the Larmor radius, there is no discontinuity in $\tilde{\rho}_{\min}$ and $\tilde{\rho}_{\max}$ for a large range of values of κ, except for κ close to $1+2/\nu_1$ (see Fig. 7). This occurs because, for a large range of values of κ, the first zero of $S_6(\tilde{\rho})$ is larger than $\tilde{\rho}_0$. In this case the value of $\tilde{\rho}_{\max}$ is roughly the value of the first zero of $S_6(\tilde{\rho})$. One can note the similarities between Fig. 7 and Fig. 5 for the first zero of $S_6(\tilde{\rho})$. It is important to note that the maximum value of $\tilde{\rho}_{max}$ is about as high when $\tilde{\rho}_0 = 5$ as when $\tilde{\rho}_0 = 53$. Thus, an ion can get a large acceleration, and may access the stochastic region, regardless of its initial energy.

When $(\nu_1 - \nu_2) = 2$, the energy gained by an ion varies in about the same way as in the case when $\nu_1 - \nu_2 = 1$. This comes from the fact that the variations of $S_6(\tilde{\rho})$ are similar when $\nu_1 - \nu_2 = 2$ or when $\nu_1 - \nu_2 = 1$. Actually, when $\mid \kappa - 1 \mid \geq 0.1$ and for values of $\tilde{\rho}$ larger than the first zero of $S_6(\tilde{\rho})$:

$$\nu_1 - \nu_2 = 2;\ S_6(\tilde{\rho}) \simeq \frac{A(\kappa, \nu_1)}{\tilde{\rho}^{0.53}} \sin\left[\frac{2\pi\,(\tilde{\rho} - 5.15/\mid \kappa - 1 \mid)}{6.3/\mid \kappa - 1 \mid}\right] \tag{15}$$

where $A(\kappa, \nu_1)$ is only a function of ν_1 and κ. The zeros of $S_6(\tilde{\rho})$ are not at the same locations for the two cases $\nu_1 - \nu_2 = 1$ and $\nu_1 - \nu_2 = 2$. Hence, the discontinuities in $\tilde{\rho}_{\min}$ and $\tilde{\rho}_{\max}$ will not occur for the same values of κ when $\nu_1 - \nu_2 = 1$ as when $\nu_1 - \nu_2 = 2$. The position of the first zero of $S_6(\tilde{\rho})$ can also be very accurately estimated by a Taylor expansion in $\tilde{\rho}$ when $\nu_1 - \nu_2 = 2$. Fig. 8 plots $\tilde{\rho}_{\max}$ versus κ when $Int(\nu_1) = 140$ and $\nu_2 = \nu_1 - 1$ and $\nu_2 = \nu_1 - 2$. As for the case when $\nu_1 - \nu_2 = 1$, when $\nu_1 - \nu_2 = 2$ there is a drop in $\tilde{\rho}_{\max}$ when $\kappa \simeq 1 + 2/\nu_1$. This drop actually spans a larger range of values of κ when $\nu_1 - \nu_2 = 2$ than when $\nu_1 - \nu_2 = 1$ and is a consequence of the effect that the first coefficient of the Taylor expansion of $S_6(\tilde{\rho})$ is a minimum when $\kappa = 1 + 2\nu_1$ in the case where $\nu_1 - \nu_2 = 2$. The peak of large acceleration when $\nu_1 - \nu_2 = 2$, is shifted to lower values of κ compared to the case when $\nu_1 - \nu_2 = 1$. This is a general trend as $\nu_1 - \nu_2$ increases. Finally, as in the case when $\nu_1 - \nu_2 = 1$, when $\nu_1 - \nu_2 = 2$, the maximum energy an ion reaches is independent of its initial energy, and an ion may access the stochastic domain regardless of its initial energy. This last feature is only true when $(\nu_1 - \nu_2) \leq 2$. When $\nu_1 - \nu_2 \geq 3$ only ions with initial energies greater than a threshold value will reach high energies or be able to access the stochastic region. This is due to the fact that $S_6(\tilde{\rho}) \sim \tilde{\rho}^{(\nu_1 - \nu_2)}$ for small values of $\tilde{\rho}$ while $S_1(\tilde{\rho})$, $S_2(\tilde{\rho}) \sim \tilde{\rho}^2$ independent of $(\nu_1 - \nu_2)$. Thus, when $(\nu_1 - \nu_2) \geq 3$, for small values of $\tilde{\rho}$, $S_6(\tilde{\rho})$ becomes very small compared to $S_1(\tilde{\rho})$ and $S_2(\tilde{\rho})$ and there is no acceleration. As $\tilde{\rho}_0$ decreases, $\mid \kappa - 1 \mid$ has to increase in order for the ions to get accelerated. The maximum value of the Larmor radius is still limited by the zeros of $S_6(\tilde{\rho})$. The first zero of $S_6(\tilde{\rho})$ moves to lower values of $\tilde{\rho}$ as $\mid \kappa - 1 \mid$ is increased, and the maximum value that $\tilde{\rho}$ can attain decreases as $\tilde{\rho}_0$ decreases (see Fig. 9 and 10).

In conclusion, we have shown that an ion, regardless of its initial energy, may be appreciably accelerated (or decelerated) by two off-resonance waves when $|Int(\nu_1 - \nu_2)| \leq 2$ and the ratio of their wavenumbers κ is in an appropriate range. In an experiment where the wave characteristics can be specified, one can have, with two waves, considerable control on the ion dynamics below the stochastic region. Indeed by changing the ratio of the two

wavenumbers or the difference between the two wave frequencies, one can choose the amount of energy an ion gains (or loses) from the waves as well as the range of initial energy of the ions that are accelerated (or decelerated).

4.2. Coherent acceleration in the case of two on-resonance waves:

We now study the dynamics defined by (2), in the case of two waves with both $\nu_1 = n_1$ and $\nu_2 = n_2$ being integers. We will restrict ourselves to the case where ρ is less than $\min(n_1, n_2)$. Thus, we again focus on a region of phase space where the motion is well described by an integrable Hamiltonian. As in the previous section, this Hamiltonian is derived from H by using perturbation theory up to second order in the waves amplitudes. Using the perturbation analysis described in Appendix A, we obtain the following transformed Hamiltonian:

$$\begin{aligned}\tilde{H}_2^{(on)} &= \varepsilon_1 J_{n_1}(\tilde{\rho})\cos[n_1(\tilde{\theta}-\tau)+\varphi_1] + \varepsilon_2 \frac{J_{n_2}(\kappa\tilde{\rho})}{\kappa}\cos[n_2(\tilde{\theta}-\tau)+\varphi_2] \\ &+\varepsilon_1^2\bar{S}_1(\tilde{\rho}) + \varepsilon_2^2\bar{S}_2(\tilde{\rho}) + \varepsilon_1^2\cos[2n_1(\tilde{\theta}-\tau)+2\varphi_1]\bar{S}_3(\tilde{\rho}) \\ &+\varepsilon_2^2\cos[2n_2(\tilde{\theta}-\tau)+2\varphi_2]\bar{S}_4(\tilde{\rho}) \\ &+\varepsilon_1\varepsilon_2\cos[(n_1+n_2)(\tilde{\theta}-\tau)+\varphi_1+\varphi_2]\bar{S}_5(\tilde{\rho}) \\ &+\varepsilon_1\varepsilon_2\cos[(n_1-n_2)(\tilde{\theta}-\tau)+\varphi_1-\varphi_2]\bar{S}_6(\tilde{\rho}) \end{aligned} \tag{16}$$

where

$$\bar{S}_2(\tilde{\rho}) = \frac{1}{2\kappa\tilde{\rho}}\sum_{m\neq n_2}\frac{mJ_m(\kappa\tilde{\rho})J'_m(\kappa\tilde{\rho})}{n_2-m} \tag{17}$$

$$\bar{S}_4(\tilde{\rho}) = \frac{1}{2\kappa\tilde{\rho}}\sum_{m\neq n_2}\frac{mJ_m(\kappa\tilde{\rho})J'_{2n_2-m}(\kappa\tilde{\rho})}{n_2-m} \tag{18}$$

$$\bar{S}_5(\tilde{\rho}) = \frac{1}{2\tilde{\rho}}\sum_{m\neq n_1}\frac{mJ_m(\tilde{\rho})J'_{n_1+n_2-m}(\kappa\tilde{\rho})}{n_1-m} + \frac{1}{2\kappa\tilde{\rho}}\sum_{m\neq n_2}\frac{mJ_m(\kappa\tilde{\rho})J'_{n_1+n_2-m}(\tilde{\rho})}{n_2-m} \tag{19}$$

$$\bar{S}_6(\tilde{\rho}) = \frac{1}{2\tilde{\rho}}\sum_{m\neq n_1}\frac{mJ_m(\tilde{\rho})J'_{n_2-n_1+m}(\kappa\tilde{\rho})}{n_1-m} + \frac{1}{2\kappa\tilde{\rho}}\sum_{m\neq n_2}\frac{mJ_m(\kappa\tilde{\rho})J'_{n_1-n_2+m}(\tilde{\rho})}{n_2-m} \tag{20}$$

$\bar{S}_1$ and $\bar{S}_3$ are obtained from $\bar{S}_2$ and $\bar{S}_4$, respectively, by replacing n_2 by n_1, and by setting $\kappa = 1$. The sums in $\bar{S}_i$ can be carried out analytically, using the results for the off-resonance case. For example

$$\begin{aligned}\bar{S}_2(\tilde{\rho}) &= \lim_{\nu_2\to n_2}\left[S_2(\tilde{\rho}) - \frac{n_2 J_{n_2}(\kappa\tilde{\rho})J'_{n_2}(\kappa\tilde{\rho})}{2\kappa\tilde{\rho}(\nu_2-n_2)}\right] \\ &= \frac{(-1)^{n_2}}{8\kappa}J_{n_2+1}(\kappa\tilde{\rho})\left[\left(\frac{\partial J_{-1-\nu}(\kappa\tilde{\rho})}{\partial\nu}\right)_{\nu=n_2} + (-1)^{n_2+1}\left(\frac{\partial J_{1+\nu}(\kappa\tilde{\rho})}{\partial\nu}\right)_{\nu=n_2}\right] \\ &+\frac{(-1)^{n_2+1}}{8\kappa}J_{n_2-1}(\kappa\tilde{\rho})\left[\left(\frac{\partial J_{1-\nu}(\kappa\tilde{\rho})}{\partial\nu}\right)_{\nu=n_2} + (-1)^{n_2+1}\left(\frac{\partial J_{\nu-1}(\kappa\tilde{\rho})}{\partial\nu}\right)_{\nu=n_2}\right] \end{aligned} \tag{21}$$

Likewise, we find

$$\bar{S}_4(\tilde{\rho}) = \frac{J_{n_2-1}(\kappa\tilde{\rho})}{4\kappa}\left(\frac{\partial J_{\nu+1}(\kappa\tilde{\rho})}{\partial\nu}\right)_{\nu=n_2} - \frac{J_{n_2+1}(\kappa\tilde{\rho})}{4\kappa}\left(\frac{\partial J_{\nu-1}(\kappa\tilde{\rho})}{\partial\nu}\right)_{\nu=n_2} + \frac{1}{4\kappa^3\tilde{\rho}^2}\int_0^{\kappa\tilde{\rho}} \rho J_{2n_2+1}(\rho)d\rho \tag{22}$$

and, when $\kappa = 1$, and $n_1 > n_2$ we find

$$\kappa = 1; \bar{S}_5(\tilde{\rho}) = \frac{J_{n_1-1}(\tilde{\rho})}{4}\left(\frac{\partial J_{\nu+1}(\tilde{\rho})}{\partial\nu}\right)_{\nu=n_2} + \frac{J_{n_2-1}(\tilde{\rho})}{4}\left(\frac{\partial J_{\nu+1}(\tilde{\rho})}{\partial\nu}\right)_{\nu=n_1} - \frac{J_{n_1+1}(\tilde{\rho})}{4}\left(\frac{\partial J_{\nu-1}(\tilde{\rho})}{\partial\nu}\right)_{\nu=n_2} - \frac{J_{n_2+1}(\tilde{\rho})}{4}\left(\frac{\partial J_{\nu-1}(\tilde{\rho})}{\partial\nu}\right)_{\nu=n_1} + 2\int_0^{\pi/2} J_{n_1+n_2}(2\tilde{\rho}\cos\theta)\sin(2\theta)\cos[(n_1-n_2)\theta]d\theta \tag{23}$$

$$\kappa = 1; \bar{S}_6(\tilde{\rho}) = \frac{J_{n_2-1}(\tilde{\rho})}{4}\left(\frac{\partial J_{\nu-1}(\tilde{\rho})}{\partial\nu}\right)_{\nu=n_1} - (-1)^{n_2}\frac{J_{n_1-1}(\tilde{\rho})}{4}\left(\frac{\partial J_{1-\nu}(\tilde{\rho})}{\partial\nu}\right)_{\nu=n_2} - \frac{J_{n_2+1}(\tilde{\rho})}{4}\left(\frac{\partial J_{\nu+1}(\tilde{\rho})}{\partial\nu}\right)_{\nu=n_1} + (-1)^{n_2}\frac{J_{n_1+1}(\tilde{\rho})}{4}\left(\frac{\partial J_{-\nu-1}(\tilde{\rho})}{\partial\nu}\right)_{\nu=n_2} \tag{24}$$

As in the off-resonance case, it can be shown that the only sums that give a non-negligible contribution to $\tilde{H}_2^{(on)}$ are $\bar{S}_1$, $\bar{S}_2$, and $\bar{S}_6$. Moreover, for $\tilde{\rho} \leq \min(n_1, n_2)$, $\bar{S}_i(\tilde{\rho}) \simeq S_i(\tilde{\rho})$ for $i = 1, 2, 6$. Indeed, because of the rapid decrease of $J_n(x)$ when x becomes less than n, the only significant terms in the S_i's and the $\bar{S}_i$'s are those which have Bessel functions of order m such that $m \leq \tilde{\rho}$. Hence, these are the same terms for S_i and $\bar{S}_i$, and for such values of m, $n_1 - m \simeq \nu_1 - m$ and $n_2 - m \simeq \nu_2 - m$ provided that $n_1 = Int(\nu_1)$ and $n_2 = Int(\nu_2)$, where $Int(\nu)$ stands for the integer part of ν. Moreover, numerically calculating $\bar{S}_i(\tilde{\rho})$ and $S_i(\tilde{\rho})$ shows that when $\tilde{\rho} \leq \min(n_1, n_2)$, $\bar{S}_i(\tilde{\rho}) \simeq S_i(\tilde{\rho})$. Therefore, for values of $\tilde{\rho}$ such that $\tilde{\rho} \leq \min(n_1, n_2)$

$$\tilde{H}_2^{(on)} \simeq \varepsilon_1 J_{n_1}(\tilde{\rho})\cos[n_1(\tilde{\theta}-\tau)+\varphi_1] + \varepsilon_2\frac{J_{n_2}(\kappa\tilde{\rho})}{\kappa}\cos[n_2(\tilde{\theta}-\tau)+\varphi_2] + \tilde{H}_2^{(off)} \tag{25}$$

It is clear from (25) that the only difference between the on and off-resonance cases comes form the presence of a first order term in $\tilde{H}_2^{(on)}$ which does not exist in $\tilde{H}_2^{(off)}$. If $\mid n_1 - n_2 \mid < \min(n_1, n_2)$ (which is the only case we consider here), when $\tilde{\rho} \to 0$, this first order term decreases more rapidly than $\tilde{H}_2^{(off)}$. This implies that there exists a value $\tilde{\rho}_l(\varepsilon_1, \varepsilon_2)$ such that for $\tilde{\rho} \leq \tilde{\rho}_l(\varepsilon_1, \varepsilon_2)$, $\tilde{H}_2^{(on)} \simeq \tilde{H}_2^{(off)}$. In other words, in the region of phase space corresponding to $\tilde{\rho} \leq \tilde{\rho}_l$ the orbits for two on-resonance waves are very close to the orbits for two off-resonance waves. In particular, if for a given initial condition the maximum value that the Larmor radius of an ion in two off-resonance waves can reach is less than $\tilde{\rho}_l$, then the Larmor radius of an ion in two on-resonance waves will never exceed $\tilde{\rho}_l$ either. Therefore, Figs. 7 to 10 are also valid for two on-resonance waves, except for values of κ where $\tilde{\rho}_{max}$ is predicted

to be larger than $\tilde{\rho}_l$. For such values of κ the first order terms in $\tilde{H}_2^{(on)}$ have to be taken into account. The effect of these first order terms is to enhance the acceleration by providing an easier access to the stochastic region. Indeed, if only these terms are retained in $\tilde{H}_2^{(on)}$, the Larmor radius of an ion will always reach the value $\tilde{\rho} = \min(n_1, n_2)$ where it is known from (4) that the motion is stochastic. This effect is illustrated in Fig. 11 where $\tilde{\rho}_{max}$ is plotted as a function of κ for $n_1 = 140$ and $n_2 = 139$. For values of κ less than 0.978 or larger than 1.001, $\tilde{\rho}_{max}$ evolves smoothly with κ and assumes the same values as those in Fig. 7 for two off- resonance waves. Two discontinuities occur at $\kappa \simeq 0.978$ and $\kappa \simeq 1.001$ due to the effects of the first order terms in $\tilde{H}_2^{(on)}$ which bring the ion up into the stochastic region. The maximum value of the Larmor radius an ion can reach after accessing the stochastic region will be discussed in section 5.

It is clear that, for smaller wave amplitudes, the first order terms will be more important in $H_2^{(on)}$ and, hence, will have a significant effect on a larger part of phase space. This implies that $\tilde{\rho}_l(\varepsilon_1, \varepsilon_2)$ is an increasing function of the wave amplitudes. Consequently, as the wave amplitudes are lowered, a larger fraction of ions can access the stochastic region where they quickly gain a large amount of energy. This is the same kind of effect as the one described in [11] for one on-resonance wave. However, for high harmonics, $\tilde{\rho}_l$ is quite insensitive to the value of the wave amplitudes and is close to $\min(n_1, n_2)$, as can be seen in Fig. 11.

4.3. Relaxation of the condition on the wave frequencies for acceleration:

Sections 4.1 and 4.2 showed that an ion can be accelerated by two waves in a magnetic field provided that the difference in the wave frequencies is an integer multiple of the cyclotron frequency. We show here that the condition on the wave frequencies can actually be relaxed and that there can be some acceleration even if

$$\nu_1 - \nu_2 = n + \delta\nu \tag{26}$$

where n is an integer, and $\mid \delta\nu \mid << 1$ is a small number scaling as $\varepsilon_1\varepsilon_2$. This scaling can be shown by requiring that the change of variables that transforms H into $H_2^{(off)}$ or into $H_2^{(on)}$ be one-to-one, or by requiring that the terms obtained up to second order give a good approximation of the perturbation series (A4). The corresponding calculations are detailed in Appendix B, and are useful for generalizing the results to the case of more than two waves. Nevertheless, in the case of two waves, the way $\delta\nu$ scales with the waves amplitudes is obvious. Indeed, instead of performing the change of variables as described in Appendix A, in order to obtain (6), it is always possible to define a canonical change of variables in such a way that the term involving $\cos[(\nu_1 - \nu_2)\tau]$ is taken into account in $\tilde{H}_2^{(off)}$, whatever the value of $(\nu_1 - \nu_2)$. In the case when $\varphi_1 = \varphi_2$, the Hamiltonian thus obtained is

$$\tilde{H} = \tilde{I} + \varepsilon_1^2 S_1(\tilde{\rho}) + \varepsilon_2^2 S_2(\tilde{\rho}) + \varepsilon_1\varepsilon_2 S_6(\tilde{\rho}) \cos\left[n(\tilde{\theta} - \tau) - \delta\nu\tau\right] \tag{27}$$

$S_6(\tilde{\rho})$ being defined by (A16) where $(\nu_1 - \nu_2)$ has to be replaced by n. The Hamiltonian (27) is integrable. This can be easily seen by performing a canonical change of variables $(\tilde{I}, \tilde{\theta}) \rightarrow (\tilde{K}, \tilde{\psi})$ using the generating function

$$G = \tilde{K}(\tilde{\theta} - \tau - \delta\nu\tau/n) \tag{28}$$

which yields $\tilde{K} = \tilde{I}$, and $\tilde{\psi} = \tilde{\theta} - \tau - \delta\nu/N\tau$. In the variables $(\tilde{K}, \tilde{\psi})$, (27) becomes

$$\tilde{H} = -\frac{\delta\nu}{n}\tilde{K} + \varepsilon_1^2 S_1(\tilde{\rho}) + \varepsilon_2^2 S_2(\tilde{\rho}) + \varepsilon_1\varepsilon_2 \cos(n\tilde{\psi}) S_6(\tilde{\rho}) \tag{29}$$

which is time independent. Hence, the orbits of (29) are obtained by solving $\tilde{H} = const.$ When solving this equation, it is clear that if there is some acceleration when $\delta\nu = 0$, this acceleration persists when $\delta\nu \neq 0$ only if $\varepsilon_1\varepsilon_2 S_6(\tilde{\rho})$ is at least of the order of $(\delta\nu/n)\tilde{I}$. This shows that $\delta\nu$ must scale as $\varepsilon_1\varepsilon_2$ for acceleration to take place. When this condition is fulfilled, it is then clear that the amount of energy gained by an ion is of the same order of magnitude as in the case when $\delta\nu = 0$. Hence, the results derived in the sections 4.1 and 4.2 remain relevant. In particular, the acceleration will be all the more important as the amplitude of $S_6(\tilde{\rho})$ is large, and the curve plotting the maximum and minimum values of $\tilde{\rho}$ as a function of k_2/k_1 also has some discontinuities, due to the existence of zeros in $S_6(\tilde{\rho})$, as in Fig. 6. Therefore, the results obtained in Sections 4.1 and 4.2 describe in a very complete way the acceleration of low energy ions by two electrostatic waves propagating perpendicularly to a uniform magnetic field.

4.4 Acceleration of low energy ions in an arbitrary discrete wave spectrum:

In this section we study the dynamics defined by (2) in the case when an arbitrary number of on and off-resonance waves are included. The study is still restricted to the part of phase space which is below the stochastic region, namely we only consider values of ρ such that $\rho \leq \min(\nu_i)$. We show here that the acceleration phenomenon described in the case of two waves also exists in the case of more than two waves, and that actually, the results obtained in the case of two waves readily apply to the case of many waves. This occurs because perturbation theory up to the second order in the waves amplitudes describes the dynamics accurately also in the case of more than two waves, as can be seen in Fig. 12 and 13 for the case of six waves. As a second order perturbation analysis only takes into account the nonlinear interaction of pairs of waves, the Hamiltonian obtained after perturbation theory in the case of N waves is a sum of Hamiltonians of the form (11) or (25). Thus, to second order, and using the same approximations as before, the Hamiltonian (2) is transformed to

$$\begin{aligned}\tilde{H} \simeq & \sum_{\nu_i \in \mathcal{N}} \frac{\varepsilon_i}{\kappa_i} J_{\nu_i}(\kappa_i\tilde{\rho}) \cos(\nu_i\tilde{\Phi} + \varphi_i) \\ & + \sum_{i=1}^{N} \varepsilon_i^2 S_2^{(i)}(\tilde{\rho}) + \sum_{(\nu_i - \nu_j) \in \mathcal{N}^*} \varepsilon_i\varepsilon_j S_6^{(i,j)}(\tilde{\rho}) \cos\left[(\nu_i - \nu_j)\Phi + \varphi_i - \varphi_j\right],\end{aligned} \tag{30}$$

where $\mathcal{N}$ denotes the set of positive integers, and $\mathcal{N}^*$ the set of striclty positive integers, $\mathcal{N}^* = \mathcal{N} \setminus \{0\}$. If ν_i is not an integer, $S_2^{(i)}$ is given by (A13) with κ replaced by κ_i and ν_2 replaced by ν_i; if ν_i is an integer, $S_2^{(i)}$ is given by (17) with the same replacements. As already noted in the case of two waves, the fact that ν_i is an integer or not does not really affect the value of $S_2^{(i)}$. As for $S_6^{(i,j)}$ it is defined by

$$S_6^{(i,j)} = \sum_{m=-\infty}^{+\infty} \frac{m J_m(\kappa_j\tilde{\rho}) J'_{\nu_i - \nu_j + m}(\kappa_i\tilde{\rho})}{\kappa_j(\nu_j - m)} + \sum_{m=-\infty}^{+\infty} \frac{m J_m(\kappa_i\tilde{\rho}) J'_{\nu_j - \nu_i + m}(\kappa_i\tilde{\rho})}{\kappa_i(\nu_i - m)} \tag{31}$$

when ν_i and ν_j are not integers. If they are integers the term involving $m = \nu_i$ has to be excluded in the first sum of (31), and the term $m = \nu_j$ has to be excluded in the second sum of (31). Again, as noted when studying the case of two waves, the fact that ν_i and ν_j are integers or not does not really affect the values of $S_6^{(i,j)}(\tilde{\rho})$ as long as $\tilde{\rho} \leq \min(\nu_i, \nu_j)$.

Now, the dependence of the acceleration mechanism on the wave spectrum parameters can be easily deduced from the case of two waves. In particular, the first order terms only play a role in a part of phase space close to the chaotic domain and can be neglected in a first approximation. Therefore, there is acceleration when the sum, S_a, of the terms $\varepsilon_i \varepsilon_j S_6^{(i,j)}(\tilde{\rho}) \cos[(\nu_i - \nu_j)\Phi + \varphi_i - \varphi_j]$ is at least of the same order as the sum, S_s, of the stabilizing terms $\varepsilon_i^2 S_2^i(\tilde{\rho})$. This yields the conditions on the different parameters of the problem in order to obtain acceleration.

In the case where the wave amplitudes are all about the same, the condition on the frequencies is simply that the number of pairs of frequencies separated by an integer multiple of the cyclotron frequency must be at least of the order of the total number of waves. If the number of stabilizing terms is much larger than the number of accelerating terms then there is no acceleration.

We can also show, as in 4.1, that the energization is a maximum when two waves whose frequencies are separated by an integer multiple of the cyclotron frequency have the same amplitudes. Moreover, if all the waves have the same normalized amplitude ε, then the orbits do not depend on ε, except when the first order terms are not negligible. In this case we find that an ion accesses the chaotic domain of phase space more easily as ε is decreased. The time needed for an ion to be accelerated scales, as in the case of two waves, as ε^{-2}.

The main difference with the case of two waves comes from the fact that changing the values of the initial phases φ_i does not only result in a shift of the orbit. The orbit explicitly depends on the choice of the φ_i's as long as there is more than one term in the sum, S_a, of the accelerating terms. When the number of terms in S_a is of the order of unity, then the amount of energy gained by an ion should be the same whatever the phases. This fact is illustrated for example in Fig. 14. Nevertheless, if the number N_a of terms in S_a is large, then this sum scales differently with N_a depending on the choice of the phases φ_i's. For example, if the φ_i's are all the same then the sum will scale as N_a, while if the φ_i's are chosen randomly the sum will scale as $\sqrt{N_a}$. Hence, for a large number of waves, one expects to obtain more acceleration when the initial phases are coherent than when they are random. Numerical results show that there is very little acceleration when the initial phases of the waves are randomly distributed.

Finally, the way the gain of energy varies with the wavenumbers can also be very easily deduced from the study performed for two waves. Indeed, for each pair of waves yielding an acceleration term, one knows how much energy an ion would gain if only these two waves existed. Then, the order of magnitude of the energy an ion gains from the whole spectrum is of the order of the sum of the energies gained from each pair of waves divided by half of the total number of waves. Therefore, $\tilde{\rho}_{\min}$ and $\tilde{\rho}_{\max}$ are expected to behave with the wavenumbers in a similar way as in the case of two waves. In order to test this point numerically without having to specify a dispersion relation, we consider the case when the wavenumbers are all about the same value. Then, it is valid to make a first order Taylor expansion of the dispersion relation $k(\omega)$ and to relate the wave numbers through a linear

relation $k_i = k_1 + \alpha(\omega_i - \omega_1)$, where α is the inverse of the group velocity evaluated at $k = k_1$. Numerically, we fix the values of the wave frequencies and compute the amount of energy gained by an ion when α is varied. Figures 15 and 16 plot $\tilde{\rho}_{\min}$ and $\tilde{\rho}_{\max}$ versus $\kappa = k_2/k_1$ in the case of multiple waves. These figures are similar to Fig. 7 plotted in the case of two waves. One can notice however that in the case of multiple waves the maximum value of $\tilde{\rho}_{\max}$ is somewhat lower that in the case of two waves. Yet, in the case of Fig. 15, four pairs of waves give rise to acceleration while there are five waves. Therefore, the ratio of the number of terms giving rise to acceleration divided by the total number of waves is higher than in the case of two waves. The fact that the maximum acceleration is not as high as for two waves simply comes from the fact that the zones of high acceleration do not correspond to the same value of the ratio of the wave numbers for each pair of waves.

When deriving (30) we did not take into account the case when the difference $(\nu_l - \nu_m)$ between two normalized wave frequencies is so close to an integer that the non-linear interaction of these waves cannot be neglected in (30), although $(\nu_l - \nu_m)$ is not an integer. If we denote $\nu_l - \nu_m = n_l + \delta\nu_l$, then we know from the results of the Appendix B that the non-linear interaction of the waves l and m has to be included in (30) for a small enough value of $\delta\nu_l$, scaling as $\varepsilon_l\varepsilon_m$. Including the corresponding term in (30) yields

$$\begin{aligned}\tilde{H} \simeq & \sum_{\nu_i \in \mathcal{N}} \frac{\varepsilon_i}{\kappa_i} J_{\nu_i}(\kappa_i\tilde{\rho})\cos(\nu_i\tilde{\Phi} + \varphi_i) + \varepsilon_l\varepsilon_m S_6^{(l,m)}(\tilde{\rho})\cos(n_l\tilde{\Phi} - \delta\nu_l\tau + \varphi_l - \varphi_m) \\ & + \sum_{i=1}^{N} \varepsilon_i^2 S_2^{(i)}(\tilde{\rho}) + \sum_{(\nu_i - \nu_j)\in\mathcal{N}^*} \varepsilon_i\varepsilon_j S_6^{(i,j)}(\tilde{\rho})\cos\left[(\nu_i - \nu_j)\Phi + \varphi_i - \varphi_j\right] \qquad (32)\end{aligned}$$

The Hamiltonian (32) is not integrable, as soon as there is more than one term in the sum S_a. Therefore, the orbits of (32) cannot be exactly calculated. Nevertheless, during a time which is of the order of $1/\delta\nu_l$, an orbit of (32) is very close to the orbit obtained by setting $\delta\nu_l = 0$ and solving $\tilde{H} = const.$ Because the maximum value of $\delta\nu_l$ scales as $\varepsilon_l\varepsilon_m$, the time $1/\delta\nu_l$ is at least of the order of the time which gives the coherent acceleration when either $\delta\nu_l = 0$, or the term due to the waves l and m is negligible. This is actually intuitively obvious, because if $1/\delta\nu_l$ were much smaller than the time of coherent acceleration, then the term $\cos(n_l\tilde{\Phi} - \delta\nu_l\tau + \varphi_l - \varphi_m)$ would behave as a fast perturbation and would henceforth be removable using perturbation theory, which is not the case. Therefore, an orbit of $\tilde{H}$ is close to the one obtained by setting $\delta\nu_l = 0$ during a time of the order of $1/\delta\nu_l$, and $1/\delta\nu_l$ is also of the order of the time during which an ion is energized by the waves when $\delta\nu_l = 0$. This implies that the analysis made on a Hamiltonian like (30) gives the order of magnitude of the energy gained by an ion also in the case of a Hamiltonian of the form (32).

In conclusion, we have shown that the results found in the case of two waves in the subsections 4.1 and 4.2 can be readily generalized to the case of an arbitrary discrete wave spectrum. This shows the universality of the results for the case of two waves, and implies that the main features of the dynamics of an ion in a discrete spectrum of waves propagating perpendicularly to a uniform magnetic field have been described in this section in a complete way, as long as the orbit of the ion remains below the stochastic region.

5. High ion energization with more that one wave:

In this section we consider the case where, in the presence of more than one wave, an ion has accessed the stochastic region of phase space. This happens when either the ion initial condition is in the chaotic domain of phase space, or when the ion has been coherently accelerated into the chaotic domain. We show here that when there are at least two on-resonance waves in the wave-spectrum, then an ion reaches energies which are much higher than with one wave, for the same values of the wave amplitudes and the same time interval. This can be seen for example in Fig. 17, plotting the Poincaré section of the dynamics of an ion acted upon by two on-resonance waves. These waves have the same amplitudes, and frequencies of the same order, as the waves in Figs. 1 and 2. Moreover, the initial condition is the same and the ion dynamics is followed for the same duration of time as in Figs. 1 and 2. Nevertheless, one can see from Fig. 17 that when acted upon by two on-resonance waves, the ion can reach an energy which is about three times higher than the maximum energy reached in the case of one wave. It is also important to note that in the case of two on-resonance waves the phase space is not quasi-uniformly visited as in the case of Fig. 1. As we will show below, this happens because the ion orbit remains close to the orbits determined from a first order perturbation analysis on the Hamiltonian (2). This implies that over a wide range of values of the wave amplitudes, the energy gained by an ion is directly related to the increase in action of the orbits found from a first order perturbation analysis. Hence, these first order orbits rule transport although the ion motion is not regular. Therefore, we study in this section the first order orbits, in order to deduce the energy an ion gains from the waves as a function of the wave-spectrum parameters. The basic results are obtained in the case of two on-resonance waves and are then generalized to an arbitrary discrete wave-spectrum.

5.1 Enhancement of the ion acceleration with two on-resonance waves:

5.1.1 Numerical illustration of the enhancement of acceleration:

In this subsection we investigate the dynamics of an ion in two on-resonance waves in the particular case when $\rho > \max(\nu_i)$. In such a case, whenever a perturbation analysis is relevant to describe the ion dynamics, the first order term dominates. Hence, the relevant perturbed Hamiltonian, $\tilde{H}$, is the Hamiltonian (16) where only the first order term is taken into account. When the wave amplitudes are small, $\tilde{H}$ describes very accurately the dynamics of the Hamiltonian (2), as is illustrated in Fig. 18 and 19. Fig. 18 shows a Poincaré section of the Hamiltonian (2) when $\varepsilon_1 = \varepsilon_2 = 0.324$, while Fig. 19 shows the orbit of $\tilde{H}$ corresponding to the same parameters as in Fig. 18. One can clearly see that for these values of the wave amplitudes, the orbits obtained from H or from $\tilde{H}$ are close to each other. One can also see in Fig. 18 that an ion can reach an energy which is about 30 times higher than its initial energy. Hence, the ion is highly energized. One off-resonance wave having an amplitude and a frequency of the same order would not energize the ion at all, because the corresponding vallue of ε is below the stochastic threshold as estimated by (3) (see Fig. 20).

When the two on-resonance wave amplitudes are increased by one order of magnitude, the ion orbit is the one shown in Fig. 17. It is thus very different from the one shown in Fig. 19 and obtained using perturbation theory. Nevertheless, the maximum energy reached by

the ion is of the same order of magnitude in the case of Fig. 17 as in the case of Fig. 19. Therefore, even if the perturbation analysis is unable to provide an accurate description of all the details of the dynamics, it nevertheless provides the good order of magnitude of the amount of energy gained by the ion. Actually, solving $\tilde{H} = const$ does not provide only one orbit but a whole set of orbits, as can be seen in Fig. 21. When the wave amplitudes are high enough in (2), some stochastic layers form about the first order orbits, allowing their interconnection. In the case of Fig. 17, 4 orbits are connected, which makes the ion orbit go a bit higher in action than in the case of Fig. 18. Nevertheless, it is clear that in the case of Fig. 17 also, the amount of energy gained by an ion is determined by the extent, in action, of the first order orbits. Therefore, increasing the wave amplitudes by one order of magnitude does not drastically change the ion energization. This situation is completely different from the one corresponding to one off-resonance wave as can be seen by comparing Fig. 1 to Fig. 20.

If the wave amplitudes are further increased, it is clear that a point is going to be reached where the width of the region of phase space which is completely stochastic is larger than the extent of the first order orbits along the action axis. In this case, acceleration is mainly stochastic and the role of the first order orbits is no longer dominant in transport. This situation is illustrated in Fig. 22, where the wave amplitudes have been increased by one order of magnitude compared to the case of Fig. 17. For such wave amplitudes, one can no longer distinguish any regular orbits, and the phase space looks completely stochastic. Actually, the first order orbits still play a role in the ion energization. These orbits bound the upper part of the chaotic domain. Therefore, after being energized in a purely stochastic way, an ion follows one of these orbits and is hence further energized in a way similar to the case of Figs. 17 and 18. This is illustrated in Fig. 22 by the fact that, as in the case of Figs. 17 and 18, the ion orbit reaches a higher value of the action in the case when θ is close to 0 or 2π than in the case when θ is close to π. The maximum value of the action reached when $\theta = \pi$, $I_{\max}(\pi) \simeq 3000$, corresponds to a purely stochastic acceleration . The difference between the highest action reached when $\theta = 0$, $I_{max}(0) \simeq 4500$, and $I_{max}(\pi)$ is close to the extent in action space of the first order orbits.

When acted upon by one off-resonance wave, an ion can only be energized in a stochastic way. In the case of one off-resonace wave having an amplitude and a frequency of the same order as the waves of Fig. 22, an ion reaches a maximum action, $I_{\max}^{(off)} \simeq 5000$ (Fig. 23), which is approximately the same as $I_{max}^{(on)}(0)$. The stochastic acceleration leads an ion to energies of the same order of magnitude with one or two waves. Therefore, no new result is to be found on stochastic acceleration with two on-resonance waves compared to what is already known for one wave. Hence, we now focus on those wave amplitudes for which transport is dominated by the first order orbits.

5.1.2 Analytical study of the acceleration mechanism dependence on wave characteristics:

As shown in the previous subsection, the key point to understanding the enhancement of acceleration by two on-resonance waves is to calculate the extent, in action, of the first order orbits. In this subsection, we evaluate the excursions in action and the dependence of the energy gained on the wave spectrum parameters.

Keeping only the first order term in (16), and going into the variables $(\tilde{I}, \tilde{\Phi} = \tilde{\theta} - \tau)$, the perturbed Hamiltonian $\tilde{H}$ is

$$\tilde{H} = \varepsilon_1 J_{n_1}(\tilde{\rho}) \cos(n_1 \tilde{\Phi} + \varphi_1) + \varepsilon_2 \frac{J_{n_2}(\kappa\tilde{\rho})}{\kappa} \cos(n_2 \tilde{\Phi} + \varphi_2) \tag{33}$$

When $\tilde{\rho} >> \max(n_1, n_2)$, one can use in (33) the large argument expansion of the Bessel functions, so that (33) becomes

$$\begin{aligned} \tilde{H} \simeq\ & \varepsilon_1 \sqrt{\frac{2}{\pi\tilde{\rho}}} \cos(\tilde{\rho} - n_1\pi/2 - \pi/4) \cos(n_1 \tilde{\Phi} + \varphi_1) \\ & + \frac{\varepsilon_2}{\kappa^{3/2}} \sqrt{\frac{2}{\pi\tilde{\rho}}} \cos(\kappa\tilde{\rho} - n_2\pi/2 - \pi/4) \cos(n_2 \tilde{\Phi} + \varphi_2) \end{aligned} \tag{34}$$

Using the approximation (34) for $\tilde{H}$, we now solve $\tilde{H} = 0$. As will be shown, such an analytic calculation completely accounts for the numerical results shown in the previous subsection. Physically, taking the constant equal to zero corresponds to a case where the initial condition is below the stochastic region, because when $\rho_0 < \min(n_1, n_2)$ the values of $J_{n_1}(\rho_0)$ and $J_{n_2}(\rho_0)$ are much less than the values assumed by $J_{n_1}(\rho)$ and $J_{n_2}(\rho)$ over a large part of the region of phase space above the chaotic domain.

For the sake of simplicity we first consider the solution of $\tilde{H} = 0$ for $\kappa = 1$. When $n_2 = n_1 + 2p + 1$, and when $\cos[(n_1 + 2p + 1)\tilde{\Phi} + \varphi_2] \neq 0$, $\tilde{H} = 0$ in (34) is equivalent to

$$\tan(R) = (-1)^{(p+1)} \frac{\varepsilon_1}{\varepsilon_2} \frac{\cos[n_1 \tilde{\Phi} + \varphi_1]}{\cos[(n_1 + 2p + 1)\tilde{\Phi} + \varphi_2]} \tag{35}$$

where $R = \tilde{\rho} - n_1\pi/2 - \pi/4$. Since changing $\tilde{\Phi}$ into $\tilde{\Phi} + \pi$ does not change the right-hand side of (35), we study this equation only over an interval of amplitude π in $\tilde{\Phi}$. In between 2 zeros of $\cos(n_1\tilde{\Phi} + \varphi_1)$ there is at least one zero of $\cos[(n_1 + 2p + 1)\tilde{\Phi} + \varphi_2]$. This implies that when $\tilde{\Phi}$ varies over the interval $I_m = [\frac{\pi/2-\varphi_1}{n_1} + \frac{m\pi}{n_1}, \frac{\pi/2-\varphi_1}{n_1} + \frac{(m+1)\pi}{n_1})$, i.e. between 2 zeros of $\cos(n_1\tilde{\Phi} + \varphi_1)$, then the right hand side of (35) runs over the whole interval $(-\infty, +\infty)$. Consequently, R changes by $\pm\pi$. In other words, a change by π/n_1 in the angle induces a change by $\pm\pi$ in the normalized Larmor radius. If, in the interval $I_{m+1} = [\frac{\pi/2-\varphi_1}{n_1} + \frac{(m+1)\pi}{n_1}, \frac{\pi/2-\varphi_1}{n_1} + \frac{(m+2)\pi}{n_1})$, the number of zeros of $\cos[(n_1 + 2p + 1)\tilde{\Phi} + \varphi_2]$ different from $\left(\frac{\pi/2-\varphi_1}{n_1} + \frac{(m+1)\pi}{n_1}\right)$ is odd, then R changes in the same way in I_m as in I_{m+1}: if R changes by $+\pi$ in I_m it also changes by π in I_{m+1} and if it changes by $-\pi$ in I_m it also changes by $-\pi$ in I_{m+1}. Conversely, if in I_{m+1} the number of zeros of $\cos[(n_1+2p+1)\tilde{\Phi}+\varphi_2]$ is even, then R changes in opposite ways in I_m and in I_{m+1}. Clearly, the most interesting case for acceleration is when the range of Larmor radius spanned by an orbit solution of (35) is maximum, i.e. when there exists an interval of amplitude π in which there is always an odd number of zeros of $\cos[(n_1+2p+1)\tilde{\Phi}+\varphi_2]$ between 2 zeros of $\cos[n_1\tilde{\Phi}+\varphi_1]$. In this case, the ion Larmor radius changes by an amount of the order of $n_1\pi$. This happens for example when the wave frequencies are separated by an ion-cyclotron frequency, i.e. $n_2 = n_1+1$. The zeros of $\cos[n_1\tilde{\Phi}+\varphi_1]$ are $\tilde{\Phi}_m = (\pi/2-\varphi_1)/n_1 + m\pi/n_1$ while the zeros of $\cos[(n_1+1)\tilde{\Phi}+\varphi_2]$ are $\tilde{\Phi}'_m = (\pi/2-\varphi_2)/(n_1+1) + m\pi/(n_1+1)$. Clearly the number of $\tilde{\Phi}'_m$'s between two $\tilde{\Phi}_m$'s

does not depend on the initial phases φ_1 and φ_2 except when they are such that one $\tilde{\Phi}'_m$ is equal to one $\tilde{\Phi}_m$. Nevertheless, with probability one, this does not happen. We thus restrict ourselves to the case when $\varphi_1 = \varphi_2 = 0$. Then, it is clear that in $[0, \pi]$ there is always one $\tilde{\Phi}'_m$ between two $\tilde{\Phi}_m$'s, and R is thus a monotonic function of $\tilde{\Phi}$ over $[0, \pi]$. Therefore, when acted upon by two on-resonance waves whose frequencies are separated by one cyclotron frequency, an ion experiences a variation in its Larmor radius of the order of $n_1\pi$. For example, in the case of Fig. 18, the minimum value of the Larmor radius is $\rho_{min} \simeq 5$ and the maximum value of the Larmor radius is $\rho_{\max} \simeq 40$, while $n_1\pi = 9\pi \simeq 28$. The discrepancy between the analytical prediction and the numerical result only comes from the lack of accuracy of the large argument expansion of the Bessel functions.

If the initial phases φ_1 and φ_2 are such that one $\tilde{\Phi}'_m$ is equal to one $\tilde{\Phi}_m$, the only consequence is that the ion Larmor radius varies by $(n_1 - 1)\pi$ instead of $n_1\pi$. Hence, as in the case of section 4, the choice of the initial phases is not important in the acceleration mechanism.

When $n_2 = n_1 + 2p$ then from (34), in the case $\kappa = 1$, $\tilde{H} = 0$ gives

$$(\varepsilon_1 + (-1)^p\varepsilon_2)\cos(R)[\cos(n_1\tilde{\Phi} + \varphi_1) + \cos[(n_1 + 2p)\tilde{\Phi} + \varphi_2)] = 0 \tag{36}$$

Solving (36) yields $R = \pi/2 + m\pi$ or $\cos(n_1\tilde{\Phi}+\varphi_1)+\cos[(n_1+2p)\tilde{\Phi}+\varphi_2)] = 0$. Therefore, the result consists of a set of rectangular cells, similar to the ones obtained in the one-wave case. Nevertheless, the large argument expansion of the Bessel functions is not precise enough to recover the result that would be obtained by using the formula (33) for $\tilde{H}$. Fig. 24 plots a set of orbits obtained by numerically solving $\tilde{H} = const$ for the case when $n_1 = 9$ and $n_1 = 11$. Comparing with Fig. 21, it can be seen that these orbits extend to lower actions than when $n_1 = 9$ and $n_2 = 10$, but nevertheless to higher actions than in the one wave case. Moreover, these orbits are close enough to be easily connected through the stochastic layers. Hence, when the wave amplitudes are small an ion is less energized than when $n_2 - n_1 = 1$, while as soon as the amplitudes are high enough for the orbits to be connected by stochasticity, the ion energization should be of the same order as when $n_2 - n_1 = 1$. This is confirmed numerically, and illustrated in Figs. 25 and 26. Therefore, when $n_2 - n_1 = 2$ stochasticity plays a more important role than when $n_2 - n_1 = 1$, nevertheless the transport is still dominated by the first order orbits. Moreover, in this case also, the energy gained by an ion corresponds to a variation in the normalized Larmor radius of the order of $n_1\pi$.

We now turn to the case when the wavenumbers are not the same, i.e. $\kappa = k_2/k_1 \neq 1$. We focus on the case when $n_2 - n_1 = 1$, and $\varepsilon_1 = \varepsilon_2$ as this corresponds to the case of maximum acceleration. As noted earlier, we can set $\varphi_1 = \varphi_2 = 0$ without loss of generality. Then, using (33), $\tilde{H} = 0$ gives:

$$J_{n_1}(\tilde{\rho})\cos[n_1\tilde{\Phi}] + \frac{J_{n_1+1}(\kappa\tilde{\rho})}{\kappa}\cos[(n_1 + 1)\tilde{\Phi}] = 0 \tag{37}$$

In order to study the variations of $\tilde{\rho}$ with $\tilde{\Phi}$, we differentiate (37), which yields

$$\begin{aligned} &d\tilde{\rho}\left\{J'_{n_1}(\tilde{\rho})\cos[n_1\tilde{\Phi}] + J'_{n_1+1}(\kappa\tilde{\rho})\cos[(n_1 + 1)\tilde{\Phi}]\right\} \\ &-d\tilde{\Phi}\left\{n_1 J_{n_1}(\tilde{\rho})\sin[n_1\tilde{\Phi}] + (n_1 + 1)\frac{J_{n_1+1}(\kappa\tilde{\rho})}{\kappa}\sin[(n_1 + 1)\tilde{\Phi}]\right\} = 0 \end{aligned} \tag{38}$$

From (37) and (38) it is easy to see that the orbit $\tilde{\rho}(\tilde{\Phi})$ has a horizontal tangent, i.e. $d\tilde{\rho}/d\tilde{\Phi} = 0$, if and only if $\tilde{\Phi}$ is an integer multiple of π, or $J_{n_1}(\tilde{\rho}) = J_{n_1+1}(\kappa\tilde{\rho}) = 0$. Note, however, that with probabilty one, this last condition is not fulfilled.

When $\kappa \neq 1$, the orbit $\tilde{\rho}(\tilde{\Phi})$ may have vertical tangents. Using (37) and (38), and making a large argument expansion of the Bessel function, we find that this happens when

$$\kappa\cos(\kappa\tilde{\rho}-n_1\pi/2-\pi/4)\cos(\tilde{\rho}-n_1\pi/2-\pi/4)+\sin(\kappa\tilde{\rho}-n_1\pi/2-\pi/4)\sin(\tilde{\rho}-n_1\pi/2-\pi/4) = 0 \tag{39}$$

In order to find the values of κ allowing (39), we denote $\kappa = 1+\delta$ and $R = \tilde{\rho}-n_1\pi/2-\pi/4$. Then (39) is equivalent to

$$\cos(\delta\tilde{\rho}) + \delta\cos(R)\cos(R+\delta\tilde{\rho}) = 0 \tag{40}$$

Because $\mid \delta\cos(R)\cos(R+\delta\tilde{\rho}) \mid \leq \mid \delta \mid$, if $\mid \delta \mid < 1$ then, on the interval$[0, \arccos(\mid \delta \mid)/\mid \delta \mid)$, $\cos(\delta\tilde{\rho}) + \delta\cos(R)\cos(R+\delta\tilde{\rho}) > 0$. Therefore, on an interval of amplitude $\arccos(\mid \delta \mid)/\mid \delta \mid$ in $\tilde{\rho}$, the orbit solution of $\tilde{H} = 0$ does not have any vertical tangent. Moreover, if $\mid \delta \mid << 1$, then, as for the case when $\kappa = 1$, a variation by π/n_1 in $\tilde{\Phi}$ induces a variation by $\pm\pi$ in $\tilde{\rho}$. Hence, if the orbit does not have vertical tangent, its extent along the $\tilde{\rho}$-axis is of the order of $n_1\pi$. In other words, if the orbit does not have any vertical tangent when $\tilde{\rho} \in [0, n_1\pi]$, then it does not have any vertical tangent at all. As we showed that the orbit does not have any vertical tangent when $\tilde{\rho} \in [0, \arccos(\mid \delta \mid)/\mid \delta \mid]$, the condition on δ for the orbit to have a vertical tangent is $\arccos(\mid \delta \mid)/\mid \delta \mid \leq n_1\pi$. The minimum value of $\mid \kappa - 1 \mid$ allowing a vertical tangent is thus of the order of $1/(2n_1)$. Therefore, if $\mid \kappa - 1 \mid < 1/(2n_1)$, the orbit solution of $\tilde{H} = 0$ does not have any vertical tangent, and the situation is similar to the case when $\kappa = 1$: the extent of the orbit along the $\tilde{\rho}$-axis is of the order of $n_1\pi$.

If $\mid \kappa - 1 \mid > 1/(2n_1)$, some orbits have vertical tangents which implies that they never go through $\tilde{\Phi} = 0$ nor $\tilde{\Phi} = \pi$. In a case where $J_{n_1}(\tilde{\rho})$ and $J_{n_1+1}(\kappa\tilde{\rho})$ have no common zeros, these orbits have no horizontal tangents. Consequently, they can reach infinite values of $\tilde{\rho}$! Nevertheless, this does not happen to the actual orbits of the Hamiltonian (2). The reason is that these orbits remain close to orbits of $\tilde{H} = C$, where C actually is a non-zero constant. When numerically solving $\tilde{H} = C$, we find that the corresponding orbits indeed have horizontal tangents for values of $\tilde{\Phi}$ different from 0 or π, as can be seen in Fig. 27. If C corresponds to an initial condition which is below the stochastic domain, then, as already mentioned, C is very small compared to the values of the Bessel functions over a large part of phase space above the chaotic region. Therefore, we expect the results obtained from $\tilde{H} = 0$ to have some relevance. In particular, we expect the orbit solutions of $\tilde{H} = C$ to have horizontal tangents either when $\tilde{\Phi}$ is an integer multiple of π or when $\tilde{\rho}$ is such that $J_{n_1}(\tilde{\rho}) \simeq J_{n_1+1}(\kappa\tilde{\rho}) \simeq 0$. Indeed, one can see in Fig. 27 that the orbit solutions of $\tilde{H} = C$ have horizontal tangents for values of $\tilde{I}$ close to 1260 and values or $\tilde{\Phi}$ different from 0 or π, while in this case $J_{n_1}(\tilde{\rho}) = 0$ for $\tilde{I} = 1262 \pm 1$ and $J_{n_1+1}(\kappa\tilde{\rho}) = 0$ for $\tilde{I} = 1263 \pm 1$. Hence, when $\mid \kappa - 1 \mid > 1/(2n_1)$, the extent of the orbits of $\tilde{H}$ in action does not correspond to $\Delta\tilde{\rho} \simeq n_1\pi$ but are related to the lowest value of $\tilde{\rho}$ such that both $J_{n_1}(\tilde{\rho})$ and $J_{n_1+1}(\kappa\tilde{\rho})$ are close to zero. In the remainder of the paper, this value will be referred to as the first common zero of $J_{n_1}(\tilde{\rho})$ and $J_{n_1+1}(\kappa\tilde{\rho})$. However, in all the simulations we performed, this value was of the order of $n_1\pi$ and one can see that the orbits of Fig. 27 do not go much higher in action than the orbits of Fig. 21.

When numerically plotting a Poincaré section of the dynamics defined by (2), for the same parameters as in Fig. 27, one can see that the maximum action reached by an orbit of (2) also corresponds to $I \simeq 1260$ (see Fig. 28). Therefore, in the case of Fig. 28, the maximum energy reached by an ion is fixed by the first common zero of $J_{n_1}(\tilde{\rho})$ and $J_{n_1+1}(\kappa\tilde{\rho})$.

Making a large argument expansion of the Bessel function in the Hamiltonian (37) shows that the orbits of $\tilde{H}$ are almost periodic in $\tilde{\rho}$. This implies that the whole set of orbits solutions of $\tilde{H} = const$ actually extends up to $\tilde{\rho} = +\infty$. In Fig. 27 we only plotted the set of orbits corresponding to values of $\tilde{\rho}$ going from 0 to the first common zero of $J_{n_1}(\tilde{\rho})$ and $J_{n_1+1}(\kappa\tilde{\rho})$. However, there is a second set of orbits of $\tilde{H}$ corresponding to values of $\tilde{\rho}$ going from the first common zero of $J_{n_1}(\tilde{\rho})$ and $J_{n_1+1}(\kappa\tilde{\rho})$ to their second common zero. And, in general, there is a set of orbits corresponding to values of $\tilde{\rho}$ going to the n^{th} common zero of $J_{n_1}(\tilde{\rho})$ and $J_{n_1+1}(\kappa\tilde{\rho})$ to their $(n+1)^{th}$ common zero. Hence, the maximum value of $\tilde{\rho}$ reached by a given set of orbits is very close to the minimum value of $\tilde{\rho}$ of the following set. This implies that the orbits of each set may easily connect through the stochastic layers which exist in the case of the dynamics of (2). If such a connection takes place, then the maximum energy reached by an ion can be much larger than in the case of Fig. 28 or Fig. 17. This is the case for example when $n_1 = 9$, $n_2 = 10$ and $\kappa = 1/\sqrt{2}$. Figure 29 plots the solution of $\tilde{H} = const$ where the constant corresponds to an initial condition where $\tilde{I}(0) = 32$ and $\tilde{\Phi}(0) = 0.94\pi$. One clearly sees in Fig. 29 the different sets of orbits solutions of $\tilde{H} = const$, and one can also see that these sets of orbits can easily connect until a value of $\tilde{I}$ close to 6300. When plotting the Poincaré section of the dynamics of (2), for the same parameter as the ones of Fig. 29, one can see that the maximum energy reached by an ion corresponds to an action close to 6300 (see Fig.30). Hence in the case of Fig. 30, the maximum energy reached by an ion is not related to the position of the first common zero of $J_{n_1}(\tilde{\rho})$ and $J_{n_1+1}(\kappa\tilde{\rho})$, but to the ability of the different orbits solutions of $\tilde{H} = const$ to connect. Actually, the value of the first common zero of $J_{n_1}(\tilde{\rho})$ and $J_{n_1+1}(\kappa\tilde{\rho})$ is about the same in the case of Fig. 28 as in Fig. 30.

By choosing the value of κ such that the orbits of $\tilde{H}$ connect over a wide range of values of the action, an ion can gain large energies from waves with moderate amplitudes. Such a case is shown in Fig. 31 where an ion can reach an energy about three times higher than in Fig. 22, while the wave amplitudes are 10 times lower. However, the situations presented in Figs. 27-31 are rather atypical. Typically, an ion reaches maximum energies which correspond to $\Delta\rho \simeq n_1\pi$, as in the case when $\kappa = 1$.

5.2 Enhancement of the ion acceleration in a discrete wave spectrum:

5.2.1 Discrete spectrum of on-resonance waves:

In this subsection, we show that the enhancement of the ion acceleration, described in the previous section for two on-resonance waves, exists in a more general spectrum of on-resonance waves. Moreover, the typical maximum energy reached by an ion is shown to be the same as for two waves, and thus corresponds to $\Delta\rho \simeq n_1\pi$.

We, thus, study the dynamics defined by (2) where all the ν_i's are integers. As in section

5.1, we perform a first order perturbation analysis which yields the perturbed Hamiltonian

$$\tilde{H} = \sum_{i=1}^{N} \frac{\varepsilon_i}{\kappa_i} J_{n_i}(\kappa_i \tilde{\rho}) \cos(n_i \tilde{\Phi} + \varphi_i) \tag{41}$$

We will not try here to perform a general analytical study of the solutions of $\tilde{H} = 0$, as we did for two waves. Instead, we will show that the concepts and results obtained in the case of two waves also apply to the case of more than two waves.

In particular, let us consider the case when the wavenumbers are identical. Then, by making a large argument expansion of the Bessel function, we find that solving $\tilde{H} = 0$ leads to

$$\tan(\tilde{R}) = \frac{\sum_{i=0}^{p}(-1)^i \varepsilon_{2i+1} \cos(n_{2i+1}\tilde{\Phi} + \varphi_{2i+1})}{\sum_{i=1}^{q}(-1)^i \varepsilon_{2i} \cos(n_{2i}\tilde{\Phi} + \varphi_{2i})} \tag{42}$$

where $n_i = n_1 + i - 1$, $q = p = (N-1)/2$ if N is odd, and $q = p + 1 = N/2$ if N is even. Let $\mathcal{N}(\tilde{\Phi})$ be the numerator of the right-hand side of (42). Then, finding the zeros of $\mathcal{N}(\tilde{\Phi})$ amounts to finding the zeros of a polynomial of degree $2n + 4p + 2$ in $e^{i\tilde{\Phi}}$. Therefore, $\mathcal{N}(\tilde{\Phi})$ has at most $2n + 4p + 2$ zeros in $[0, 2\pi)$. As $\mathcal{N}(\tilde{\Phi} + \pi) = (-1)^{n+1}\mathcal{N}(\tilde{\Phi})$, $\mathcal{N}(\tilde{\Phi})$ has at most $n + 2p + 1$ zeros in $[0, \pi)$. For values of $\tilde{\Phi}$ which are not an integer multiple of π/n_1, $\mathcal{N}(\tilde{\Phi}) = 0$ is equivalent to $\tan(n_1\tilde{\Phi}) = g(\tilde{\Phi})$, where $g(\tilde{\Phi})$ is a function that can be readily found by expanding the cosines in $\mathcal{N}(\tilde{\Phi})$. Therefore, $\mathcal{N}(\tilde{\Phi})$ has at least n_1 zeros in $[0, \pi)$. Similarly, one can show that the number of zeros of the denominator of the right-hand side of (42) is larger than $n_1 + 1$ and smaller than $n_1 + 2q$. Therefore, when the total number of waves is not large compared to n_1, the situation is similar to the two waves case, and an ion is expected to reach a maximum energy corresponding to a variation of the normalized Larmor radius of the order of $n_1\pi$. Moreover, as in the case of two waves, the amount of energy gained by an ion depends on the parity of the number of poles of the right hand side of (42) between 2 of its zeros. The energization is maximum when there is an odd number of poles between 2 zeros.

In Fig. 32 we plot the solution of $\tilde{H} = const$ in the case of four waves having all the same initial phases but slightly different amplitudes and wavenumbers. One can see that the orbits plotted in Fig. 32 for the case of four waves reach energies of about the same value as the orbits plotted in Fig. 21 for the case of two waves, except for values of $\tilde{\Phi}$ close to π. Therefore, depending on the initial condition, stochasticity may be necessary for the ion to be highly energized. Nevertheless, for amplitudes of the same order as the ones chosen in the case of two waves in section 5.1, an ion reaches energies of the same order as in the case of Fig. 17 for two waves, as can be seen in Fig. 33. Moreover, by comparing the figures 32 and 33, it is clear that also in the case of more than two waves, the ion motion is dominated by the orbits found using a first order perturbation analysis.

When the wavenumbers are different, then, as in the case of two waves, an ion can reach very high energies through the connection, due to stochasticity, of different sets of first order orbits. Such an effect is illustrated in Fig. 34.

In conclusion, we find that all the results derived in the case of two waves also apply for more than two waves. This implies that, in the case of more than two waves, the typical maximum energy reached by an ion also corresponds to $\Delta\rho \simeq n_1\pi$. However, by an

appropriate choice of the wavenumbers an ion can be energized to energies much higher than the typical one corresponding to $\Delta\rho \simeq n_1\pi$. In this case, the ion energization occurs mainly through the connection of first-order orbits.

Contrasting our results with previous works, we note that in Ref. 15 the acceleration of ions through patterns in phase space has been investigated in the case of one on-resonance wave, and in the case where the electric field is an infinite sum of on-resonance waves: $\vec{E} = \hat{x}E_0 \sum_{i=-\infty}^{+\infty} \sin(kx - \omega t - i\Delta\omega t)$. In Ref. 16 and 17, the same kind of electric field is assumed, but the effect of a finite number of waves is investigated. In the case of one wave, as already mentioned, stochasticity is essential to energize ions. Therefore, the acceleration mechanism is different from the ones given here. In the case of many waves, for the particular electric field assumed in[13-15], stochasticity also seems to be essential, so that the results obtained are quite different from the one presented here. In particular, in[13-15] no mention is made about a typical energy reached by the ions. Moreover, as all the waves have the same wavenumber in[13-15], the effect presented in Fig. 31 could not be found in previous studies.

5.2.2 Discrete spectrum of on and off-resonance waves:

In this subsection we numerically check that the enhanced acceleration described in the case of on-resonance waves also exists in a wave spectrum composed of a mixture of on and off-resonance waves. We first show that the enhanced acceleration exists in the case of two waves where one wave is on-resonance and the other wave is slightly off-resonance. This effect is similar to the one described is section 4.3. We then show that the enhanced acceleration also exists in the case of three waves where two of them are on-resonance and the third one is off-resonance. Moreover, we estimate the maximum amplitude of the off-resonance wave allowing the enhanced acceleration.

In the previous subsections, we showed that the enhanced acceleration was linked to the nature of the orbits of the Hamiltonian $\tilde{H}$ deduced from (2) by performing a perturbation analysis to first order in the waves amplitudes. As shown, an ion is highly energized when following the orbits of $\tilde{H}$ only if there are at least two on-resonance waves in the wave spectrum. However, for the same reasons as the ones developed in section 4.3, when one off-resonance wave frequency is very close to an integer multiple of the cyclotron frequency, its contribution to $\tilde{H}$ can no longer be neglected. In particular, let us consider the case of two waves such that one of them is on-resonance, and the other one is slightly off-resonance. Let the first wave frequency be such that $\omega_1/\Omega = n_1$, where n_1 is an integer, and the second wave frequency be such that $\omega_2/\Omega = n_2 + \delta\nu$, where n_2 is an integer and $\delta\nu << 1$. Then, it is always possible to define a canonical change of variables such that at first order in the wave amplitudes, the Hamiltonian (2) is transformed into

$$\tilde{H} = \varepsilon_1 J_{n_1}(\tilde{\rho}) \cos(n_1\tilde{\Phi} + \varphi_1) + \frac{\varepsilon_2}{\kappa} J_{n_2}(\kappa\tilde{\rho}) \cos(n_2\tilde{\Phi} - \delta\nu\tau + \varphi_2) \qquad (43)$$

The Hamiltonian (43) can be considered as constant for a time of the order of $2\pi/\delta\nu$. Hence, during the time $2\pi/\delta\nu$, the orbits of $\tilde{H}$ are the same as the ones obtained when $\delta\nu = 0$. Therefore, if $2\pi/\delta\nu$ is larger, or of the order of, the time needed for an ion to be energized when $\delta\nu = 0$, then it is clear that the enhanced acceleration described previously still exists even when $\delta\nu \neq 0$. Such a situation is illustrated in Fig. 35. Therefore, the enhanced

acceleration can take place even if there are less than two on-resonance waves in the wave spectrum.

Now, let us consider the case of three waves such that two of them are on-resonance, and the third one is so radically off-resonance that it plays no role in the Hamiltonian $\tilde{H}$ derived using a first order perturbation analysis. In this case, the enhanced acceleration can still be observed, as can be seen in Fig. 36. Actually, there is an upper bound in the off-resonance wave amplitude for the enhanced acceleration to remain, as is shown in Fig. 37. The off-resonance wave amplitude has to be small enough so that $\tilde{H}$ still has some relevance to describe the dynamics of (2). For the case corresponding to Figs. 36 and 37, we numerically find that the upper bound for the off-resonance wave amplitude is close of $\varepsilon_{off} = 1.8$, while the amplitude of each off-resonance wave is $\varepsilon_{on} = 0.2592$. Actually, when performing the perturbation analysis up to second order, we know from section 4.1 that the off-resonance wave induces a stabilizing term at second order. This term was denoted by $\varepsilon_{off}^2 S_1(\tilde{\rho})$ in section 4.1. It has to be compared with the accelerating term coming from the first order. The root mean square of the first order term (33), with respect to the angle $\tilde{\Phi}$, is $\langle \tilde{H} \rangle = \varepsilon_{on}\sqrt{[J_{n_1}(\tilde{\rho}) + J_{n_2}(\tilde{\rho})]/2}$. For values of $\tilde{\rho}$ corresponding to the maximum energy reached by an ion in the case of Fig. 37, $\langle \tilde{H} \rangle / (\varepsilon_{off}^2 S_2(\tilde{\rho})) \simeq 1$. Therefore, the upper bound in the amplitude of the off-resonance wave allowing the enhanced acceleration is such that the accelerating terms due to the on-resonance waves are balanced by the stabilizing term due to the off-resonance wave.

In conclusion, we have shown that the enhanced acceleration described in section 5.2 is not restricted to the case where the wave spectrum is only composed of on-resonance waves. This shows the physical relevance of the phenomenon of enhanced acceleration for multiple waves.

6. Conclusion:

In this paper we have shown that multiple electrostatic waves propagating across a uniform magnetic field are more efficient in energizing ions than a single wave. In particular, there is no threshold in energy for ions to be accelerated by the waves. Furthermore, the acceleration of low-energy ions is coherent, and there is no threshold for the electric field amplitudes of the waves for the acceleration to take place. The stochasticity threshold that is usually studied in wave-particle interactions is not relevant for this case. The time needed to accelerate low-energy ions is shown to scale inversely as the square of the wave amplitudes. The maximum energy that the ions can achieve and the ion population that is energized can be determined by appropriately choosing the wave frequencies and wavenumbers. Appropriate choices for the frequencies and wavenumbers can also induce a deceleration of ions, extracting their energies. If an accelerated ion reaches the chaotic domain, the maximum energy it reaches can be much higher in the case of multiple waves than in the case of one wave. When the energization is enhanced, the ion orbit follows a path obtained from a first order, in wave amplitudes, perturbation analysis. Therefore, the ion acceleration is not determined by stochasticity. As shown in section 5, a variation in the wavenumbers could induce a dramatic increase in the ion acceleration. However, there is a typical maximum energy reached by an ion, corresponding to an increase in the ion Larmor radius close to $(\pi\omega_1)/(k\Omega)$, where

k is a typical wavenumber, ω_1 is the lowest frequency, and Ω is the cyclotron frequency.

The results we have presented can be readily applied to many physical situation involving coherent wave-particle interactions in a magnetic field. In particular, they prove to be relevant in explaining recent results[10] regarding the acceleration of O^+ and H^+ ions in the ionosphere; this will be shown in a forthcoming paper.[9] Our results can also be applied to new means of ion heating (and/or energy extraction from energetic α-particles) in magnetically confined fusion plasmas.[16] Finally, we remark that for the case when two waves are both below the ion-cyclotron frequency,[12] the perturbation analysis presented here carries through in the same manner as in Section 4, but with the sum S_6 replaced by the sum S_5.

7. Acknowledgements:

This work was supported by the National Science Foundation under grant number 94-24282-ATM, and the Department of Energy under contract number DE-FG02-91ER-54109. One of us (D.B.) was also supported by a Lavoisier grant from the French Ministère des Affaires Etrangères.

APPENDIX A

In order to perform a perturbation analysis using the formalism of the Lie transform[17], one introduces a generating Lie Hamiltonian χ, and defines the transformation operator T, acting on any function g of the dynamical variables I and θ. T is such that $T\{g\}(I,\theta) = g(\tilde{I},\tilde{\theta})$, where $(\tilde{I},\tilde{\theta})$ is the position in phase space at "time" ε, of the trajectory defined by the Hamiltonian χ, with initial conditions (I,θ). In particular, when g is the identity, this leads to the definition of the change of variables $(\tilde{I},\tilde{\theta}) = T(I,\theta)$. This change of variables is clearly canonical. The time introduced to define the transformation operator is a "fake" time for the auxiliary dynamics defined by χ, and is not related to the real time τ in (2). For the sake of simplicity, we consider the case when all the waves have the same reduced amplitude ε. The generalization to the case of different waves amplitudes is straightforward. Following Deprit's method[18], we expand χ in a power series in ε:

$$\chi = \sum_{i=0}^{+\infty} \varepsilon^i \chi_{i+1} \tag{A1}$$

The Hamiltonian (2) is already expanded in power series in ε: $H = H_0 + \varepsilon H_1$, where

$$H_0 = I \tag{A2}$$

$$H_1 = \sum_{n=-\infty}^{\infty} \left[J_n(\rho)\cos(n\theta - \nu_1\tau + \varphi_1) + \frac{J_n(\kappa\rho)}{\kappa}\cos(n\theta - \nu_2\tau + \varphi_2) \right] \tag{A3}$$

where J_n is the Bessel function of order n and $\kappa = k_2/k_1$ is the ratio of the two wavenumbers. In the new variables $(\tilde{I},\tilde{\theta})$ the dynamics is given by a new Hamiltonian $\tilde{H}$ that can also be expanded in power series in ε

$$\tilde{H} = \sum_{i=0}^{+\infty} \varepsilon^i \tilde{H}_i. \tag{A4}$$

It is clear that $\tilde{H}_0 = H_0$ because when $\varepsilon = 0$, $(\tilde{I},\tilde{\theta}) = (I,\theta)$.
Finally, we also expand the inverse transformation operator T^{-1} as a power series in ε

$$T^{-1} = \sum_{i=0}^{+\infty} \varepsilon^i T_i^{-1} \tag{A5}$$

where T_0^{-1} is the identity since for $\varepsilon = 0$ $(\tilde{I},\tilde{\theta}) = (I,\theta)$. For $i \geq 1$, it can be shown that T_i^{-1} is defined by the recursion relation

$$T_i^{-1} = \frac{1}{i} \sum_{j=0}^{i-1} L_{i-j} T_j^{-1} \tag{A6}$$

where $L_i = \{\chi_i, .\}$, and $\{.,.\}$ stands for the Poisson bracket.
One of the results of Deprit's method is the relation between the $\tilde{H}_i$'s, the H_i's, the χ_i's and the T_i^{-1}'s:

$$\frac{\partial \chi_i}{\partial \tau} + \{\chi_i, H_0\} = i(\tilde{H}_i - H_i) - \sum_{j=1}^{i-1} \left(L_{i-j}\tilde{H}_j + j T_{i-j}^{-1} H_j \right) \tag{A7}$$

This is a functional relation. In (A7) H and $\tilde{H}$ are functions of the same canonical variables. This is the main advantage of the Lie transform, to not involve mixed variables. Using the definition (A2) of H_0, (A7) becomes

$$\frac{\partial \chi_i}{\partial \tau} + \frac{\partial \chi_i}{\partial \theta} = i(\tilde{H}_i - H_i) - \sum_{j=1}^{i-1} \left(L_{i-j} \tilde{H}_j + j T_{i-j}^{-1} H_j \right) \tag{A8}$$

In (A8), $\tilde{H}_i$ is chosen so that no secularity appears in χ_i. Once $\tilde{H}_i$ is thus specified, (A8) is solved for χ_i.

At first order in perturbation theory (i=1), (A8) becomes

$$\begin{aligned} \frac{\partial \chi_1}{\partial \tau} + \frac{\partial \chi_1}{\partial \theta} = \tilde{H}_1 \; &- \sum_{n=-\infty}^{\infty} J_n(\rho) \cos(n\theta - \nu_1 \tau + \varphi_1) \\ &- \frac{1}{\kappa} \sum_{n=-\infty}^{\infty} J_n(\kappa\rho) \cos(n\theta - \nu_2 \tau + \varphi_2) \end{aligned} \tag{A9}$$

No term leads to secularities in χ_1 when neither ν_1 nor ν_2 are integers. Thus, we choose $\tilde{H}_1 = 0$. Then, the contribution of the first order to the generating Lie Hamiltonian is

$$\chi_1 = \sum_{m=-\infty}^{+\infty} \left[\frac{J_m(\tilde{\rho}) \cos(m\tilde{\theta} - \nu_1 \tau + \varphi_1)}{m - \nu_1} + \frac{J_m(\kappa\tilde{\rho}) \cos(m\tilde{\theta} - \nu_2 \tau + \varphi_2)}{\kappa(m - \nu_2)} \right] \tag{A10}$$

To second order, (A8) gives

$$\frac{\partial \chi_2}{\partial \tau} + \frac{\partial \chi_2}{\partial \theta} = 2(\tilde{H}_2 - H_2) - L_1(\tilde{H}_1 + H_1) \tag{A11}$$

Following the same kind of calculations as in[19] we can show that, in order to avoid secularities in χ_2, we have to choose

$$\begin{aligned} \tilde{H}_2 \; = \; & S_1(\tilde{\rho}) + S_2(\tilde{\rho}) + \delta_1 \cos[2\nu_1(\tilde{\theta} - \tau) + 2\varphi_1] S_3(\tilde{\rho}) \\ & + \delta_2 \cos[2\nu_2(\tilde{\theta} - \tau) + 2\varphi_2] S_4(\tilde{\rho}) \\ & + \delta_3 \cos[(\nu_1 + \nu_2)(\tilde{\theta} - \tau) + \varphi_1 + \varphi_2] S_5(\tilde{\rho}) \\ & + \delta_4 \cos[(\nu_1 - \nu_2)(\tilde{\theta} - \tau) + \varphi_1 - \varphi_2] S_6(\tilde{\rho}) \end{aligned} \tag{A12}$$

where δ_1, δ_2, δ_3, and δ_4, are unity respectively if $2\nu_1$, $2\nu_2$, $(\nu_1+\nu_2)$, and $(\nu_1-\nu_2)$ are integers, and zero otherwise, and

$$S_2(\tilde{\rho}) = \frac{1}{2\kappa\tilde{\rho}} \sum_{m=-\infty}^{+\infty} \frac{m J_m(\kappa\tilde{\rho}) J'_m(\kappa\tilde{\rho})}{\nu_2 - m} \tag{A13}$$

$$S_4(\tilde{\rho}) = \frac{1}{2\kappa\tilde{\rho}} \sum_{m=-\infty}^{+\infty} \frac{m J_m(\kappa\tilde{\rho}) J'_{2\nu_2 - m}(\kappa\tilde{\rho})}{\nu_2 - m} \tag{A14}$$

$$S_5(\tilde{\rho}) = \frac{1}{2\tilde{\rho}} \sum_{m=-\infty}^{+\infty} \frac{m J_m(\tilde{\rho}) J'_{\nu_1+\nu_2-m}(\kappa\tilde{\rho})}{\nu_1 - m} + \frac{1}{2\kappa\tilde{\rho}} \sum_{m=-\infty}^{+\infty} \frac{m J_m(\kappa\tilde{\rho}) J'_{\nu_1+\nu_2-m}(\tilde{\rho})}{\nu_2 - m} \tag{A15}$$

$$S_6(\tilde{\rho}) = \frac{1}{2\tilde{\rho}} \sum_{m=-\infty}^{+\infty} \frac{m J_m(\tilde{\rho}) J'_{\nu_2-\nu_1+m}(\kappa\tilde{\rho})}{\nu_1 - m} + \frac{1}{2\kappa\tilde{\rho}} \sum_{m=-\infty}^{+\infty} \frac{m J_m(\kappa\tilde{\rho}) J'_{\nu_1-\nu_2+m}(\tilde{\rho})}{\nu_2 - m} \tag{A16}$$

where the prime denotes the derivative with respect to the argument of the Bessel function. S_1 and S_3 are deduced from S_2 and S_4 by changing ν_2 into ν_1 and by setting $\kappa = 1$. The sums in S_2 and S_4 (and thus the sums S_1 and S_3) can be carried out analytically, following the same kind of method as the one developed in[19]:

$$S_2(\tilde{\rho}) = \frac{\pi}{8\kappa \sin(\pi\nu_2)}[J_{\nu_2+1}(\kappa\tilde{\rho})J_{-\nu_2-1}(\kappa\tilde{\rho}) - J_{\nu_2-1}(\kappa\tilde{\rho})J_{-\nu_2+1}(\kappa\tilde{\rho})] \quad \text{(A17)}$$

$$S_4(\tilde{\rho}) = \frac{\pi\cot(\pi\nu_2)}{8\kappa}[J^2_{\nu_2-1}(\kappa\tilde{\rho}) - J^2_{\nu_2+1}(\kappa\tilde{\rho})] + \frac{1}{4k^3\tilde{\rho}^2}\int_0^{2\kappa\tilde{\rho}} \rho J_{2\nu_2}(\rho)d\rho \quad \text{(A18)}$$

In the case when $\kappa = 1$, the sums in S_5 and S_6 can also be carried out analytically

$$\kappa = 1;\ S_5(\tilde{\rho}) = \frac{\pi\cot(\pi\nu_1)}{4}[J_{\nu_2-1}(\tilde{\rho})J_{\nu_1-1}(\tilde{\rho}) - J_{\nu_2+1}(\tilde{\rho})J_{\nu_1+1}(\tilde{\rho})] + \int_0^{\pi/2} J_{\nu_1+\nu_2}(2\tilde{\rho}\cos\theta)\sin(2\theta)\cos(\nu_1-\nu_2)\theta\ d\theta \quad \text{(A19)}$$

$$\kappa = 1, (\nu_1 - \nu_2) \in \mathcal{N};\ S_6(\tilde{\rho}) = \frac{\pi[J_{-\nu_2-1}(\tilde{\rho})J_{\nu_1+1}(\tilde{\rho}) - J_{-\nu_2+1}(\tilde{\rho})J_{\nu_1-1}(\tilde{\rho})]}{4\sin(\pi\nu_2)} \quad \text{(A20)}$$

Hence, up to second order in the waves amplitudes, the Hamiltonian (2) is changed into

$$\begin{aligned}\tilde{H} = {} & \tilde{I} + \varepsilon^2 S_1(\tilde{\rho}) + \varepsilon^2 S_2(\tilde{\rho}) + \varepsilon^2\delta_1\cos[2\nu_1(\tilde{\theta}-\tau) + 2\varphi_1]S_3(\tilde{\rho}) \\ & + \varepsilon^2\delta_2\cos[2\nu_2(\tilde{\theta}-\tau) + 2\varphi_2]S_4(\tilde{\rho}) \\ & + \varepsilon^2\delta_3\cos[(\nu_1+\nu_2)(\tilde{\theta}-\tau) + \varphi_1 + \varphi_2]S_5(\tilde{\rho}) \\ & + \varepsilon^2\delta_4\cos[(\nu_1-\nu_2)(\tilde{\theta}-\tau) + \varphi_1 - \varphi_2]S_6(\tilde{\rho}) \end{aligned} \quad \text{(A21)}$$

When the calculation developed in this appendix is generalized to the case when the waves amplitudes are not all the same, one obtains the Hamiltonian (6).

APPENDIX B

In this appendix we show that the term resulting from the non-linear interaction of two waves may have to be taken into account when deriving the Hamiltonian obtained after perturbation theory, even though the difference between the normalized wave frequencies is not an exact integer. Moreover, we show that the maximum departure from an integer allowed to make this non-linear interaction non-perturbative, scales as the product of the two waves amplitudes. For the sake of simplicity we make all the calculations in the case when there are only two waves having the same amplitudes in (2), and then generalize the results thus obtained. Let us denote the difference between the two normalized wave frequencies

$$\nu_1 - \nu_2 = n + \delta\nu \quad \text{(B1)}$$

where n is an integer and $\delta\nu$ is a small non-zero quantity. In order to find the maximum value of $\delta\nu$ that makes the result of the non-linear interaction between the two waves be non-negligible, one has to investigate the domain of validity of the calculation performed in the sections 4.1 and 4.2. Actually, whatever the value of ν_1 and ν_2, one can always

define a canonical change of variables which, up to second order in the waves amplitudes, transforms the Hamiltonian (2) into the Hamiltonians (6) or (16). Nevertheless, when $\delta\nu$ goes to zero, while remaining different from zero, the dynamics defined by $\tilde{H}_2^{(on)}$ or $\tilde{H}_2^{(off)}$ become irrelevant to describe the dynamics ruled by H.

One of the reasons why this is so is that when $\delta\nu$ is too small, the change of variables performed to get from H to $\tilde{H}_2^{(on)}$ or $\tilde{H}_2^{(off)}$ is no longer one-to-one. Consequently, an orbit of $\tilde{H}_2^{(on)}$ or $\tilde{H}_2^{(off)}$, calculated in the transformed variables $(\tilde{\theta}, \tilde{\rho})$, does not give any useful information on an orbit of H, i.e. in the original variables (θ, ρ), as making the inverse transform $(\tilde{\theta}, \tilde{\rho}) \to (\theta, \rho)$ would lead to some unphysical results like an orbit crossing itself in phase space.

Another reason why $\tilde{H}_2^{(on)}$ or $\tilde{H}_2^{(off)}$ become irrelevant when $\delta\nu \to 0$ is that they were derived by neglecting the terms of the perturbation series which are of order higher than 2. However, the amplitudes of those terms increase when $\delta\nu$ decreases while the amplitudes of $\tilde{H}_2^{(on)}$ and $\tilde{H}_2^{(off)}$ remain constant. Hence, when $\delta\nu$ is too small, the second order term is no longer a good approximation of the perturbation series. Moreover the amplitudes of the neglected terms increase all the more as their order is high. Hence, when $\delta\nu$ is too small, the perturbation series may not converge.

We are now going to develop all the previous points, and show that they all lead to a $\delta\nu$ scaling as $\varepsilon_1\varepsilon_2$.

1. One-to-one character of the change of variables:

In this subsection, we calculate the minimum value of $\delta\nu$ such that the change of variables defined to go from the Hamiltonian (2) to the Hamiltonians (6) or (16) would be one-to-one. This yields an upper bound of the maximal value of $\delta\nu$ making the result of the non-linear interaction of the two waves non-negligible. Such a method, based on the one-to-one character of a canonical change of variables, has already been used in[20] to estimate the threshold for the destruction of a KAM torus. A similar method has also proven in[21] to give the good scaling, with the wave amplitudes, of the range of interaction in phase velocities of a particle with an electrostatic wave spectrum, in an unmagnetized plasma.

Let us denote χ the Hamiltonian of the Lie transform. If we only go up to second order, then $\chi = \varepsilon\chi_1 + \varepsilon^2\chi_2$, and the new variables are related to the old ones through

$$\tilde{I} = I - \varepsilon\frac{\partial\chi_1}{\partial\theta} - \frac{\varepsilon^2}{2}\frac{\partial\chi_2}{\partial\theta} + \frac{\varepsilon^2}{2}\left(\frac{\partial\chi_1}{\partial\theta}\frac{\partial^2\chi_1}{\partial\theta\partial I} - \frac{\partial\chi_1}{\partial I}\frac{\partial^2\chi_1}{\partial\theta^2}\right) \tag{B2}$$

$$\tilde{\theta} = \theta + \varepsilon\frac{\partial\chi_1}{\partial I} + \frac{\varepsilon^2}{2}\frac{\partial\chi_2}{\partial I} + \frac{\varepsilon^2}{2}\left(\frac{\partial\chi_1}{\partial I}\frac{\partial^2\chi_1}{\partial\theta\partial I} - \frac{\partial\chi_1}{\partial\theta}\frac{\partial^2\chi_1}{\partial I^2}\right) \tag{B3}$$

χ_1 is defined by

$$\chi_1 = \sum_{m\in\mathcal{N}_1} \frac{J_{m_1}(\tilde{\rho})\cos(m\theta - \nu_1\tau)}{\nu_1 - m} + \sum_{m\in\mathcal{N}_2} \frac{J_{m_1}(\tilde{\rho})\cos(m\theta - \nu_2\tau)}{\nu_2 - m} \tag{B4}$$

where $\mathcal{N}_1 = \mathcal{N}$ if ν_1 is not an integer, $\mathcal{N}_1 = \mathcal{N}\backslash\{\nu_1\}$ if ν_1 is an integer, and a similar definition holds for $\mathcal{N}_2$. Hence, when $\delta\nu \to 0$, i.e. when $\nu_1 - \nu_2$ gets closer and closer to an integer, χ_1

remains bounded, while, as we are going to show it, χ_2 diverges. Therefore, when $\delta\nu << 1$, the terms involving χ_1 in (B2) and (B3) can be ignored. In this case, demanding that $\partial\tilde{I}/\partial I$ and $\partial\tilde{\theta}/\partial\theta$ have a constant sign amounts to the same condition

$$\frac{\varepsilon^2}{2}\left|\frac{\partial^2\chi_2}{\partial I\partial\theta}\right| \leq 1 \tag{B5}$$

χ_2 is calculated through the differential equation

$$\frac{\partial\chi_2}{\partial\tau} + \frac{\partial\chi_2}{\partial\theta} = 2\tilde{H}_2 - \{\chi_1, \tilde{H}_1\} - \{\chi_1, H_1\} \tag{B6}$$

where $\{.,.\}$ denotes the Poisson bracket. We consider here only the case where neither ν_1 nor ν_2 are integer. In this case $\tilde{H}_1 = 0$. Even if ν_1 or ν_2 were an integer, the term $\{\chi_1, \tilde{H}_1\}$ would remain bounded when $\delta\nu \to 0$ and thus would be negligible in (B5) when $\delta\nu << 1$. We only consider here the case when $2\nu_1$, $2\nu_2$ and $\nu_1 + \nu_2$ are far away from integers, i.e. that they differ from an integer by an amount larger than $\delta\nu$. We really focus on the case when $\nu_1 - \nu_2$ is close to an integer because we showed in sections 4.2. and 4.3. that it is the only case where there can be acceleration. If $\nu_1 - \nu_2$ is an integer, the terms that give rise to secularities in χ_2 are $2\tilde{H}_2$, as calculated in the appendix A. Therefore, if $\nu_1 - \nu_2 = n + \delta\nu$, it is clear that when $\delta\nu << 1$, the terms that make χ_2 diverge are the ones which appear in $2\tilde{H}_2$ when $\delta\nu = 0$. Namely, when $\delta\nu << 1$

$$\begin{aligned}
\frac{2\tilde{H}_2 - \{\chi_1, H_1\}}{\cos[n\theta - (n+\delta\nu)\tau]} &= \frac{1}{2\tilde{\rho}}\sum_{m=-\infty}^{+\infty} mJ_m(\tilde{\rho})J'_{m-n}(\kappa\tilde{\rho})\left(\frac{1}{\nu_1 - m} + \frac{1}{\nu_1 - \delta\nu - m}\right) \\
&\quad + \frac{1}{2\kappa\tilde{\rho}}\sum_{m=-\infty}^{+\infty} mJ_m(\kappa\tilde{\rho})J'_{m+n}(\tilde{\rho})\left(\frac{1}{\nu_2 - m} + \frac{1}{\nu_2 + \delta\nu - n}\right) \\
&\simeq \frac{1}{\tilde{\rho}}\sum_{m=-\infty}^{+\infty}\frac{mJ_m(\tilde{\rho})J'_{m-n}(\kappa\tilde{\rho})}{\nu_1 - m} \\
&\quad + \frac{1}{\kappa\tilde{\rho}}\sum_{m=-\infty}^{+\infty}\frac{mJ_m(\kappa\tilde{\rho})J'_{m+n}(\tilde{\rho})}{\nu_2 - m} \\
&\simeq 2S_6(\tilde{\rho})
\end{aligned} \tag{B7}$$

From (B6) and (B7) one easily finds

$$\chi_2 \simeq \frac{2S_6(\tilde{\rho})}{\delta\nu}\sin[n\theta - (n+\delta\nu)\tau] \tag{B8}$$

so that Eq. (B5) now writes

$$\frac{n\varepsilon^2}{\tilde{\rho}}\left|\frac{dS_6(\tilde{\rho})}{d\tilde{\rho}}\frac{\cos[n\theta - (n+\delta\nu)\tau]}{\delta\nu}\right| \leq 1 \tag{B9}$$

This condition is fulfilled whatever θ and τ if

$$|\delta\nu| \geq \frac{n\varepsilon^2}{\tilde{\rho}}\frac{dS_6(\tilde{\rho})}{d\tilde{\rho}} \tag{B10}$$

Hence, the right hand side of (B10) gives an estimate of the maximum value of $\delta\nu$ that makes the non-linear interaction of the two waves be non-negligible, based on the one-to-one character of the change of variables.

Let us now consider a more general situation where there are more than two waves in (2) and where the waves do not all have the same amplitudes. In this case we consider a given pair of frequencies (ν_l, ν_m) and still denote $\nu_l - \nu_m = n + \delta\nu$. If we evaluate χ_2 when $\delta\nu \to 0$ then we only have to consider the terms involving the non-linear interaction of the waves l and m. Hence we are back to a problem similar to the two-waves case. Therefore, (B5) remains valid. The terms involving the non-linear interaction of the waves l and m are proportional to the product of the amplitudes of these two waves. Hence, in the general case, ε^2 has to be replaced by $\varepsilon_l\varepsilon_m$ in (B10), which implies in turn that $\delta\nu$ scales as $\varepsilon_l\varepsilon_m$.

2. Estimate of the high order terms of the perturbation series:

Let us now come back to the case of two waves having the same amplitudes and let us evaluate the amplitudes of the high order terms of the perturbation series when the condition

$$l_1\nu_1 + l_2\nu_2 + l_3 \neq 0 \tag{B11}$$

$(l_1, l_2, l_3) \in \mathcal{Z}^3$, is satisfied, where $\mathcal{Z}$ is the set of the relative integers. The condition (B11) corresponds to the most general case. We show here that when $\delta\nu$ goes to zero, while being different from zero:

$$\tilde{H}_{2p+1} = 0 \tag{B12}$$

$$\tilde{H}_{2p+2} \sim \frac{h_{2p+2}(\tilde{\rho})}{\delta\nu^p} \tag{B13}$$

$$\chi_{2p+2} \sim \frac{\xi_{2p+2}(\tilde{\theta}, \tilde{\rho})}{\delta_\nu^{p+1}} \tag{B14}$$

$$\chi_{2p+1} \sim \frac{\xi_{2p+1}(\tilde{\theta}, \tilde{\rho})}{\delta_\nu^{p}} \tag{B15}$$

where h_p and ξ_p are functions that we will not try to calculate. The $\tilde{H}_i$'s and χ_i's are obtained via the differential equation

$$\frac{\partial\chi_i}{\partial\tau} + \frac{\partial\chi_i}{\partial\tilde{\theta}} - i\tilde{H}_i = \sum_{j=1}^{i-1}\{\chi_{i-j}, \tilde{H}_j\} - T_{i-1}^{-1}H_1 \tag{B16}$$

In particular, $i\tilde{H}_i$ is just the opposite of the sum of the terms of the right hand side of (B16) giving rise to secularities in χ_i. All the terms of the right-hand side of (B16) are the result of the i-linear interaction of the terms present in the Hamiltonian (2). Hence they contain products of i factors of the form $\cos(m\tilde{\theta} - \nu_1\tau + \varphi_1)$ or $\cos(m\tilde{\theta} - \nu_2\tau + \varphi_2)$. This implies that they will depend on $\tilde{\theta}$ and τ through terms of the form $\cos[\sum_{j=1}^{i}\varepsilon_j(m_j\tilde{\theta} - \nu_j\tau + \varphi_j)]$, where $\varepsilon_j = \pm 1$, $m_j \in \mathcal{Z}$, $\nu_j = \nu_{1,2}$, and $\varphi_i = \varphi_{1,2}$. These terms yield secularities in χ_i if

$$\sum_{j=1}^{i}\varepsilon_j(m_j - \nu_j) = 0 \tag{B17}$$

It is clear that when i is odd, and when (B11) is satisfied, (B17) can never be fulfilled. Consequently, $\tilde{H}_{2p+1} = 0$, which proves (B12).

When i is even, because of (B11), (B17) is fulfilled if and only if $\sum_{j=1}^{i} \varepsilon_j \nu_j = \sum_{j=1}^{i} \varepsilon_j m_j = 0$, which occurs when $\sum_{j=1}^{i} \varepsilon_j = 0$ and when all the ν_j's are the same. Hence, the $\tilde{H}_{2p}$'s only depend on $\tilde{\rho}$.

Let us now prove (B13), (B14) and (B15) by induction. The calculation of $\tilde{\chi}_1$, $\tilde{H}_2$, and $\tilde{\chi}_2$ already proved that these equations are true for $p = 0$. Let us suppose that they are true up to a given order p. Then, for any even j such that $1 \leq j \leq 2i+3$, $\{\chi_{2p+4-j}, \tilde{H}_j\} \sim \{\xi_{2p+4-j}(\tilde{\theta}, \tilde{\rho}), h_j(\tilde{\rho})\}/\delta\nu^{p+1}$, while if j is odd $\{\chi_{2p+2-j}, \tilde{H}_j\} = 0$. Moreover, $T_{2p+3}^{-1} H_1$ writes as a sum of Poisson brackets of the form:
$\{\chi_{m_1}, \{\chi_{m_2}, ..., \{\chi_{m_l}, H_1\}, ...\}$, where $\sum_{j=1}^{l} m_j = 2p+3$, and each m_j is larger than 1. Using (B14) and (B15) it is easy to show that such a Poisson bracket scales as $1/\delta\nu^{\alpha}$, with $0 \leq \alpha \leq p+1$, and $\alpha = p+1$ when only one of the m_j's is odd. Hence, when $\delta\nu \to 0$, $T_{2p+3}^{-1} H_1$ scales as $1/\delta\nu^{p+1}$. Therefore, the right hand side of (B16), when $i = 2p+4$, scales as $1/\delta\nu^{p+1}$. Similarly, when $i = 2p+3$ in (B16), the right hand side of this equation also scales as $1/\delta\nu^{p+1}$. As $(2p+4)\tilde{H}_{2p+4}$ is only the opposite of the sum of the terms of the right hand side of (B16) that could give rise to secularities in χ_{2p+4}, and as we already showed that $\tilde{H}_{2p+4}$ only depends on $\tilde{\rho}$, we readily deduce (B13).

As already mentioned, the right hand side of (B16) depends on $\tilde{\theta}$ and τ through terms of the form $\cos[\sum_{j=1}^{i} \varepsilon_j (m_j \tilde{\theta} - \nu_j \tau + \varphi_j)]$. When i is even, when half of the ν_j's are such that $\nu_j = \nu_1$, and when there is the same number of ε_j's such that $\varepsilon_j = +1$ and $\nu_j = \nu_1$ as the number of ε_j's such that $\varepsilon_j = -1$ and $\nu_j = \nu_2$, then $\sum_{j=1}^{i} \varepsilon_j \nu_j = \sum_{j=1}^{i/2} \varepsilon_j (\nu_1 - \nu_2) = \sum_{j=1}^{i} \varepsilon_j (n + \delta\nu)$. When, moreover, the m_j's are such that $\sum_{j=1}^{i} \varepsilon_j m_j = \sum_{j=1}^{i/2} \varepsilon_j n$, then $\cos[\sum_{j=1}^{i} \varepsilon_j (m_j \tilde{\theta} - \nu_j \tau + \varphi_j)] = \cos\left[\sum_{j=1}^{i/2} \varepsilon_j n(\tilde{\theta} - \tau + \varphi_j) - \sum_{j=1}^{i/2} \varepsilon_j \delta\nu\tau\right]$. When solving for χ_i, such a cosine yields in χ_i the term
$-\sin\left[\sum_{j=1}^{i/2} n(\tilde{\theta} - \tau + \varphi_j) - \sum_{j=1}^{i/2} \delta\nu\tau\right] / \sum_{j=1}^{i/2} \varepsilon_j \delta\nu$. Therefore, if $i = 2p+4$, as the right hand side of (B16) scales as $1/\delta\nu^{p+1}$, χ_{2p+4} scales as $1/\delta\nu^{p+2}$, which proves (B14).

If i is odd, then when solving (B16) for χ_i, each $\cos[\sum_{j=1}^{i} \varepsilon_j (m_j \tilde{\theta} - \nu_j \tau + \varphi_j)]$ yields $\sin[\sum_{j=1}^{i} \varepsilon_j (m_j \tilde{\theta} - \nu_j \tau + \varphi_j)] / \sum_{j=1}^{i} \varepsilon_j (m_j - \nu_j)$ which has no singularity when $\delta\nu \to 0$. Therefore, χ_{2p+3} scales with $\delta\nu$ exactly as the right hand side of (B16), i.e. as $1/\delta\nu^{p+1}$, which proves (B15).

Therefore, the perturbation series for $\tilde{H}$ writes

$$\tilde{H} \sim \delta\nu \sum_{i=1}^{+\infty} \left(\frac{\varepsilon^2}{\delta\nu}\right)^i h_{2i}(\tilde{\rho}) \tag{B18}$$

It is clear from (B18) that when $\delta\nu \to 0$, $\tilde{H}$ can no longer be approximated by $\varepsilon^2 \tilde{H}_2$. It is also clear from (B18) that the maximum value of $\delta\nu$ requiring the inclusion of high order terms in the evaluation of $\tilde{H}$ scales as ε^2. In fact, demanding that $\varepsilon^2 \tilde{H}_2$ would be larger than a finite number of the following terms of the perturbation series would give the following condition on $\delta\nu$

$$\delta\nu \geq \varepsilon^2 F(\tilde{\rho}) \tag{B19}$$

where $F(\tilde{\rho})$ is the sum of the corresponding h_{2i}'s. This condition is similar to (B10).

Actually, if the radius of convergence $R(\tilde{\rho})$ of (B18) is finite, then this series diverges when $\delta\nu$ is too small. In this case, a perturbation analysis cannot give any indication on the dynamics defined by (2). In particular, the Hamiltonians (6) or (16) do not give a good approximation of the dynamics of the Hamiltonian (2). The series (B18) is convergent if

$$\delta\nu \geq \varepsilon^2/R(\tilde{\rho}) \tag{B20}$$

which is of the form (B10) or (B19).

Let us note here that if the condition (B11) is not fulfilled, then it can be proven in a similar way as for the evaluation of $\tilde{H}_{2p}$ that $\tilde{H}_{2p+1} \sim h_{2p+1}(\tilde{\theta},\tilde{\rho})/\delta\nu^p$. Therefore, if the condition (B11) is not fulfilled, the perturbation series writes

$$\tilde{H} = \delta\nu \sum_{j=1}^{+\infty} \left(\frac{\varepsilon^2}{\delta\nu}\right)^j h_{2j}(\tilde{\theta},\tilde{\rho}) + \varepsilon \sum_{j=0}^{+\infty} \left(\frac{\varepsilon^2}{\delta\nu}\right)^j h_{2j+1}(\tilde{\theta},\tilde{\rho}) \tag{B21}$$

and can thus be seen as a sum of 2 series. If these series have 2 different radii of convergence, R_1 and R_2, then the perturbation series converges only if $\delta\nu \geq \varepsilon^2/R$ where $R = \min(R_1, R_2)$. Hence, the scaling ε^2 is still valid.

Let us now consider the more general case when there are more than two waves in (2) and when the waves do not all have the same amplitude. If we consider a given pair of frequencies (ν_l, ν_m) and denote $\nu_l - \nu_m = n + \delta\nu$, then, when deriving the high order terms of the perturbation series in the limit when $\delta\nu \to 0$, one only has to take into account the non-linear interaction of the waves l and m. Hence, as in the section 1 of this appendix, one finds that in the general case ε^2 has to be replaced by $\varepsilon_l\varepsilon_m$ in (B21). Hence, once again, we find that the maximum value of $\delta\nu$ scales as $\varepsilon_l\varepsilon_m$.

REFERENCES

[1] C.F.F. Karney and A. Bers, Phys. Rev. Lett., **39**, 550, (1977).
[2] C.F.F. Karney, Phys. Fluids, **21**, 1584, (1978).
[3] C.F.F. Karney, Phys. Fluids, **22**, 2188, (1979).
[4] A. Fukuyama, H. Momota, R. I. Tatani, and T. Takizuka, Phys. Rev. Lett., **38**, 701, (1977).
[5] S. Riyopolous, Phys. Fluids, **28**, 1097 (1985).
[6] H.Pacher, C. Gormezano, W. Hess, G. Ichtchenko, R. Magne, T.-K. Nguyen, G.W. Pacher, F. Söldner, G. Tonon and J.-G. Wegrowe, in *heating in toroidal plasmas*, proceedings of the 2nd Joint Grenoble-Varenna international symposium. Ed. E. Canobbio, H.P. Eubank, G.G. Leotta, A. Malein and E. Sindoni, p.329 (1980).
[7] J.J. Schuss, T.M. Antonsen, Jr., and M. Porkolab, *Nucl. Fusion* **23**, 201 (1983).
[8] F. Skiff, F. Anderegg, and M.Q. Tran, *Phys. Rev. Lett.,* **58**, 1430 (1987).
[9] A.K. Ram, A. Bers, and D. Benisti, to be published in the Journal of Geophysical Research; presented at the 1997 Conference on the Interrelationship Between Experiments in Laboratory and Space Plasmas, Maui, Hawaii, June 1997.
[10] J.L. Vago, P.M. Kintner, S. Chesney, R.L. Arnoldy, K.A. Lynch, T.E. Moore, and C.J. Pollock, J. *Geophys. Res.*, **97**, 16935 (1992).
[11] D. Bénisti, A.K. Ram and A. Bers, accepted for publication in Phys. Lett. A (1997).
[12] After the completion of this work we became aware of the following paper: M. Temerin and I. Roth, *Geophys. Res. Lett.*, **13**, 1109 (1986). This paper deals with multiple waves below the ion-cyclotron frequency in contrast to our study which considers mainly waves above the ion-cyclotron frequency.
[13] G.M. Zaslavsky, R.Z. Sagdeev, D.A. Usikov, and A.A. Chernikov, *Weak Chaos and Quasi-Regular Patterns*, (Cambridge University Press, 1991).
[14] S. Murakami, T. Sato, and A. Hasegawa Physica D **32** 269 (1988)
[15] G. Schmidt Comments Plasma Phys. Controlled Fusion Vol. 13, No. 2, 77-84 (1989)
[16] A. Bers, A.K. Ram, and D. Benisti, to be published.
[17] J. Cary, Phys. Rep., **79**, 129, (1981).
[18] A. Deprit, Celest. Mech., **1**, 12, (1969).
[19] Ping-Kun Chia, L. Schmitz, and R.W. Conn, Phys. Plasmas, **3**, 1545, (1996)
[20] D.F. Escande and F. Doveil in "Proceedings of the International Conference on Plasma Physics", Fusion Associaton of Japan, Nagoya, **1**, 387, (1980)
[21] D. Bénisti, Ph.D. thesis, Université de Provence, Marseille, 1995.

FIGURE CAPTIONS

Fig. 1: Poincaré section of the dynamics defined by the Hamiltonian (2) for the case of one off-resonance wave, $\nu = 9.25$, $\varepsilon = 3.42$, and 2 initial conditions: $I(0) = 4.125$, $\theta(0) = 0.94\pi$, and $I(0) = 32$ and $\theta(0) = 0.94\pi$. The total time of integration corresponds to 8000 cyclotron periods.

Fig. 2: Poincaré section of the dynamics defined by the Hamiltonian (2) for the case of one on-resonance wave, $\nu = 9$, $\varepsilon = 3.24$, and for the same initial conditions and the same time of integration as for Fig. 1.

Fig. 3: Poincaré section of the dynamics defined by the Hamiltonian (2) in the case of two on-resonance waves, $\nu_1 = 140$, $\nu_2 = 139$, $\varepsilon_1 = \varepsilon_2 = 98$. The initial condition is $\rho(0) = 69, \theta(0) = \pi/2$.

Fig. 4: Orbit obtained from second order perturbation theory for the same parameters as in Fig. 3.

Fig. 5: Position of the first zero of the 7^{th} order Taylor series expansion of $S_6(\tilde{\rho})$ as a function of κ when $Int(\nu_1) = 140$ and $\nu_2 = \nu_1 - 1$.

Fig. 6: Maximum and minimum values of the normalized Larmor radius of the orbits of $\tilde{H}^{(off)}$, for the initial condition $\tilde{\rho}_0 = 53$, $\tilde{\Phi}_0 = 1.57$, versus κ for two waves such that $Int(\nu_1) = 140$ and $\nu_2 = \nu_1 - 1$.

Fig. 7: Maximum and minimum values of the normalized Larmor radius of the orbits of $\tilde{H}^{off}$, for the initial condition $\tilde{\rho}_0 = 5$, $\tilde{\Phi}_0 = 1$, versus κ for two waves such that $Int(\nu_1) = 140$ and $\nu_2 = \nu_1 - 1$.

Fig. 8: Maximum values of the normalized Larmor radius of the orbits of $\tilde{H}_2^{(off)}$, for the initial condition $\tilde{\rho}_0 = 10$, $\tilde{\Phi}_0 = 0.4$, versus κ, for two waves such that $Int(\nu_1) = 140$ and $\nu_2 = \nu_1 - 2$ (solid line) and $Int(\nu_1) = 140$ and $\nu_2 = \nu_1 - 1$ (dashed line).

Fig. 9: Maximum values of the normalized Larmor radius of the orbits of $\tilde{H}_2^{(off)}$, for the initial condition $\tilde{\rho}_0 = 80$, $\tilde{\Phi}_0 = 0.4$, versus κ, for two waves such that $Int(\nu_1) = 140$ and $\nu_2 = \nu_1 - 10$.

Fig. 10: Maximum values of the normalized Larmor radius of the orbits of $\tilde{H}_2^{(off)}$, for the initial condition $\tilde{\rho}_0 = 20$, $\tilde{\Phi}_0 = 0.4$, versus κ, for two waves such that $Int(\nu_1) = 140$ and $\nu_2 = \nu_1 - 10$.

Fig. 11: Maximum values of the normalized Larmor radius of the orbits of $\tilde{H}_2^{(on)}$, for the initial condition $\tilde{\rho}_0 = 50$ $\tilde{\Phi}_0 = \pi/2$, versus κ, for two waves such that $n_1 = 140$ and $n_2 = 139$ and $\varepsilon_1 = \varepsilon_2 = 15$.

Fig. 12: Poincaré section of the dynamics defined by (2) for six waves with frequencies such that $\nu_1 = 30$, $\nu_2 = 29$, $\nu_3 = 31.75$, $\nu_4 = 31.25$, $\nu_5 = 30.5$, $\nu_6 = 29.25$; the normalized wavenumbers are $\kappa_1 = 1$, $\kappa_2 = 0.98$, $\kappa_3 = 1$, $\kappa_4 = 1$, $\kappa_5 = 1$, $\kappa_6 = 0.98$. All the waves have the same amplitude $\varepsilon = 4.5$, and all have a zero initial phase: $\varphi_i = 0$. The initial condition is $\rho_0 = 5$, $\Phi_0 = \pi/2$.

Fig. 13: Orbit obtained from second order perturbation theory for the same parameters as in Fig. 12.

Fig. 14: Orbit obtained from second order perturbation theory for the same parameters as in Fig. 12 and 13, but with initial random phases.

Fig. 15: Maximum and minimum values of the normalized Larmor radius of the orbits of $\tilde{H}$ for the initial condition $\tilde{\rho}_0 = 10$, $\tilde{\Phi}_0 = 0.2$, versus k_2/k_1 for five waves such that $\nu_1 = 141$ and $\nu_2 = 140$, $\nu_3 = 139$, $\nu_4 = 143.5$, $\nu_5 = 140.5$, having all the same amplitudes and the same initial phases.

Fig. 16: Maximum and minimum values of the normalized Larmor radius of the orbits of $\tilde{H}$ for the initial condition $\tilde{\rho}_0 = 10$, $\tilde{\Phi}_0 = 0.2$, versus k_2/k_1 for six waves such that $\nu_1 = 141$ and $\nu_2 = 140$, $\nu_3 = 140.5$, $\nu_4 = 138.5$, $\nu_5 = 143.2$, $\nu_6 = 140.2$, having all the same amplitudes while the initial phases are chosen randomly.

Fig. 17: Poincaré section of the dynamics defined by the Hamiltonian (2) for the case of two on-resonance waves, $\nu_1 = 9$, $\nu_2 = 10$, $\varepsilon_1 = \varepsilon_2 = 3.24$, $\kappa = 1$. The initial condition is $I(0) = 32$ and $\theta(0) = 0.94\pi$. The total time of integration corresponds to 8000 cyclotron periods.

Fig. 18: Same as Fig. 17 except for the wave amplitudes: $\varepsilon_1 = \varepsilon_2 = 0.324$.

Fig. 19: Orbit solution of $\tilde{H} = const$ for the same parameters as in Fig. 18.

Fig. 20: Same as Fig. 1 but for an amplitude corresponding to $\varepsilon = 0.346$ and only one initial condition: $I(0) = 32$ and $\theta(0) = 0.94\pi$.

Fig. 21: Solution of $\tilde{H} = const$ for different initial phase conditions, when the constant is the same as in Fig. 19.

Fig. 22: Same as Fig. 17 and 18 but for $\varepsilon_1 = \varepsilon_2 = 32.4$.

Fig. 23: Same as Fig. 20 but for $\varepsilon = 34.6$.

Fig. 24: Orbit solutions for $\tilde{H} = const$ for two waves having the same amplitude and wavenumbers, and with $n_1 = 9$, $n_2 = 11$. The constant corresponds to an initial condition such that $I(0) = 32$ and $\Phi(0) = 0.2$.

Fig. 25: Poincaré section of the dynamics defined by (2) in the case of two waves such that $n_1 = 9$, $n_2 = 11$, $\varepsilon_1 = \varepsilon_2 = 0.324$, and having the same wavenumbers. The initial condition corresponds to $I(0) = 32$ and $\theta_0 = .4\pi$. The time of integration corresponds to 8000 cyclotron periods.

Fig. 26: Same as Fig. 25 but for $\varepsilon_1 = \varepsilon_2 = 3.24$.

Fig. 27: Solution of $\tilde{H} = C$ for two on-resonance waves such that $n_1 = 9$, $n_2 = 10$, $\varepsilon_1 = \varepsilon_2 = 3.24$, $k_1 = 1$ and $k_2 = 0.9$. The constant C corresponds to an initial condition such that $I(0) = 32$ and $\Phi(0) = 0.94\pi$.

Fig. 28: Poincaré section of the dynamics defined by (2) for two on-resonance waves having the same characteristics as in Fig. 27, and for the same initial condition as in Fig. 27.

Fig. 29: Solution of $\tilde{H} = const$ for two on-resonance waves such that $n_1 = 9$, $n_2 = 10$, $\varepsilon_1 = \varepsilon_2 = 3.24$, $k_1 = 1$ and $k_2 = 1/\sqrt{2}$. The constant corresponds to an initial condition such that $I(0) = 32$ and $\Phi(0) = 0.94\pi$.

Fig. 30: Poincaré section of the dynamics defined by (2) for two on-resonance waves having the same characteristics as in Fig. 29, and for the same initial condition as in Fig. 29.

Fig. 31: Poincaré section of the dynamics defined by (2) for two on-resonance waves such that $n_1 = 9$, $n_2 = 10$, $\varepsilon_1 = \varepsilon_2 = 3.24$, $k_1 = 1$ and $k_2 = 0.85$. The initial condition is $I(0) = 32$ and $\Phi(0) = 0$.

Fig. 32: Solution of $\tilde{H} = const$ for four on-resonance waves such that $n_1 = 9$, $n_2 = 10$, $n_3 = 11$, $n_4 = 12$, $\varepsilon_1 = 3.24$, $\varepsilon_2 = 3.078$, $\varepsilon_3 = 3.321$, $\varepsilon_4 = 3.159$, $k_1 = 1$ and $k_2 = 0.95$, $k_3 = 1.02$, $k_4 = 0.98$. The constant corresponds to an initial condition such that $I(0) = 32$ and $\Phi(0) = 0.94\pi$.

Fig. 33: Poincaré section of the dynamics defined by (2) for the same parameters as in Fig. 32.

Fig. 34: Poincaré section of the dynamics defined by (2) for four waves such that $n_1 = 9$, $n_2 = 10$, $n_3 = 11$, $n_4 = 12$, $\varepsilon_1 = \varepsilon_2 = \varepsilon_3 = \varepsilon_4 = 3.24$, $k_1 = 1$, $k_2 = 0.85$, $k_3 = 0.7$, $k_4 = 0.6$. The initial condition is $I(0) = 31.5$, $\theta(0) = 0$.

Fig. 35: $I(\tau)$ as a function of $\theta(\tau)$ for values of τ which are multiples of 2π in the case of two waves such $\varepsilon_1 = \varepsilon_2 = 0.81$, $k_1 = k_2$, $\nu_1 = 9$, $\nu_2 = 10.03$ (this is not a Poincaré section). The initial condition is $I(0) = 32$, $\theta(0) = .7\pi$.

Fig. 36: Poincaré section of the dynamics defined by (2) in the case of three waves such that $\nu_1 = 9$, $\nu_2 = 10$, $\nu_3 = 8.25$, $\varepsilon_1 = \varepsilon_2 = 0.2592$, $\varepsilon_3 = 1.62$, $k_1 = k_2 = k_3$. The initial condition

is $I(0) = 32, \theta(0) = .7\pi$.

Fig. 37: Same as Fig. 36 except for $\varepsilon_3 = 1.782$.

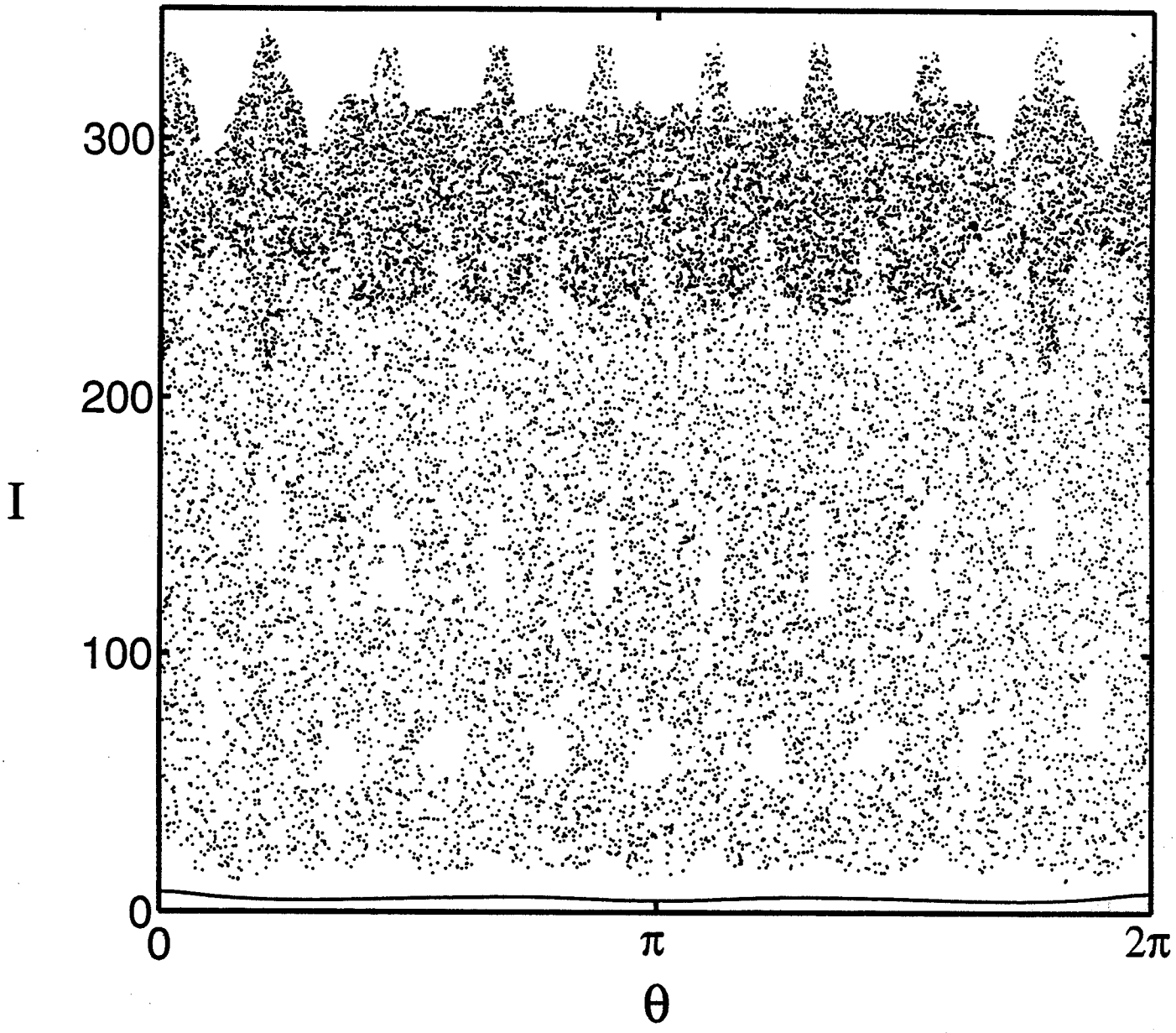

Figure 1

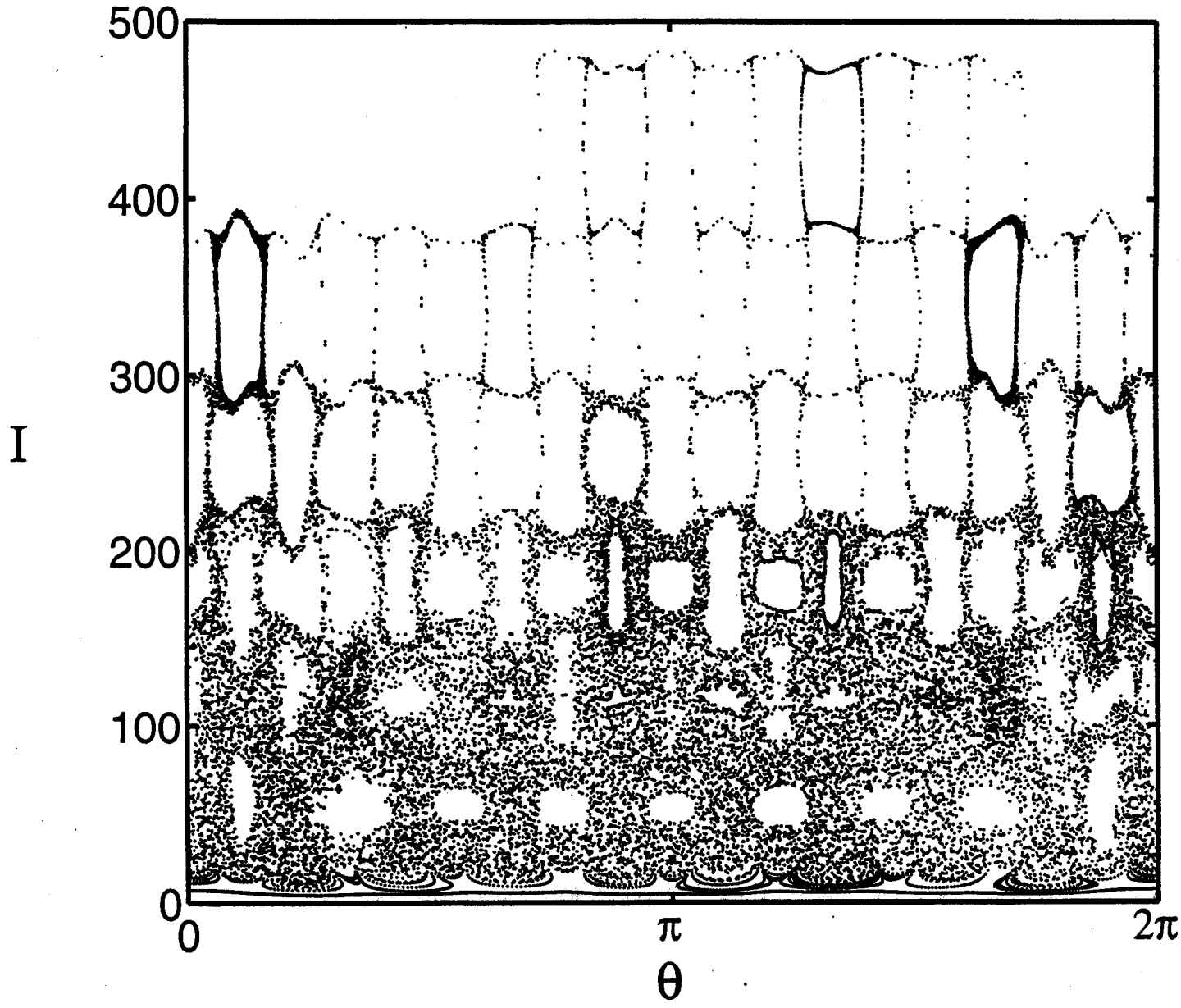

Figure 2

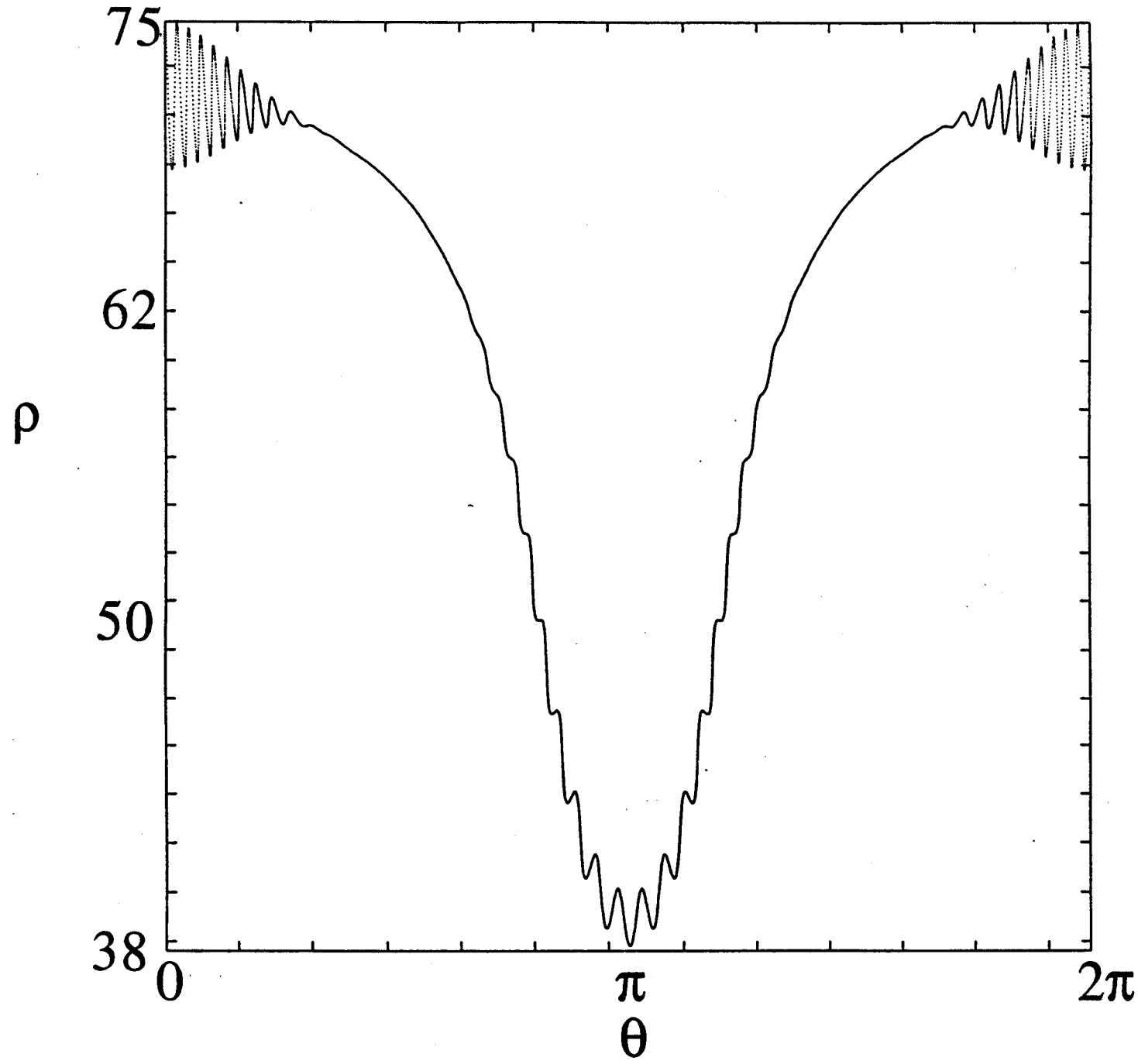

Figure 3

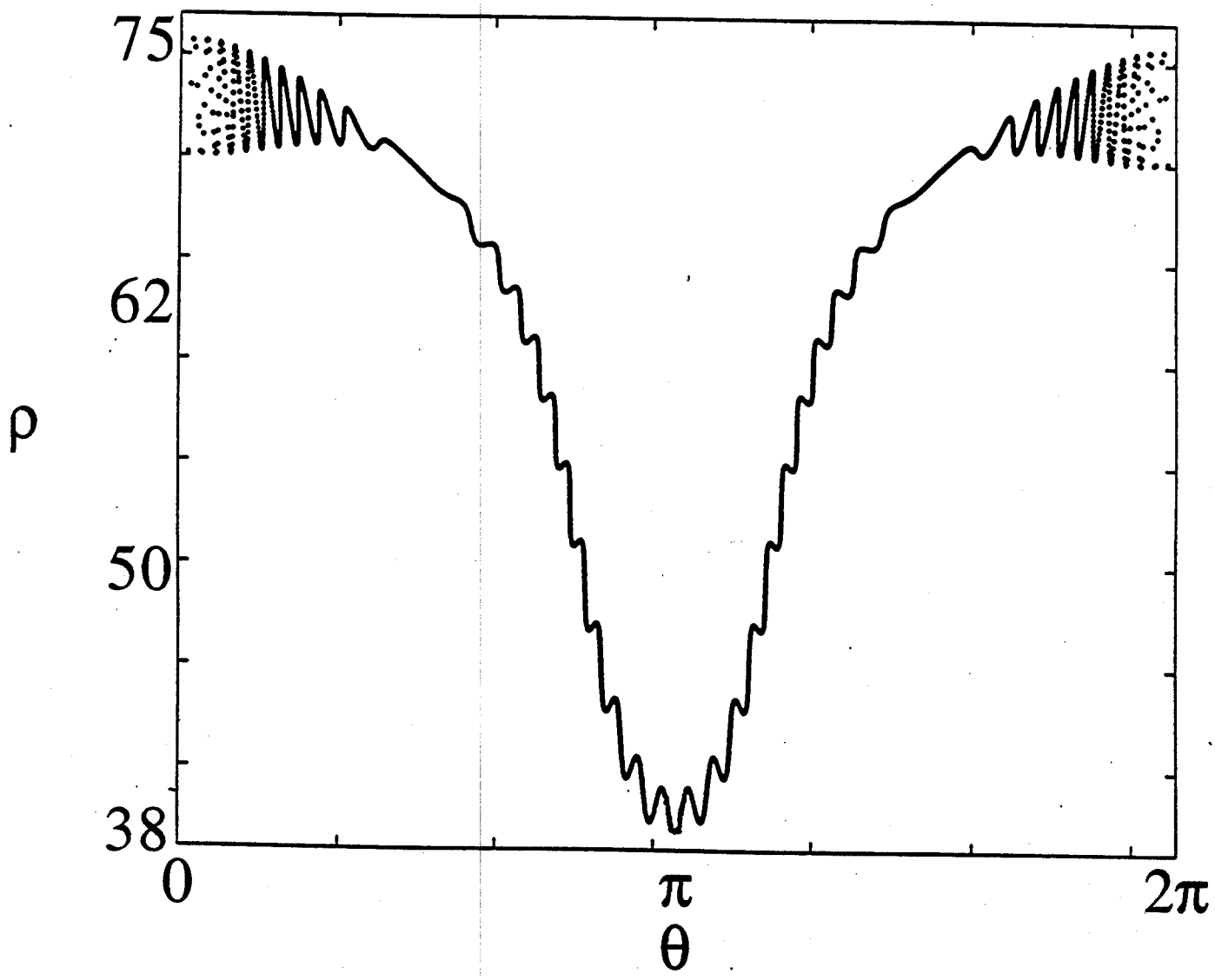

Figure 4

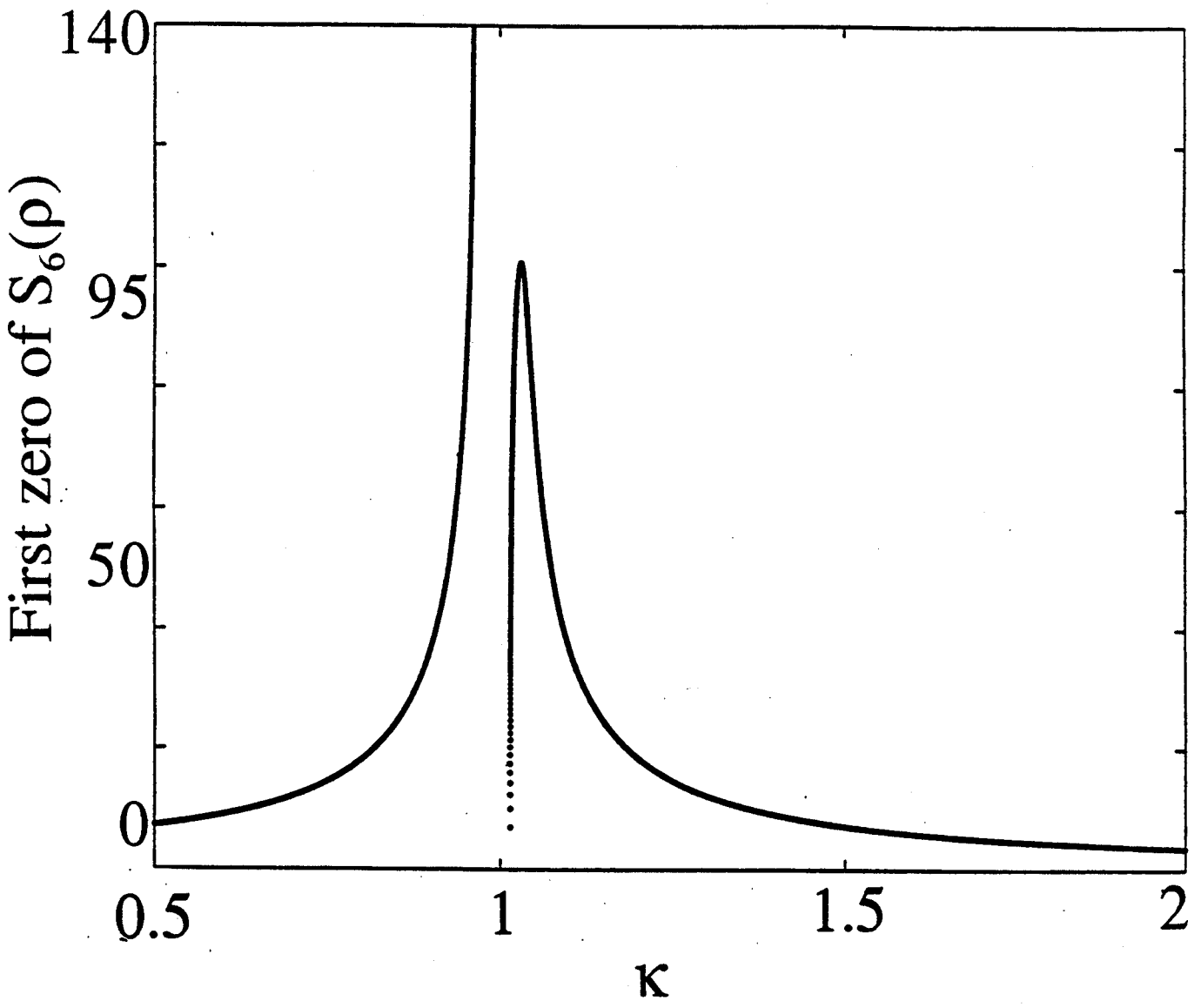

Figure 5

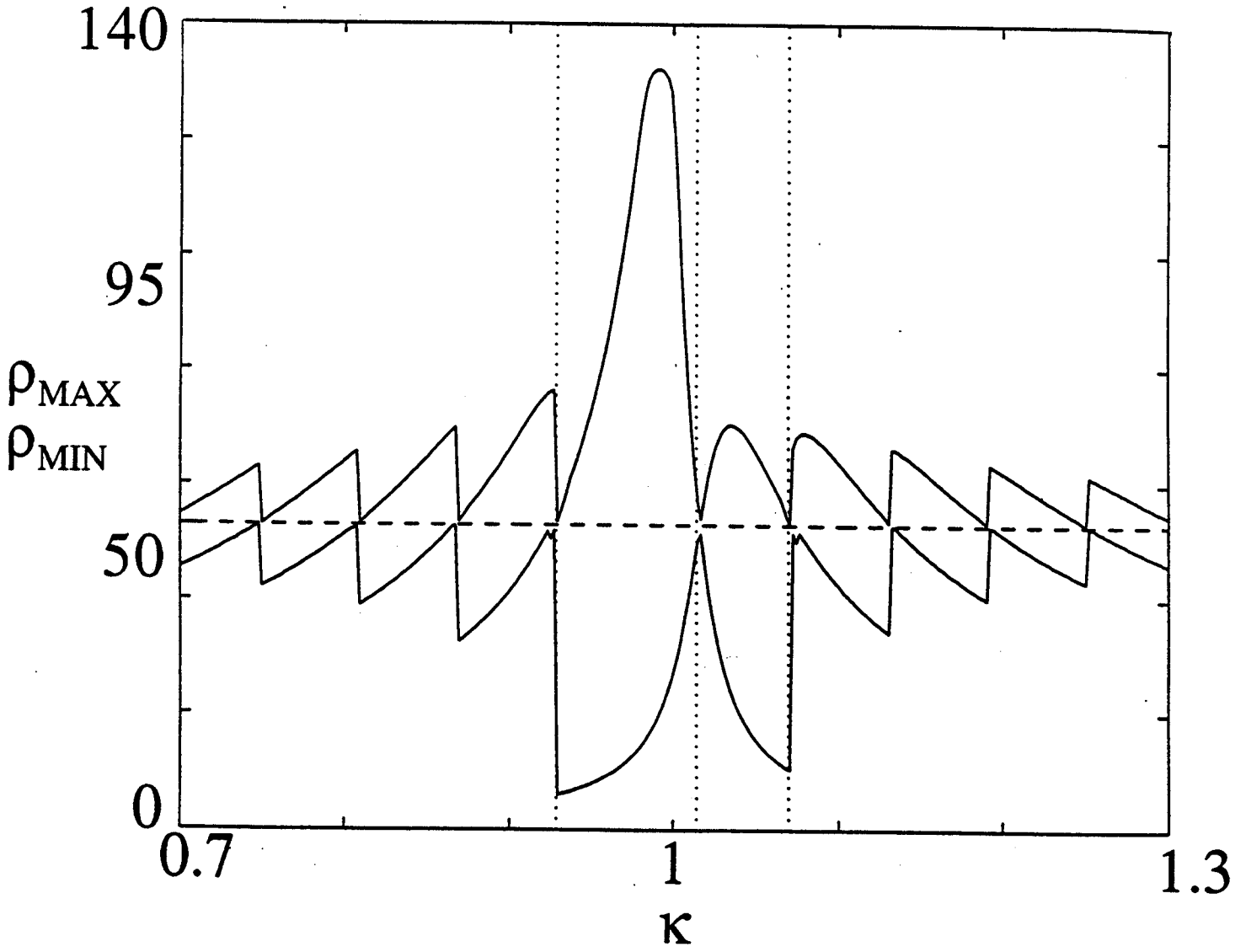

Figure 6

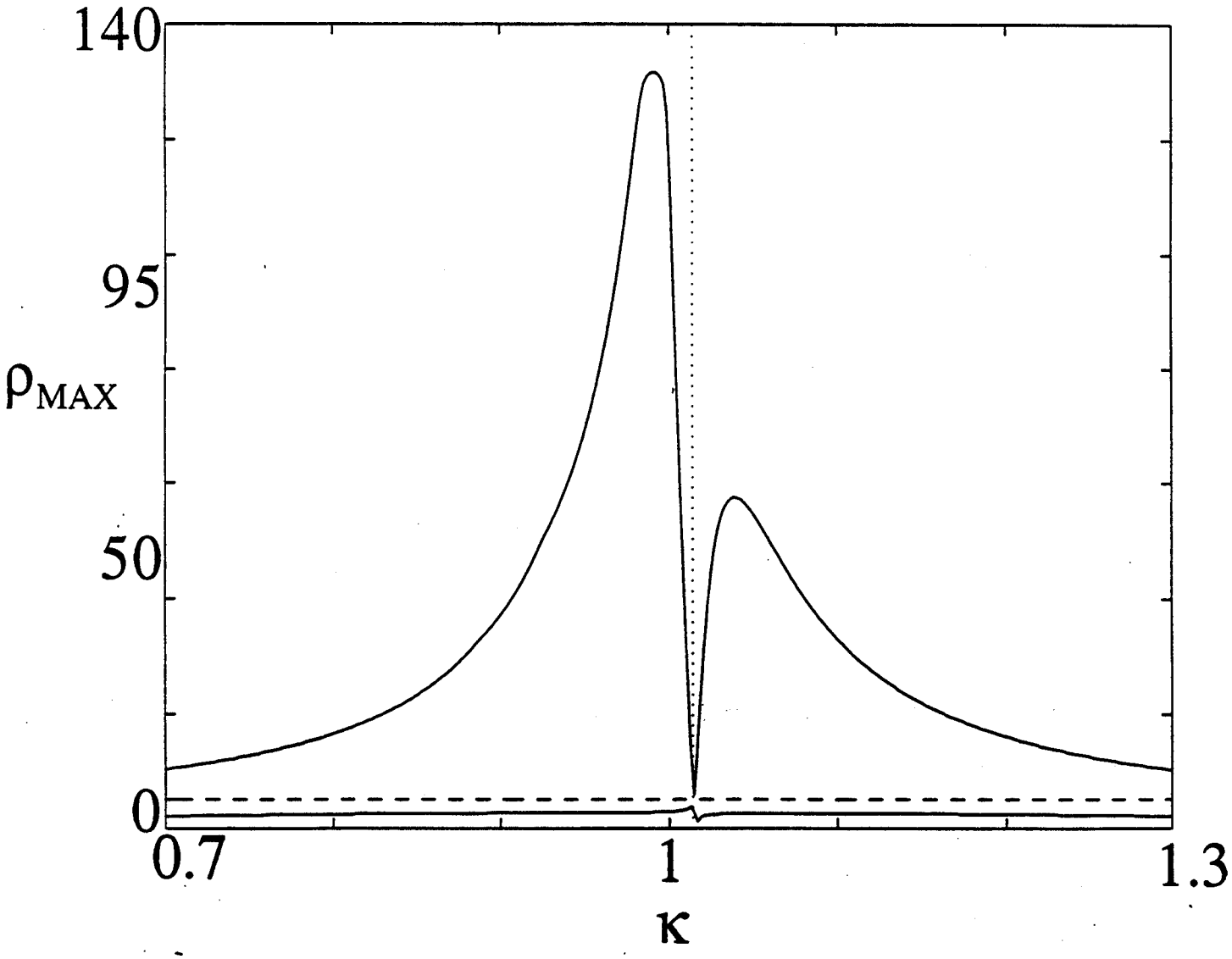

Figure 7

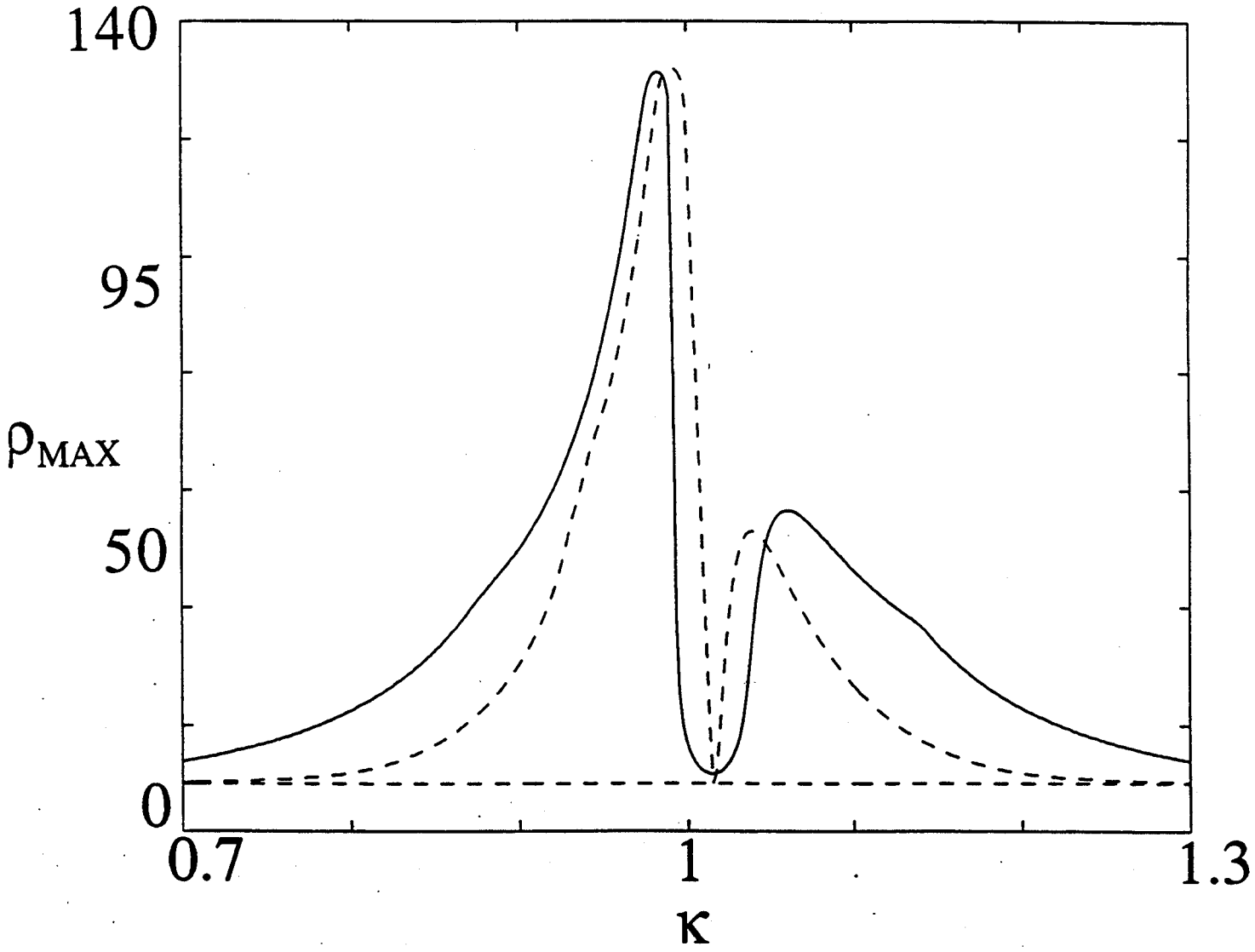

Figure 8

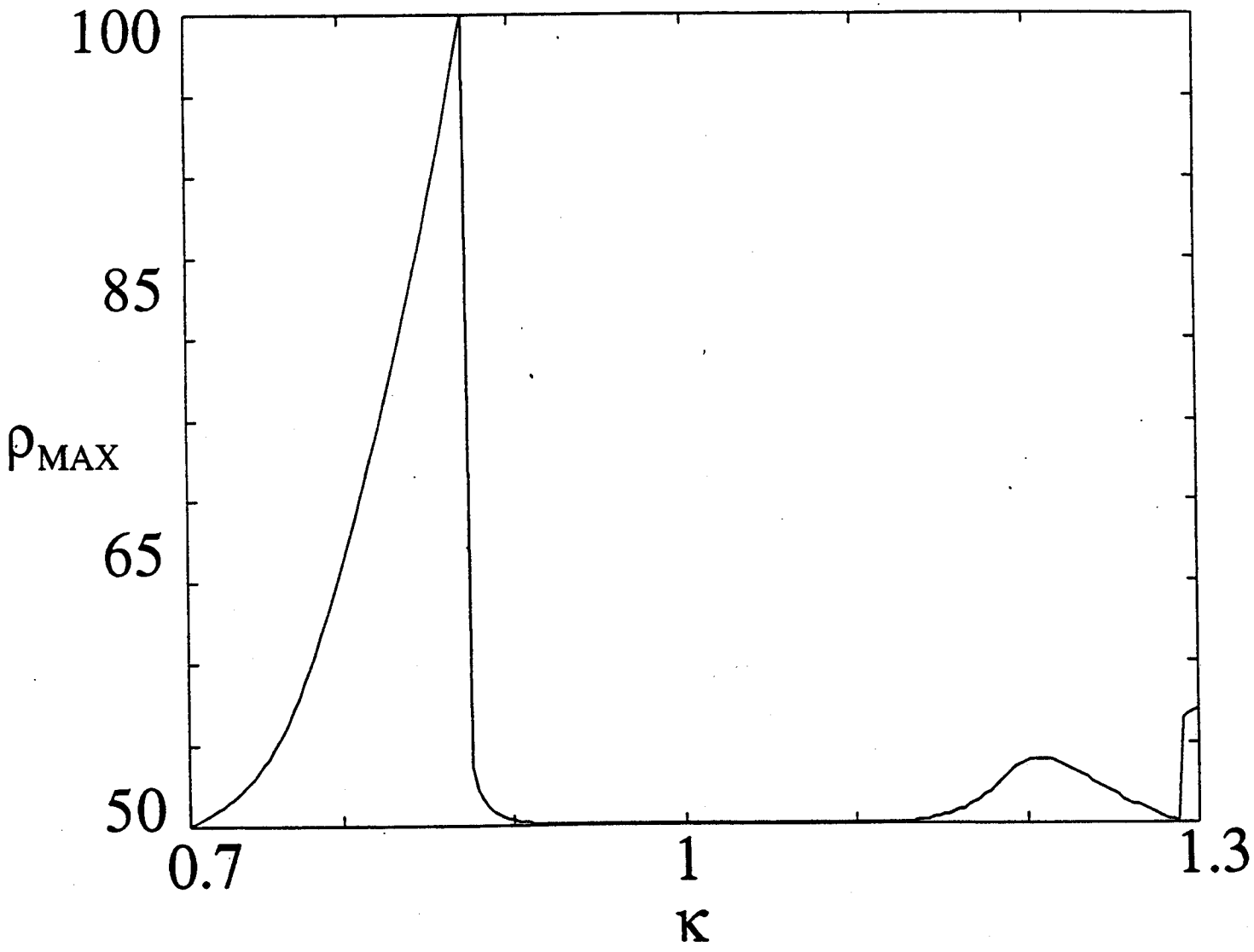

Figure 9

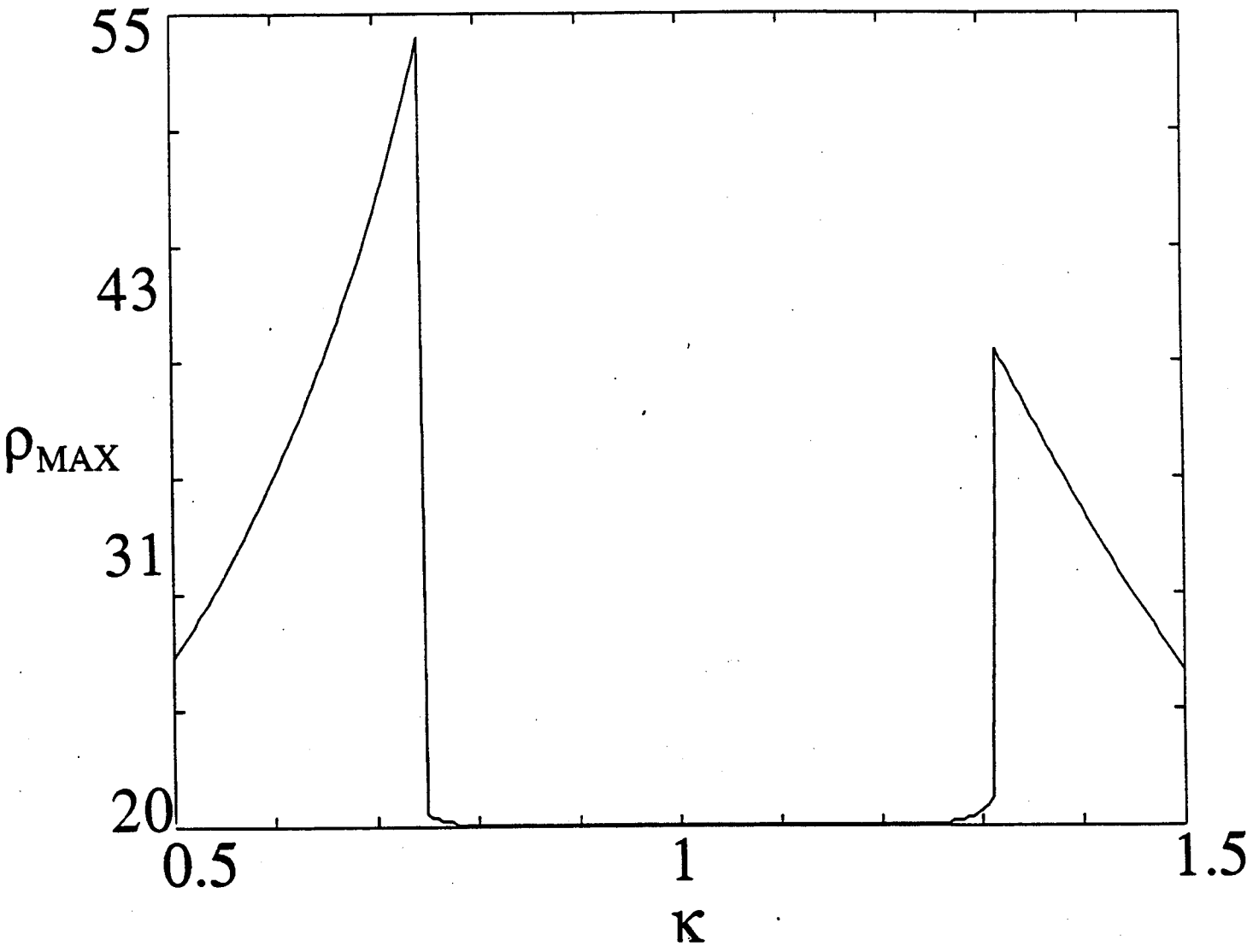

Figure 10

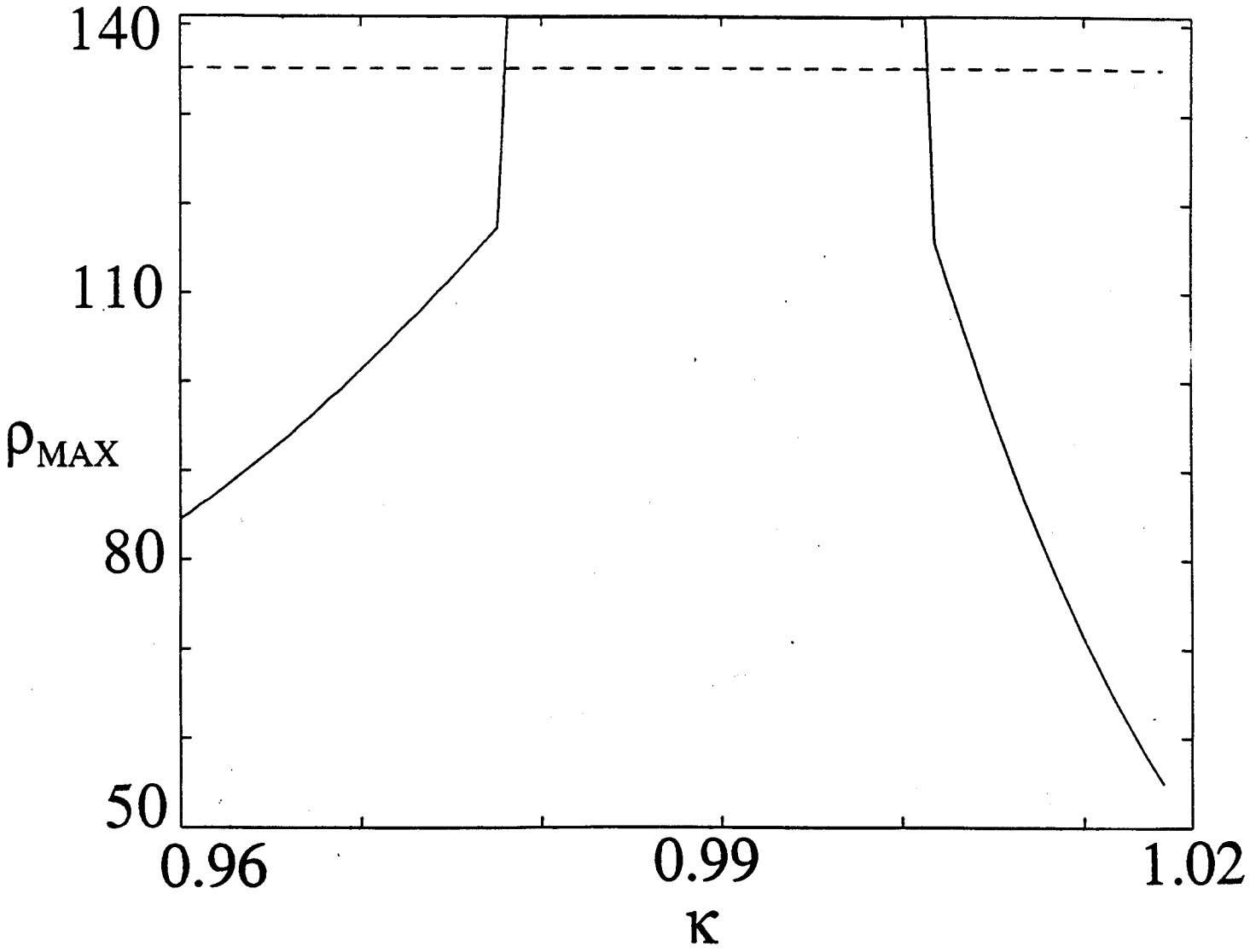

Figure 11

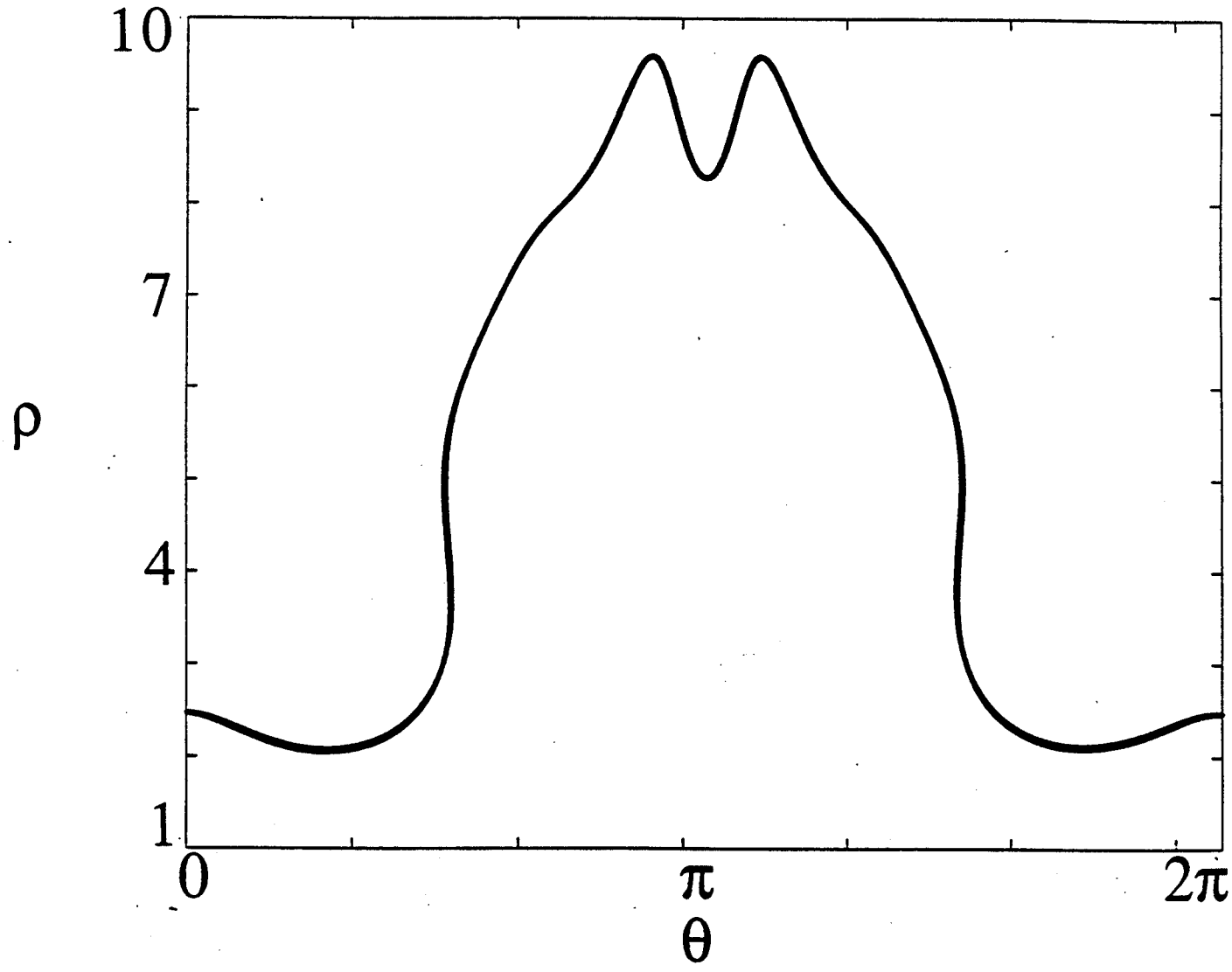

Figure 12

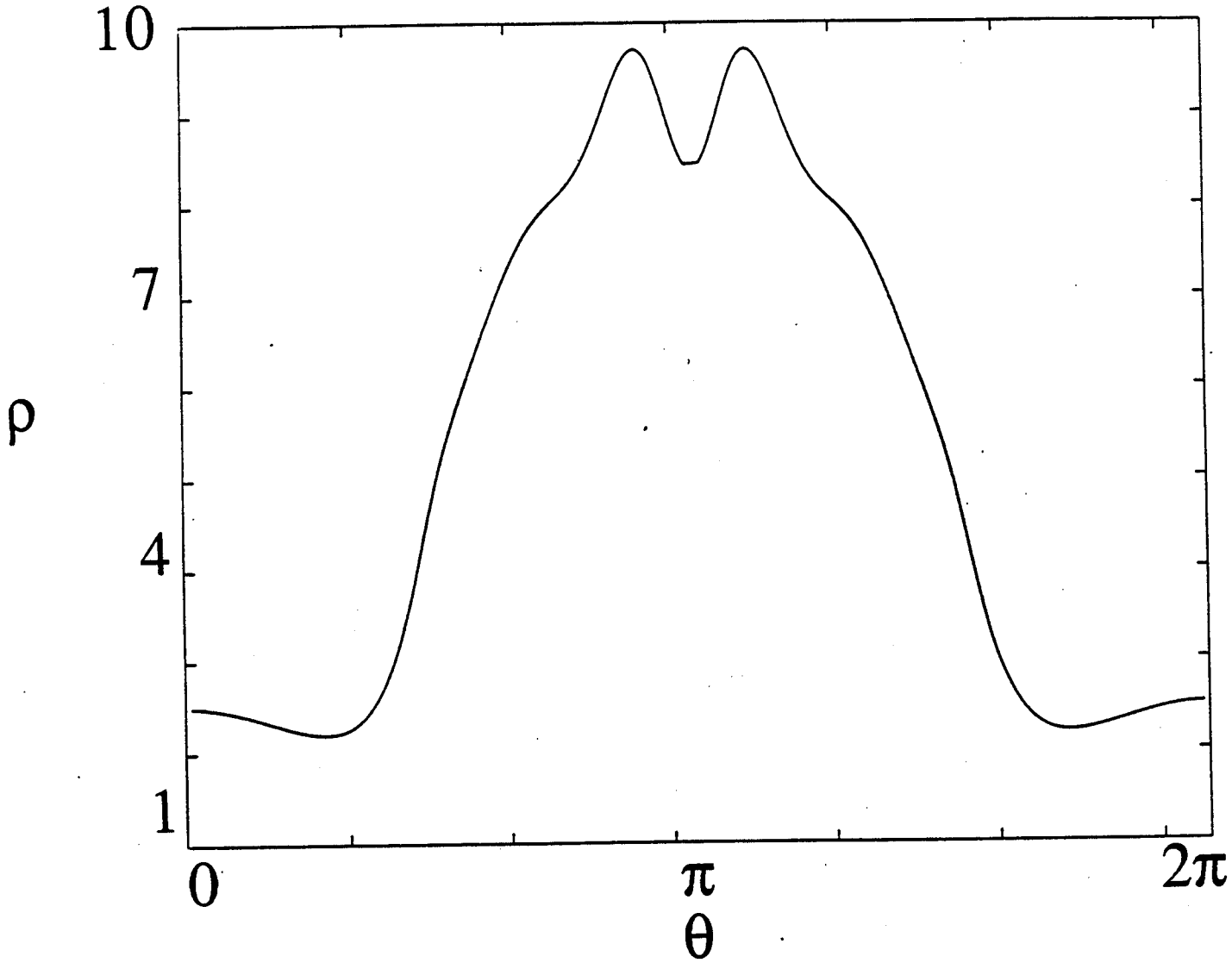

Figure 13

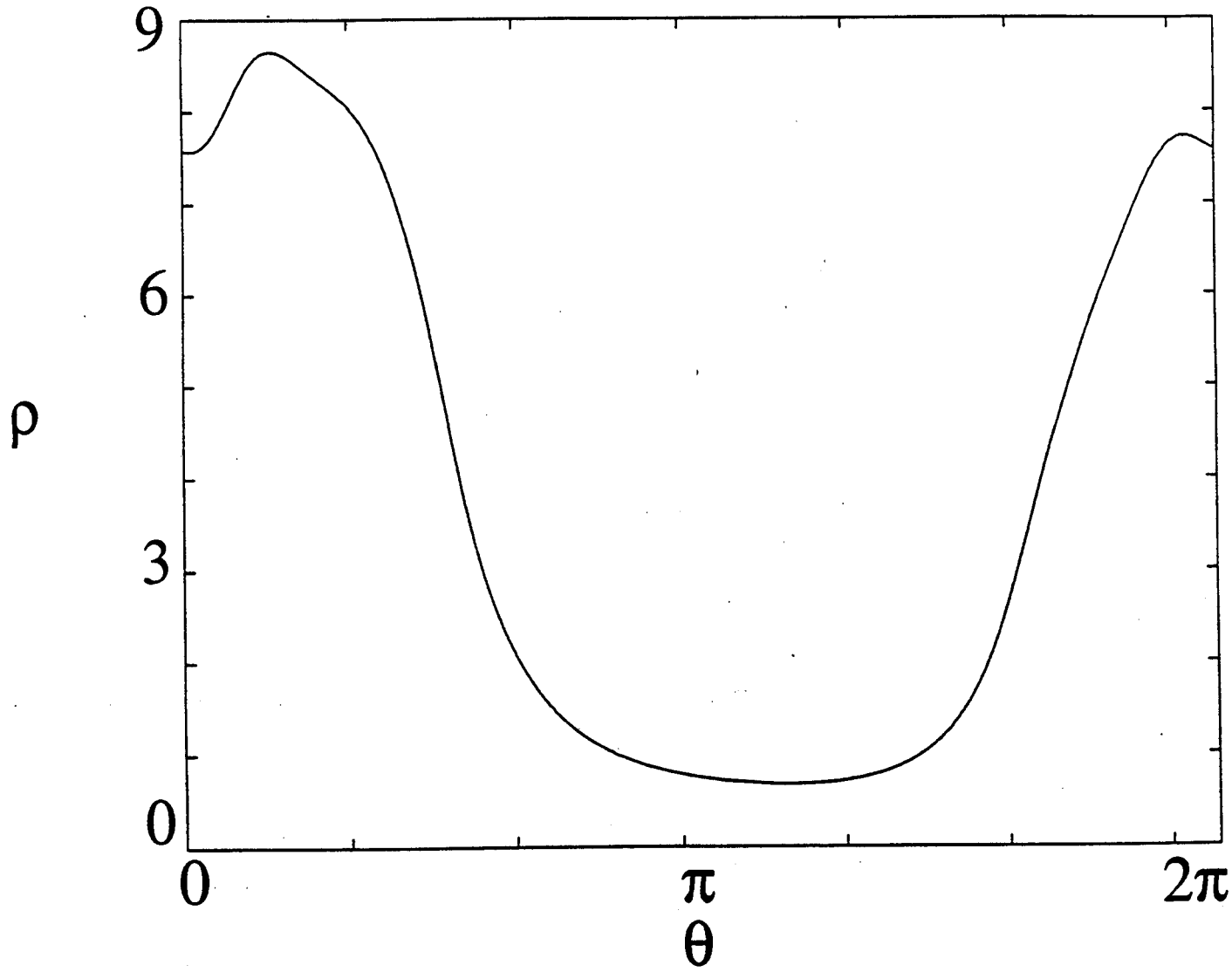

Figure 14

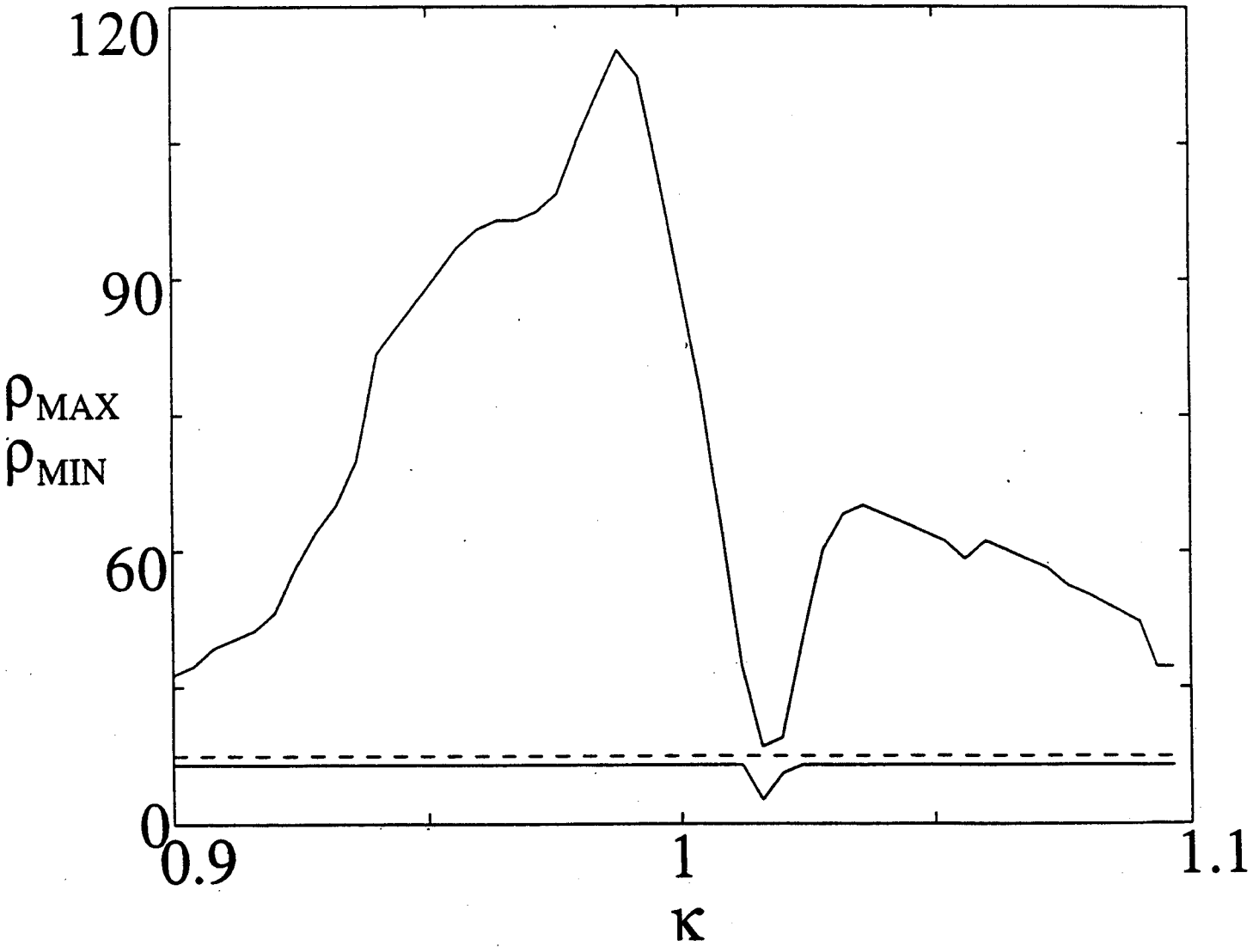

Figure 15

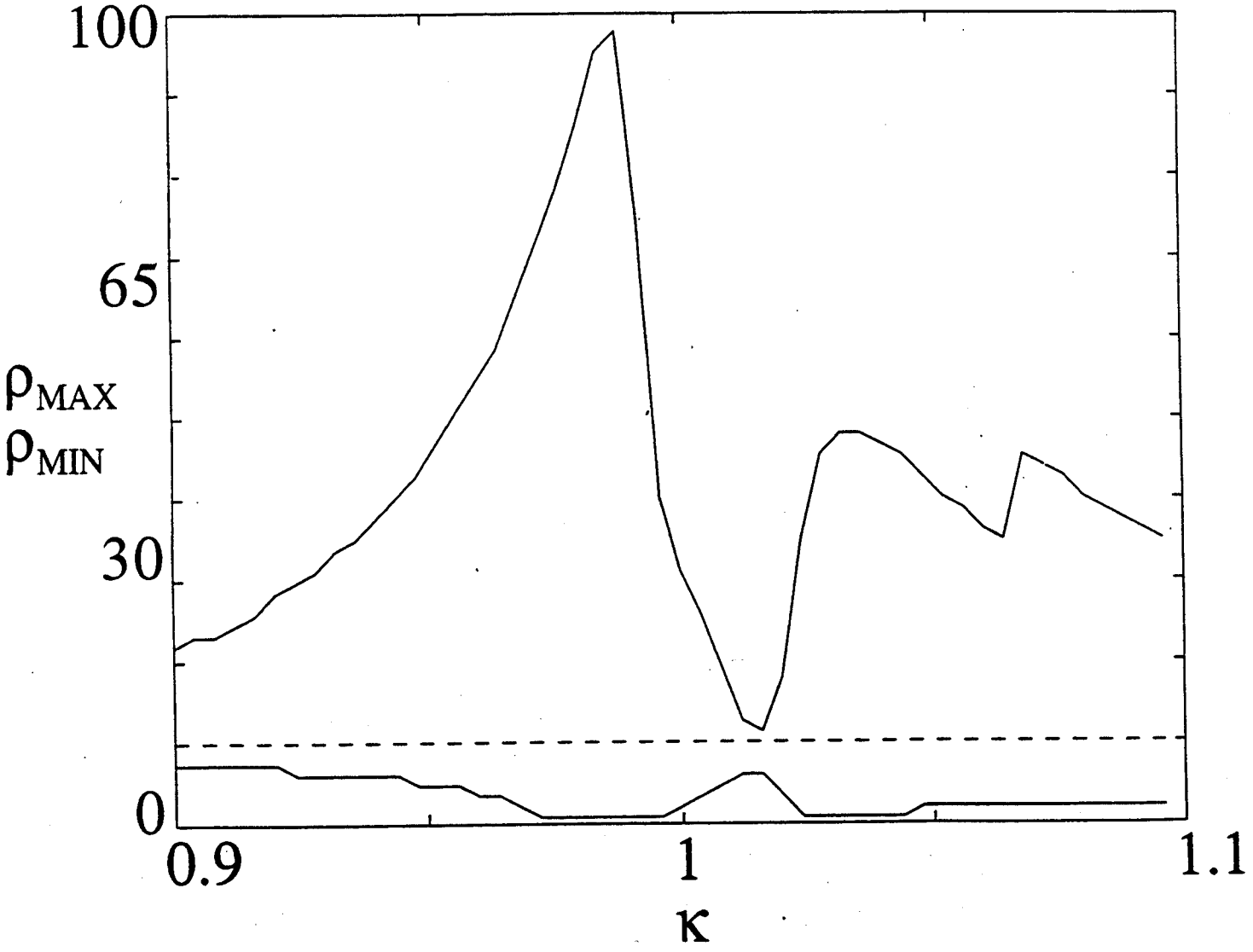

Figure 16

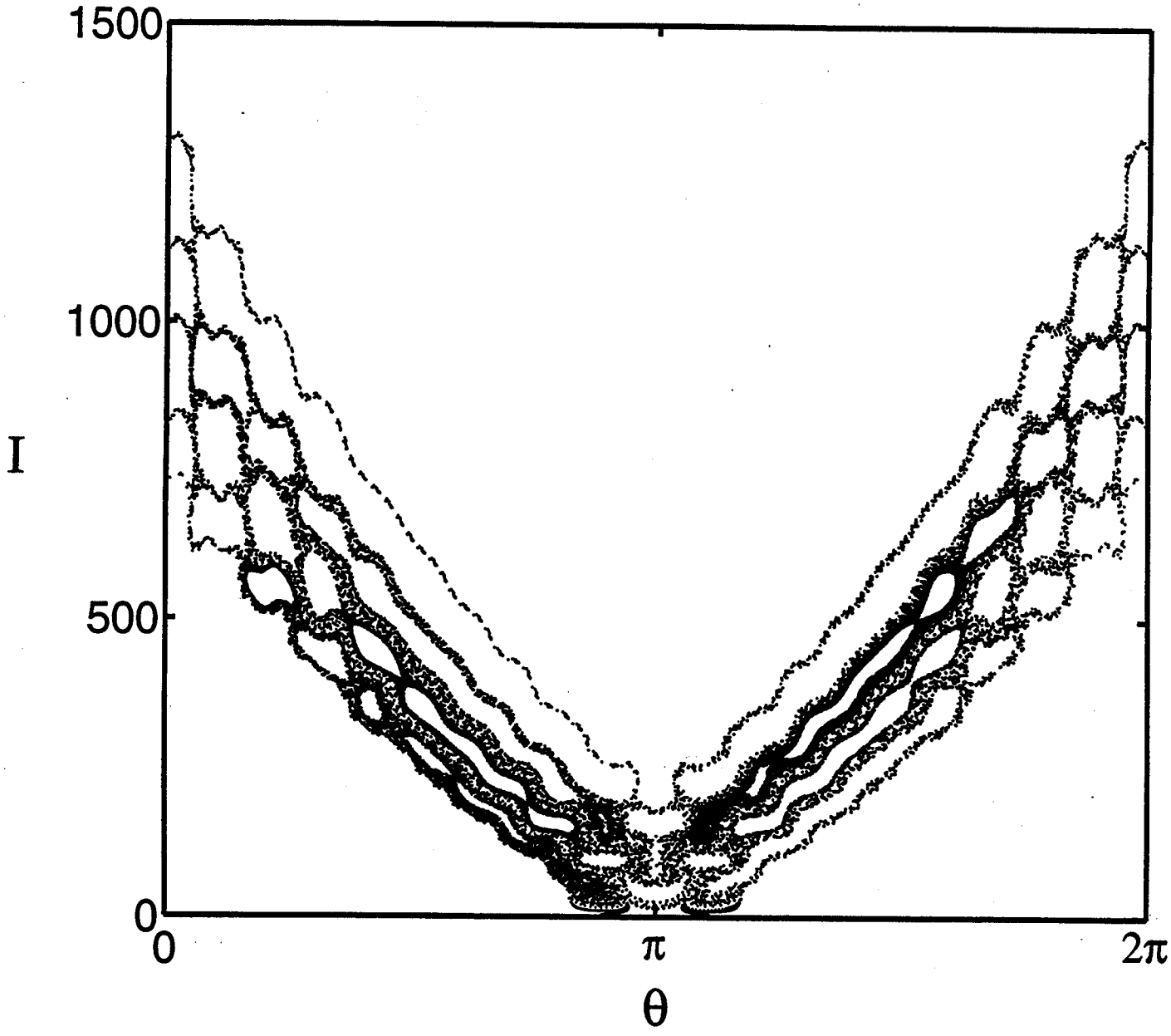

Figure 17

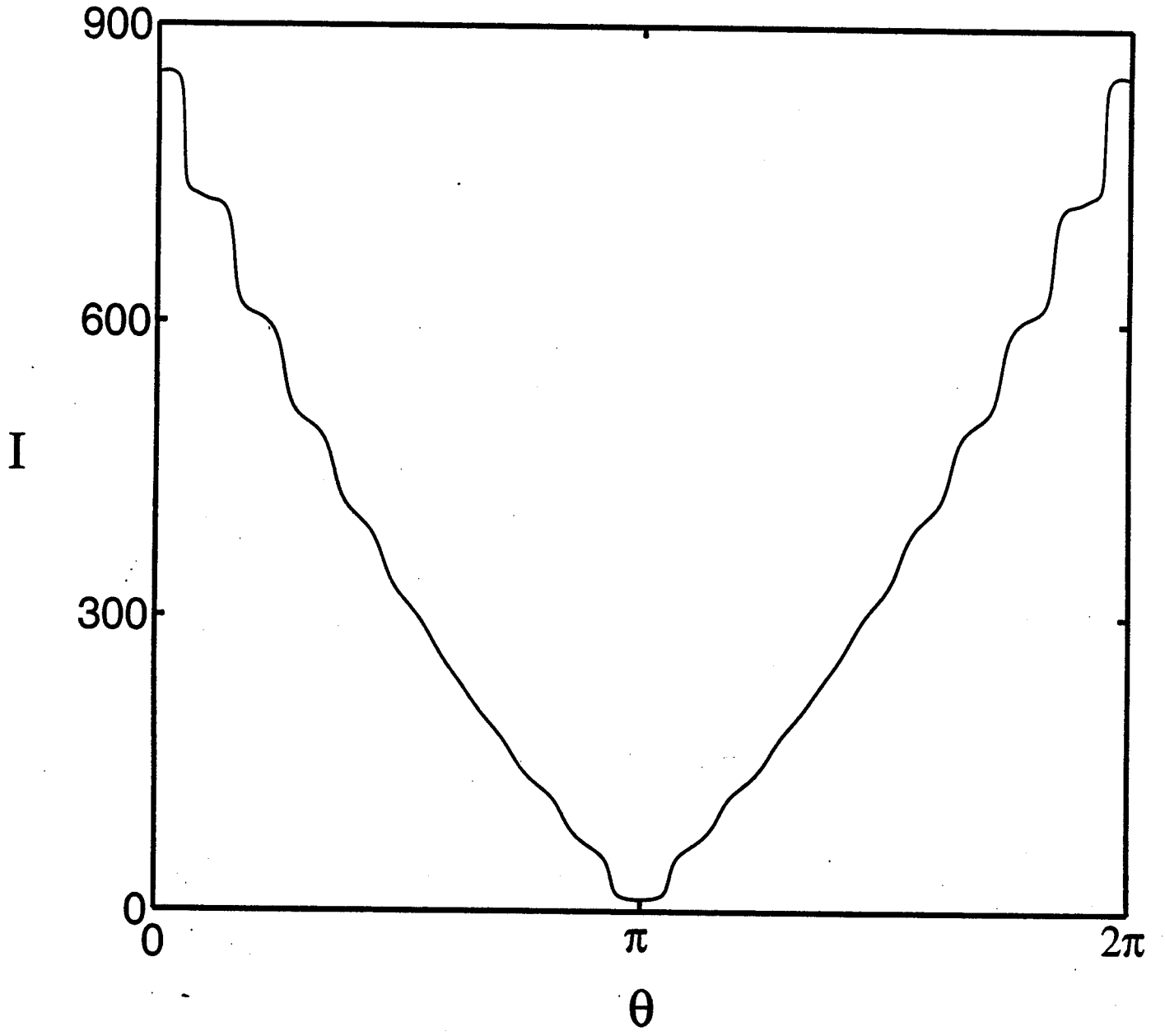

Figure 18

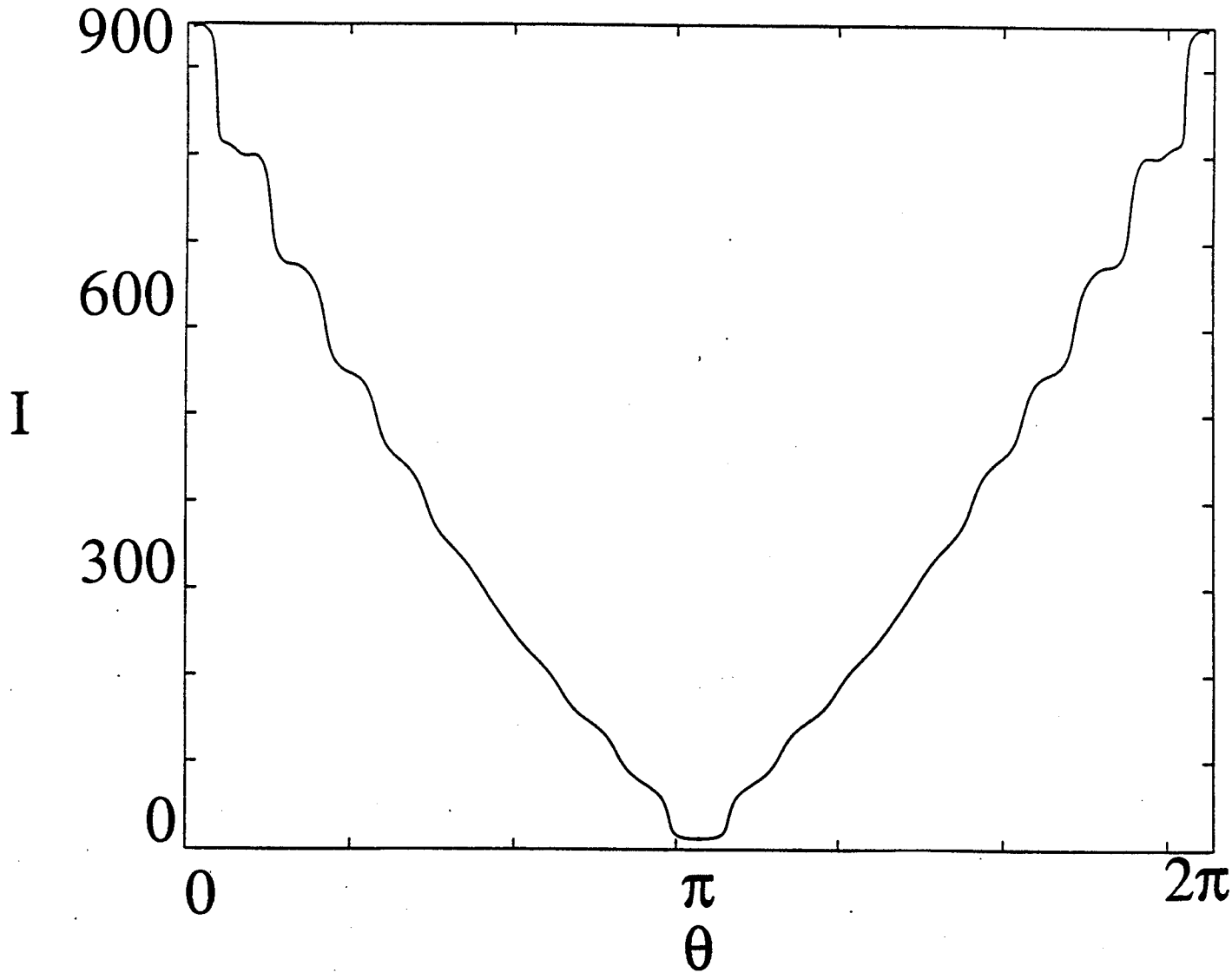

Figure 19

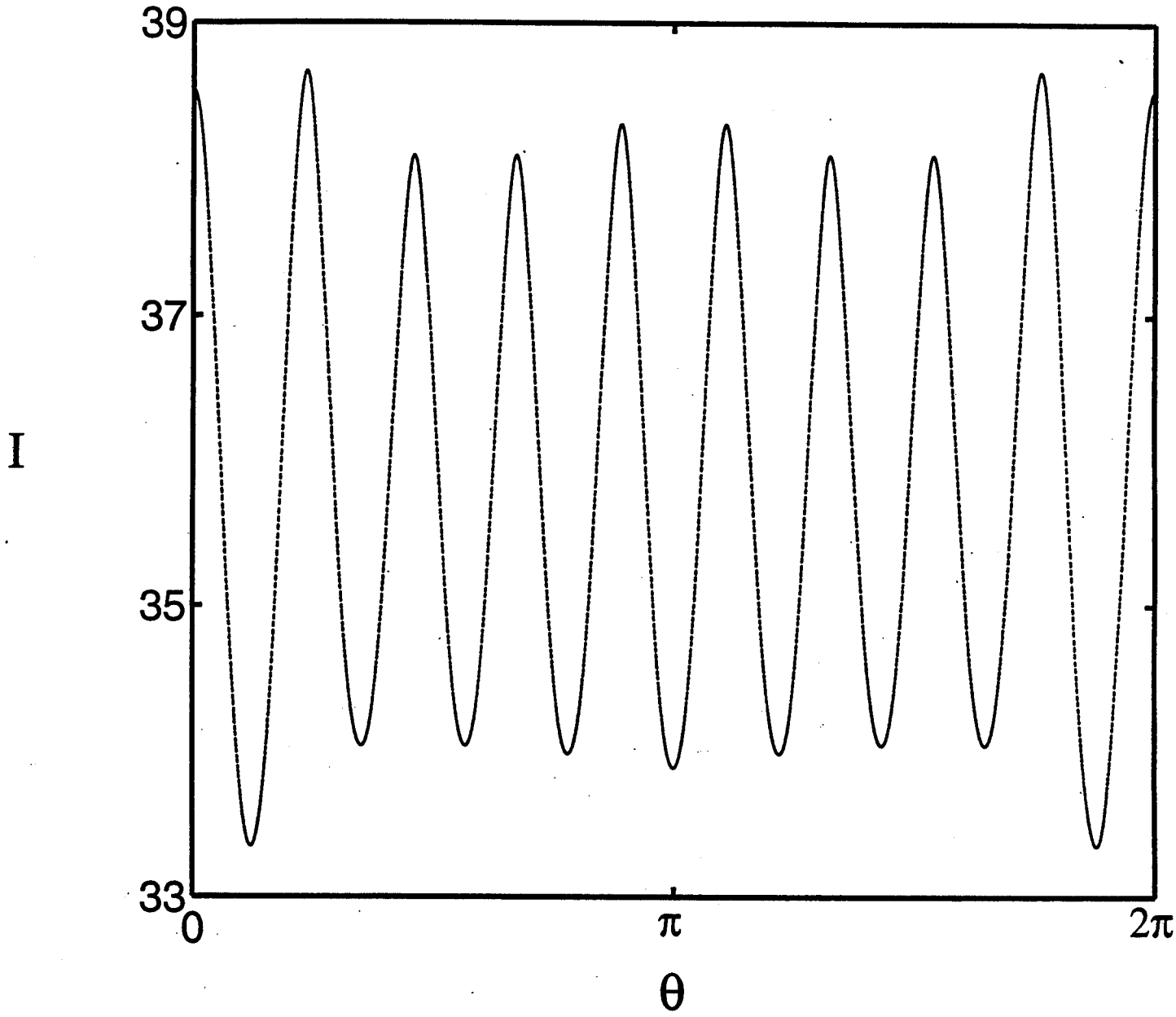

Figure 20

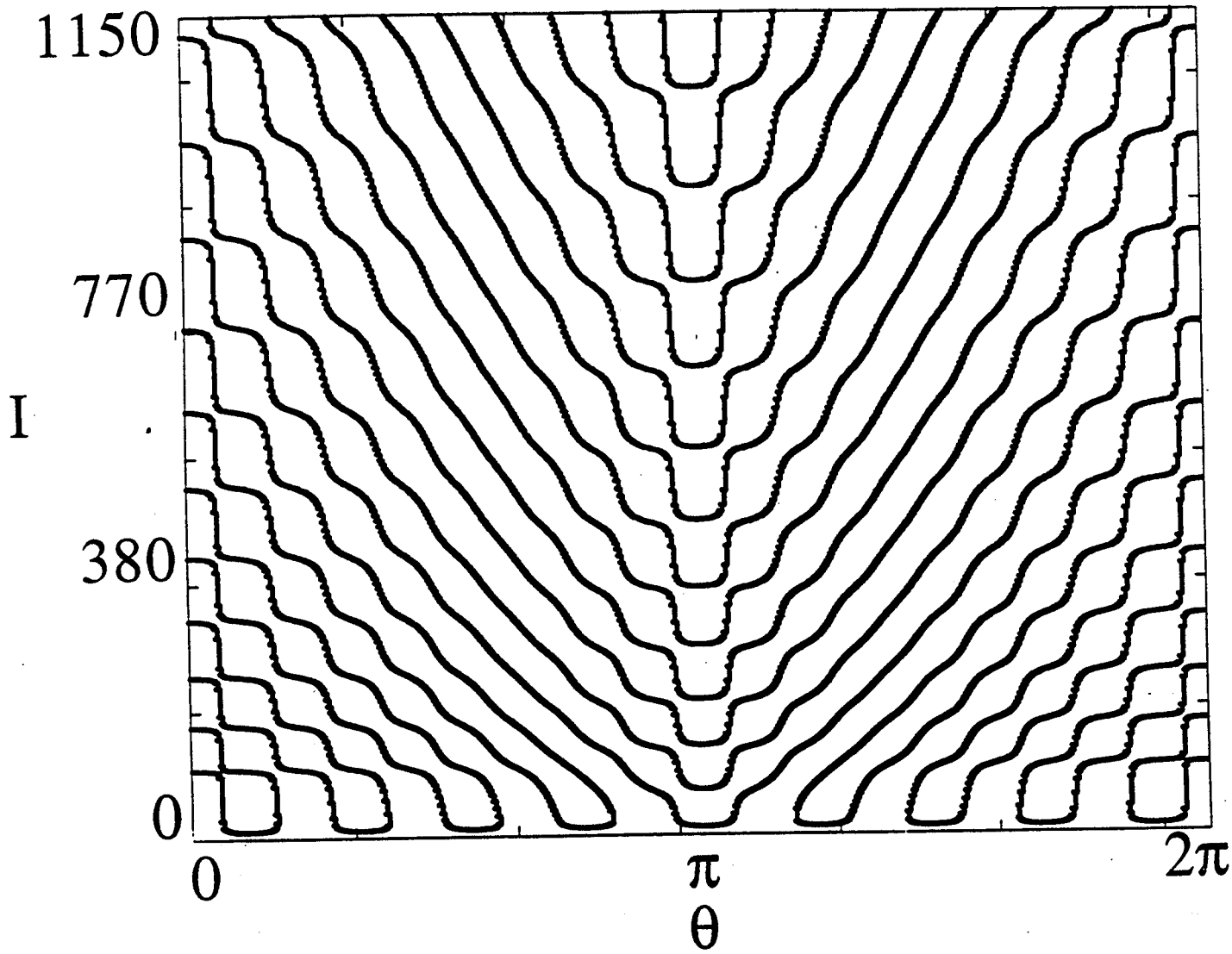

Figure 21

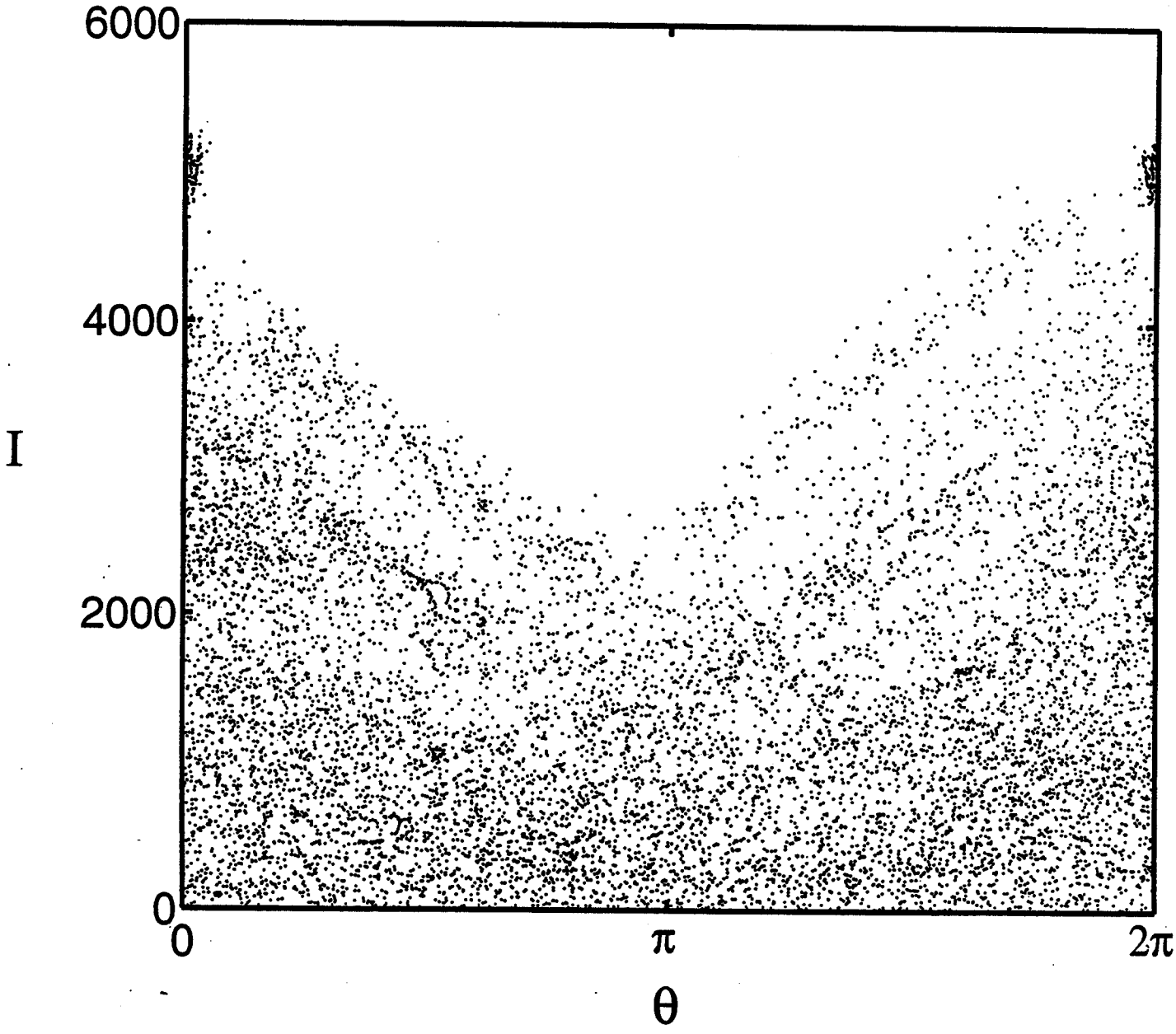

Figure 22

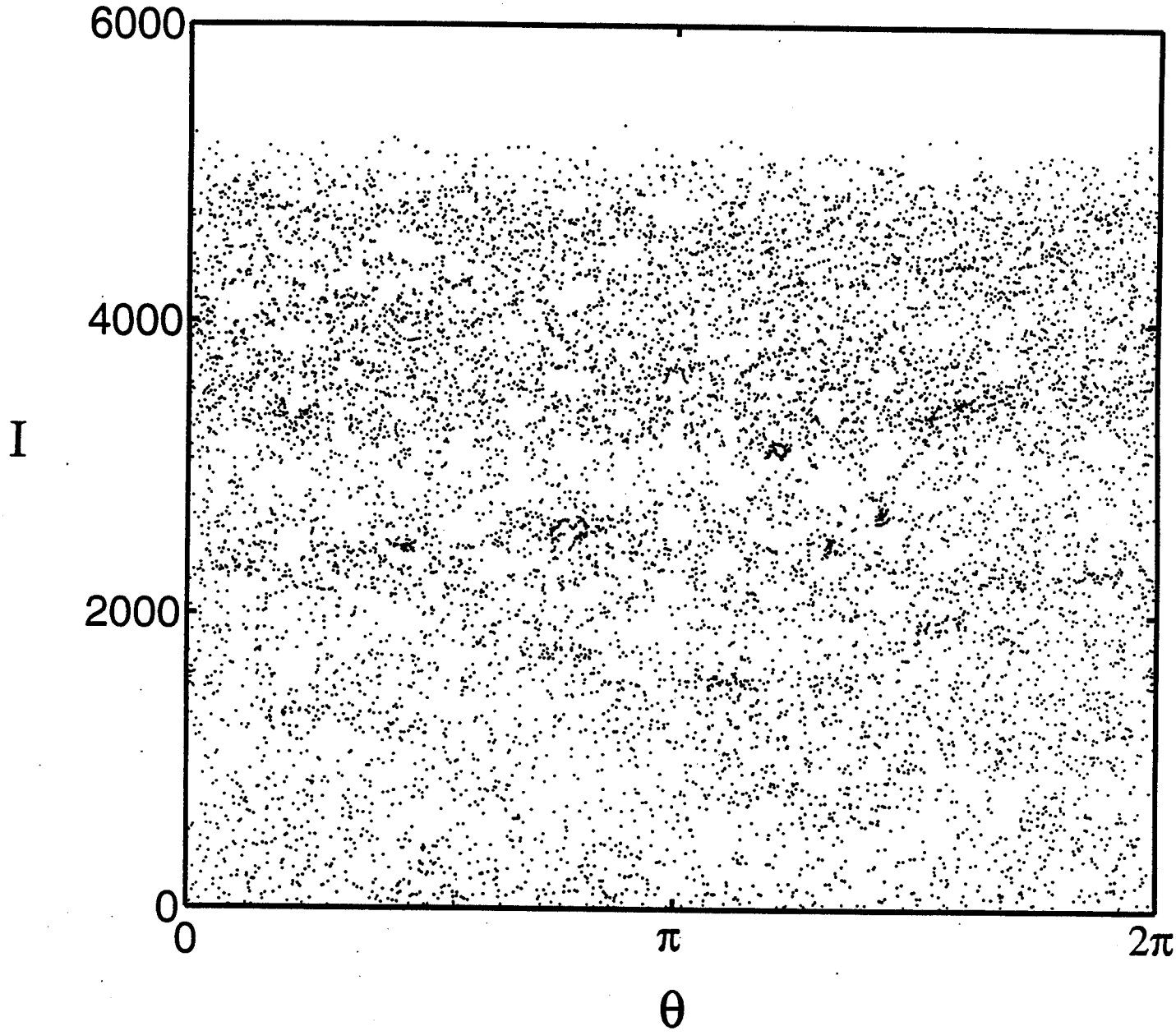

Figure 23

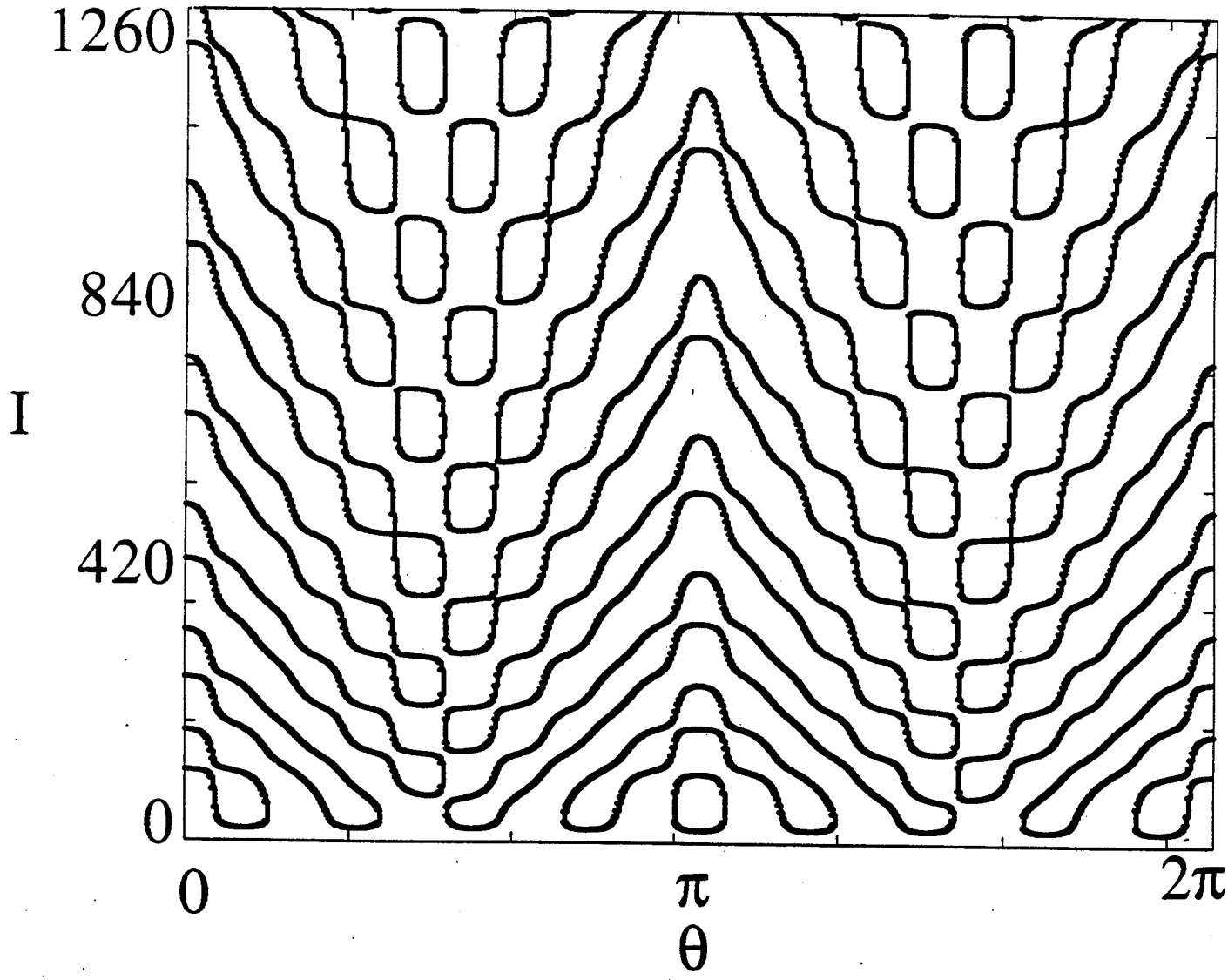

Figure 24

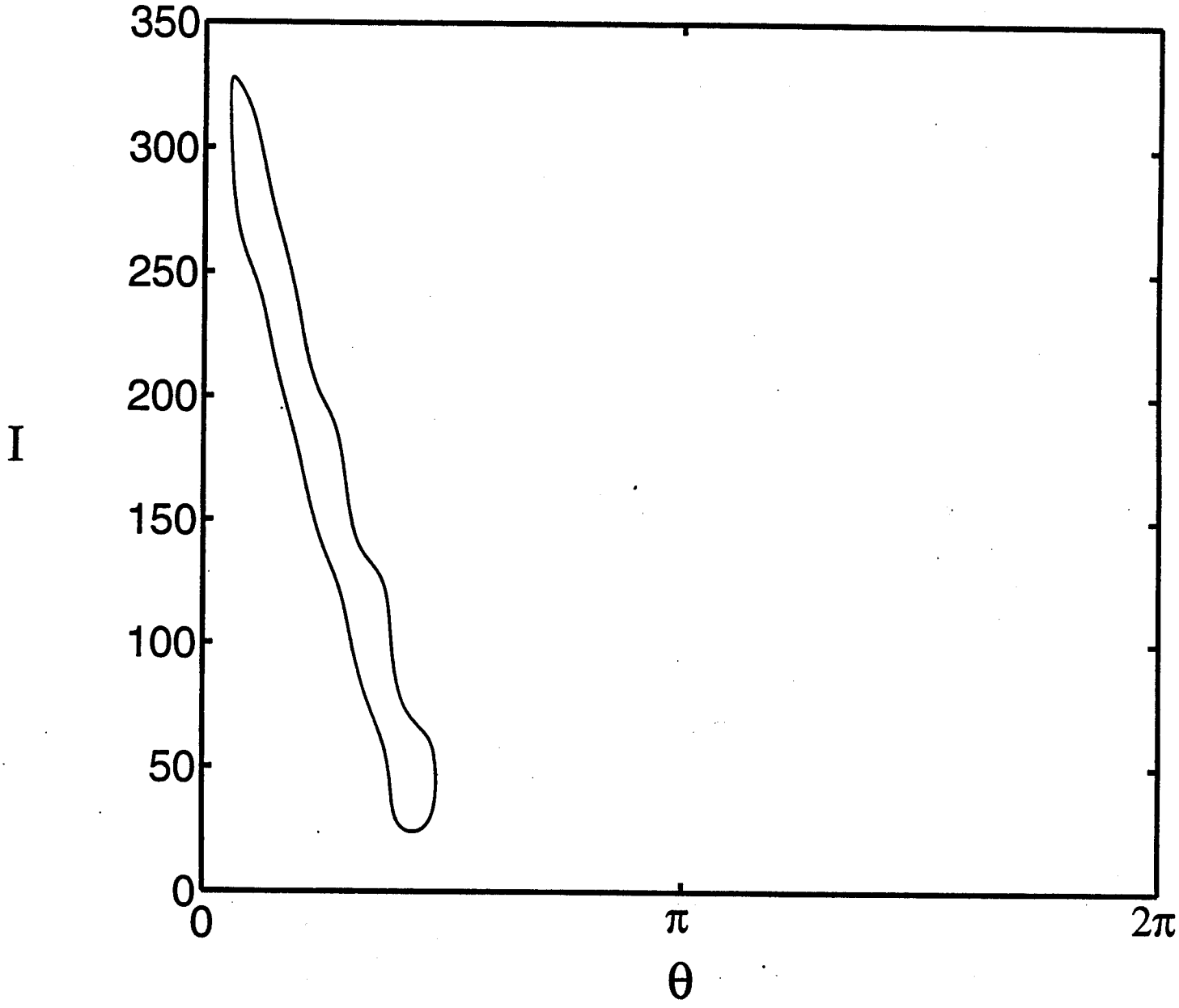

Figure 25

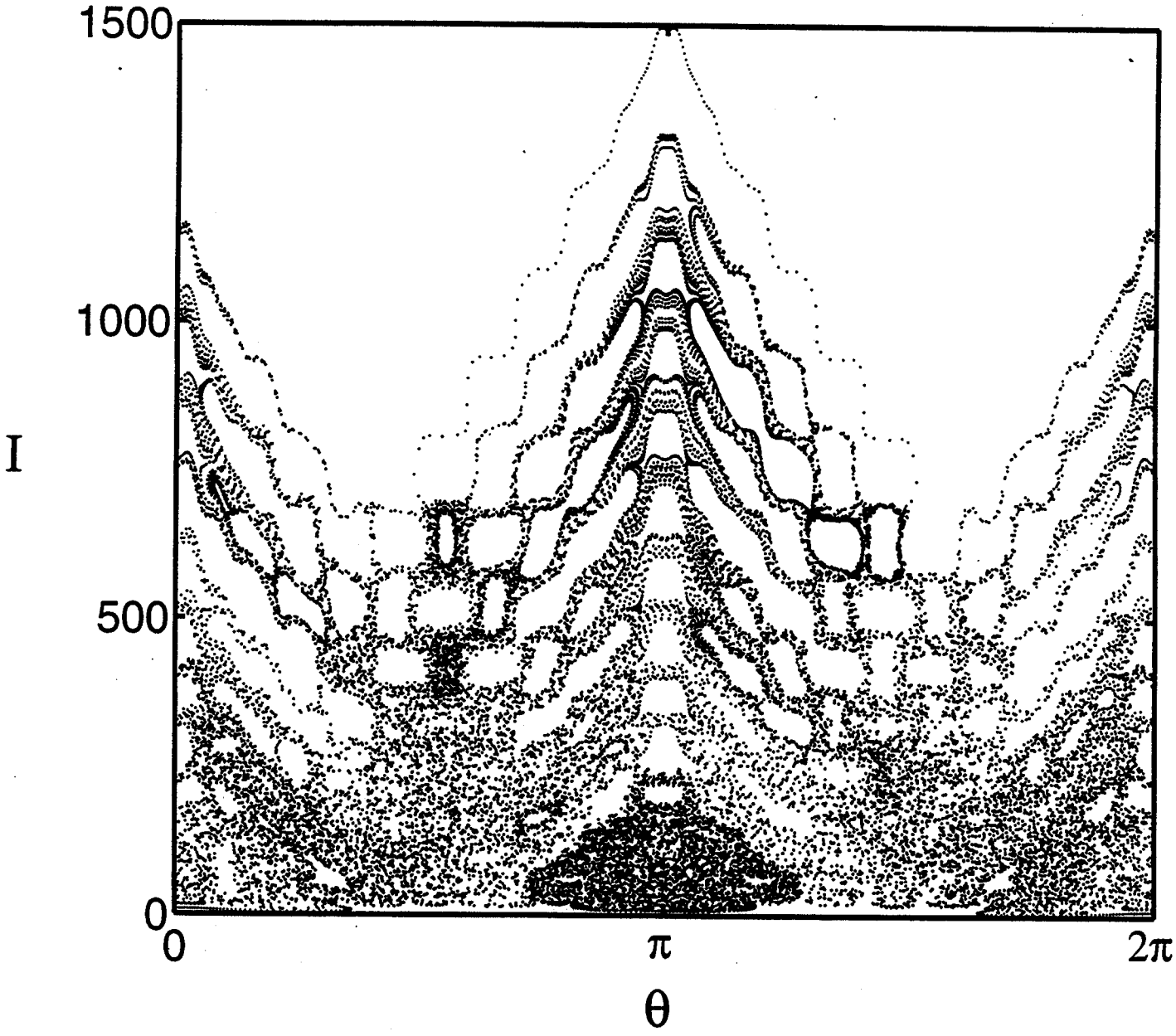

Figure 26

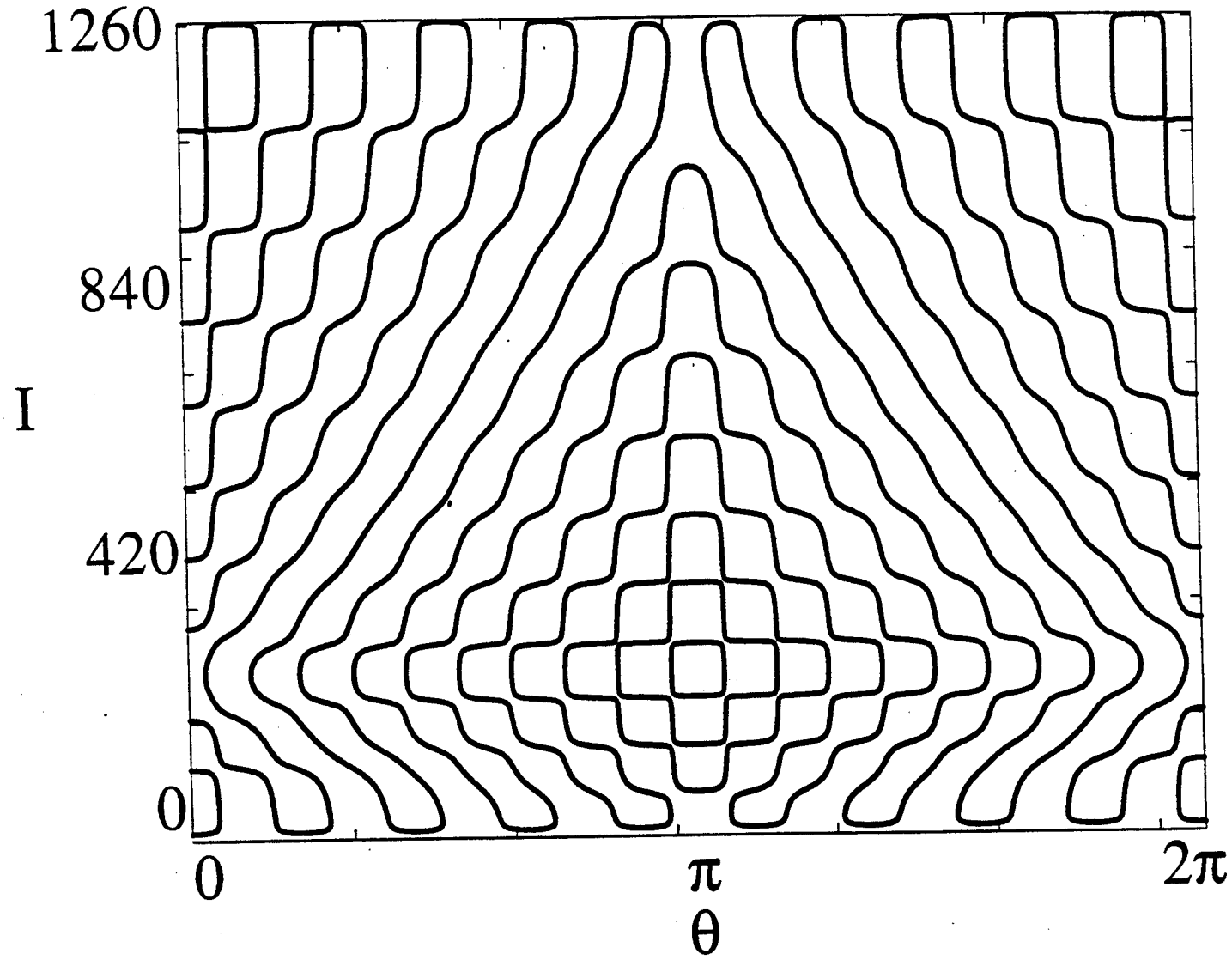

Figure 27

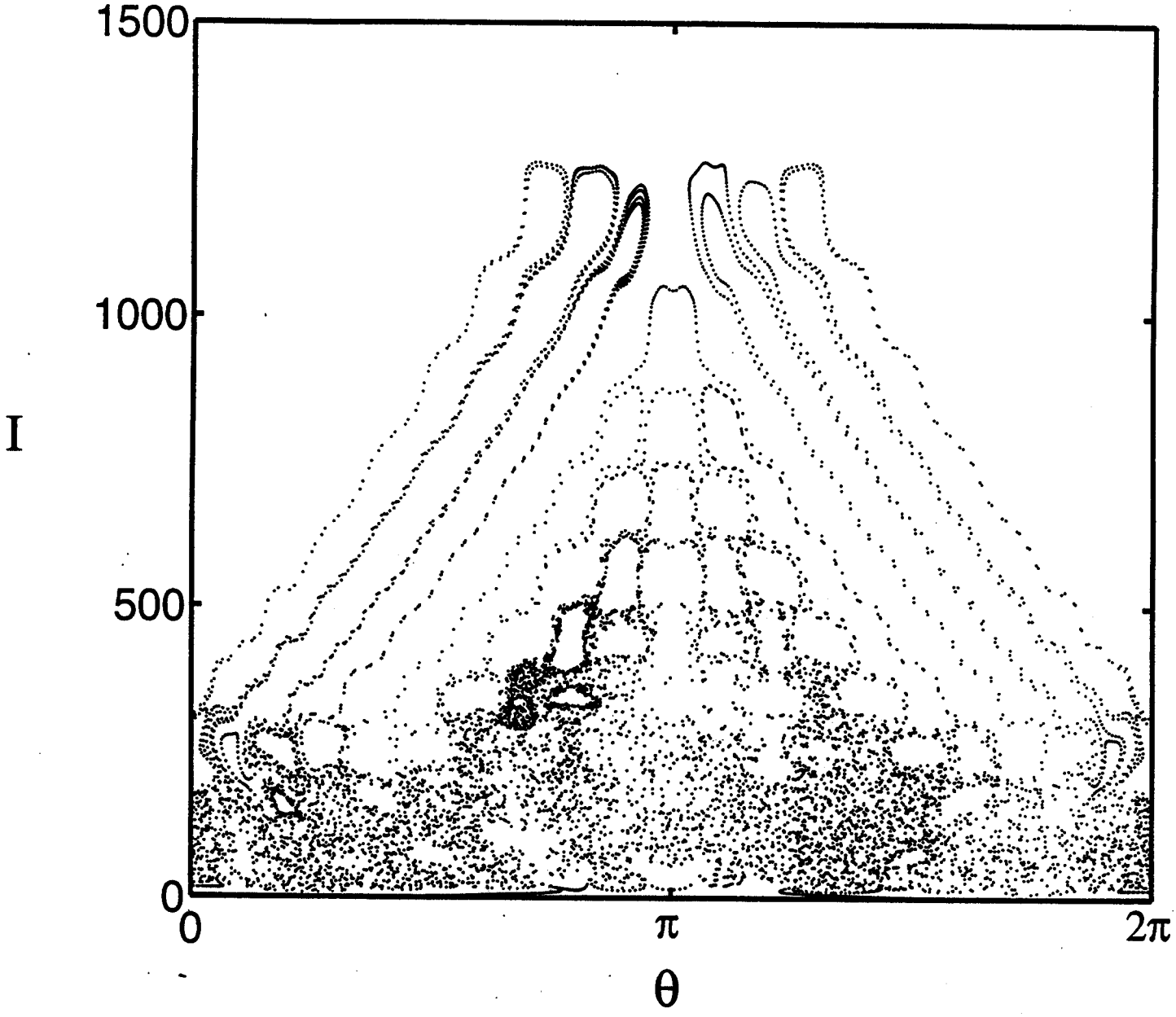

Figure 28

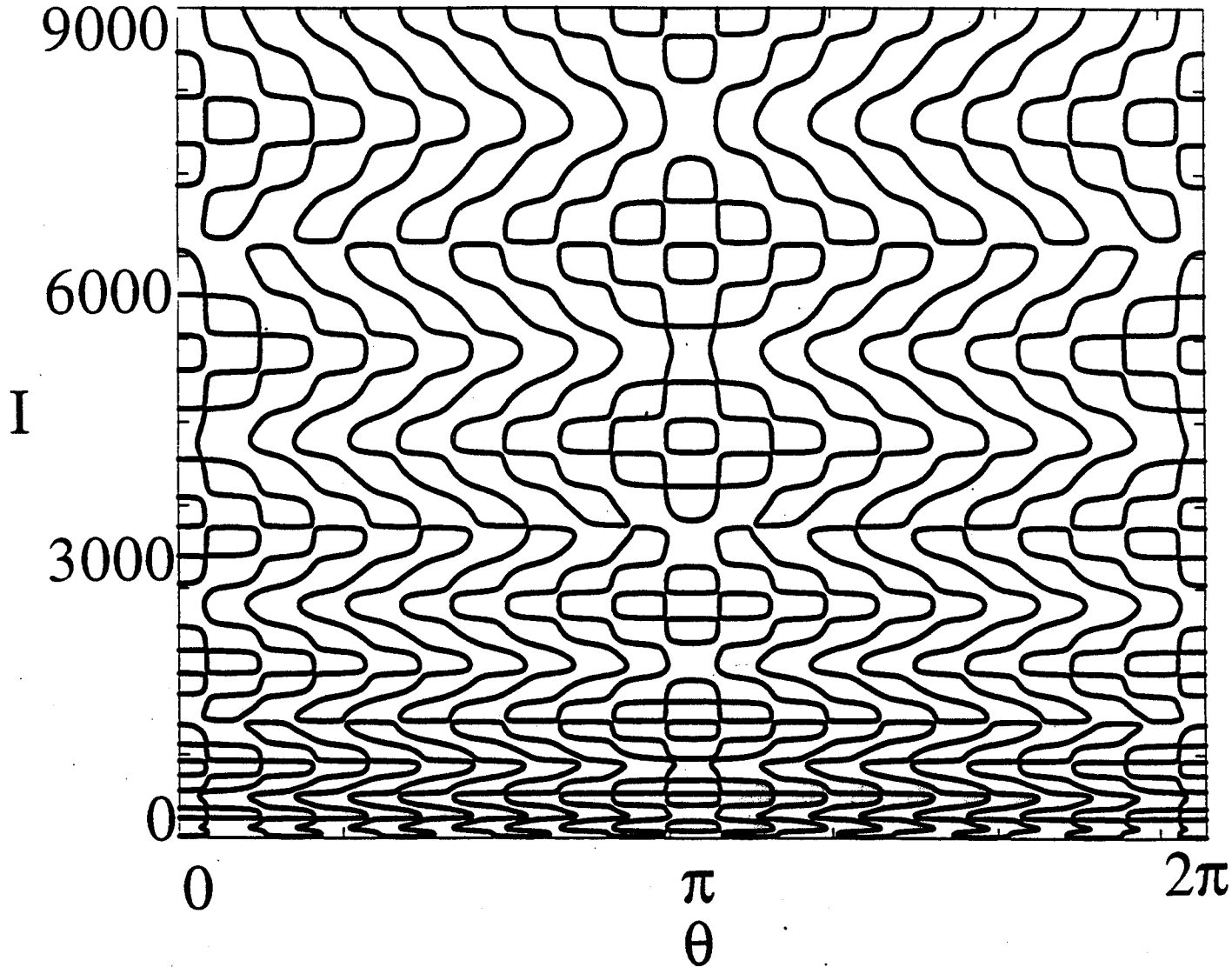

Figure 29

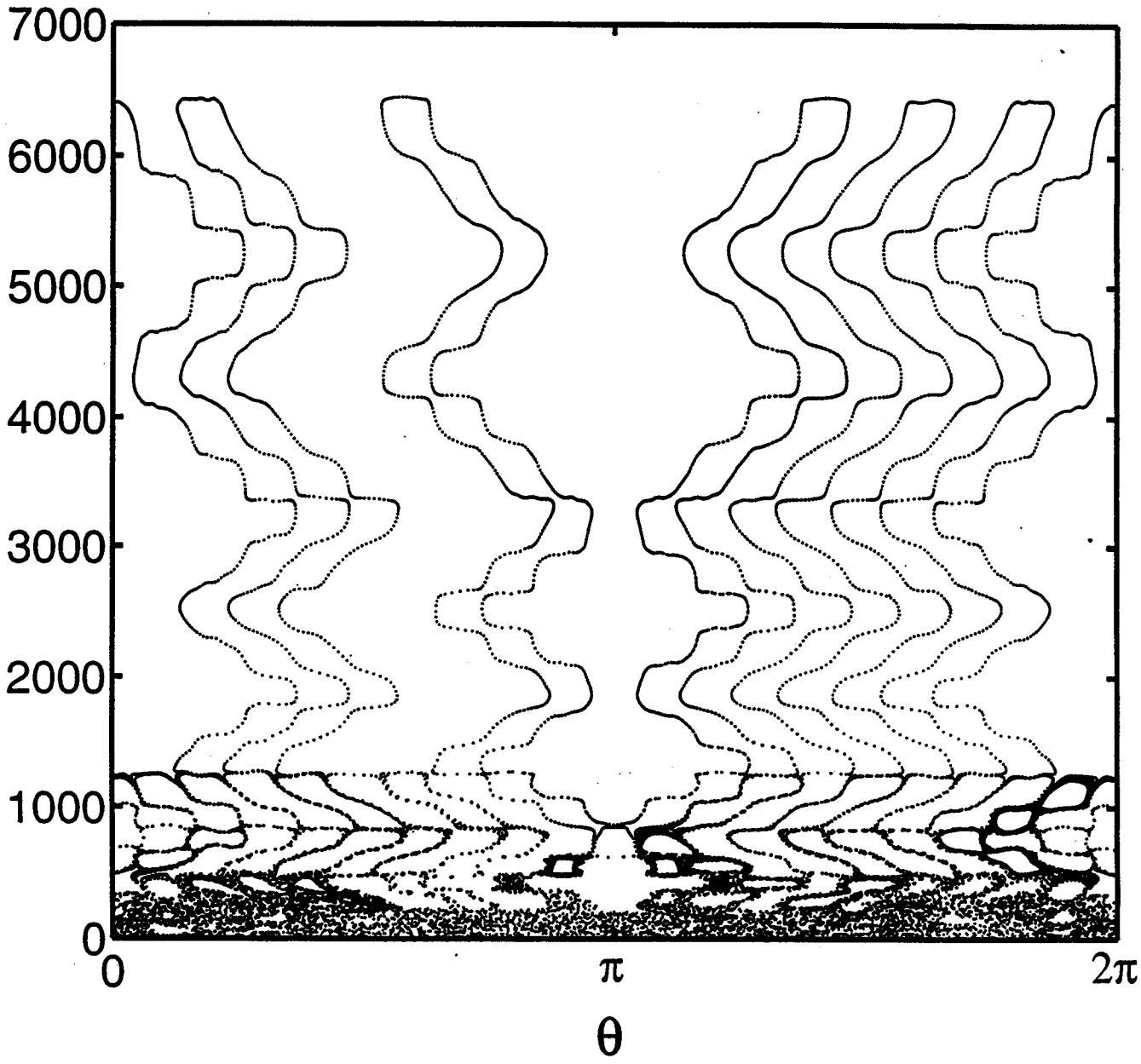

Figure 30

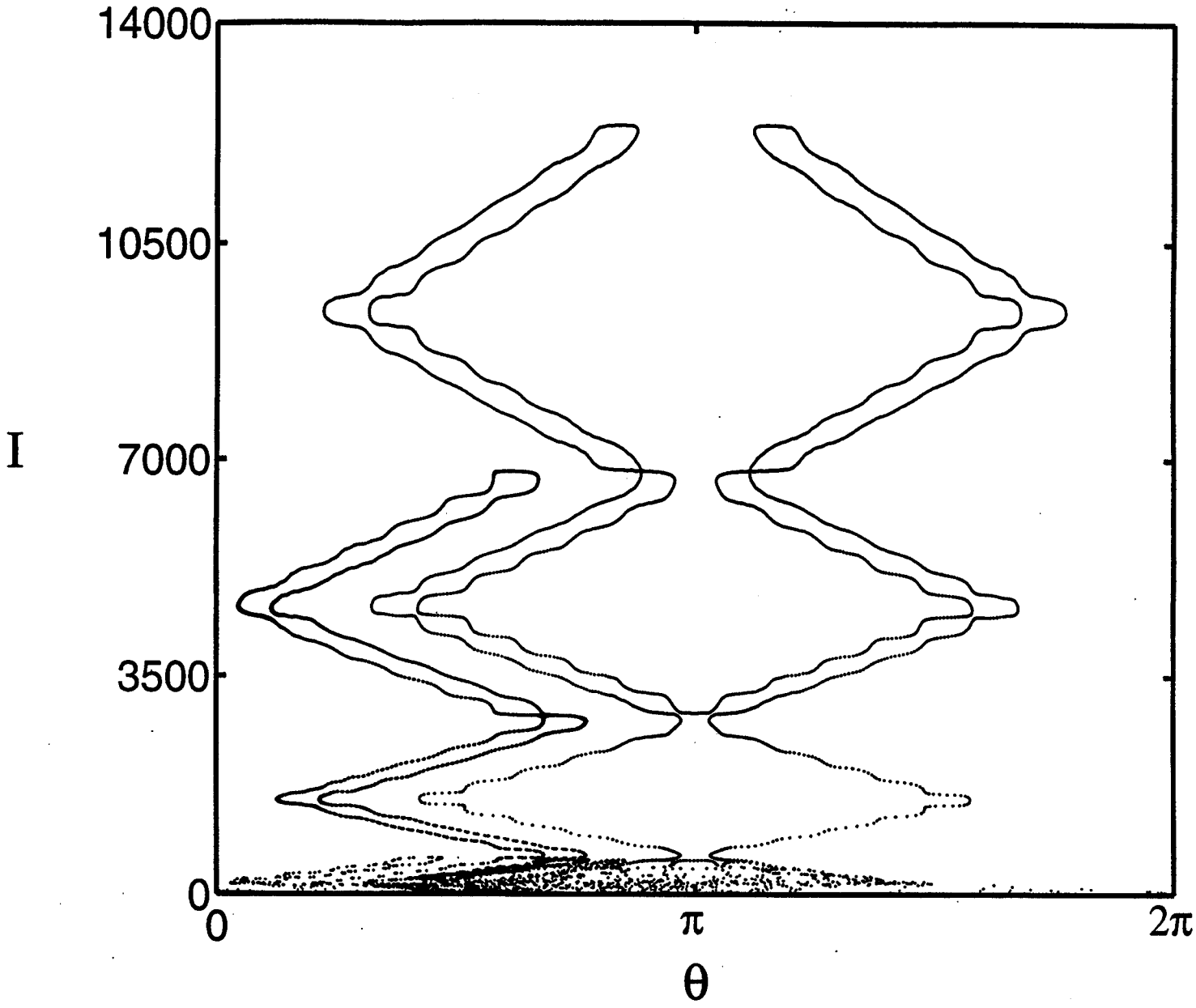

Figure 31

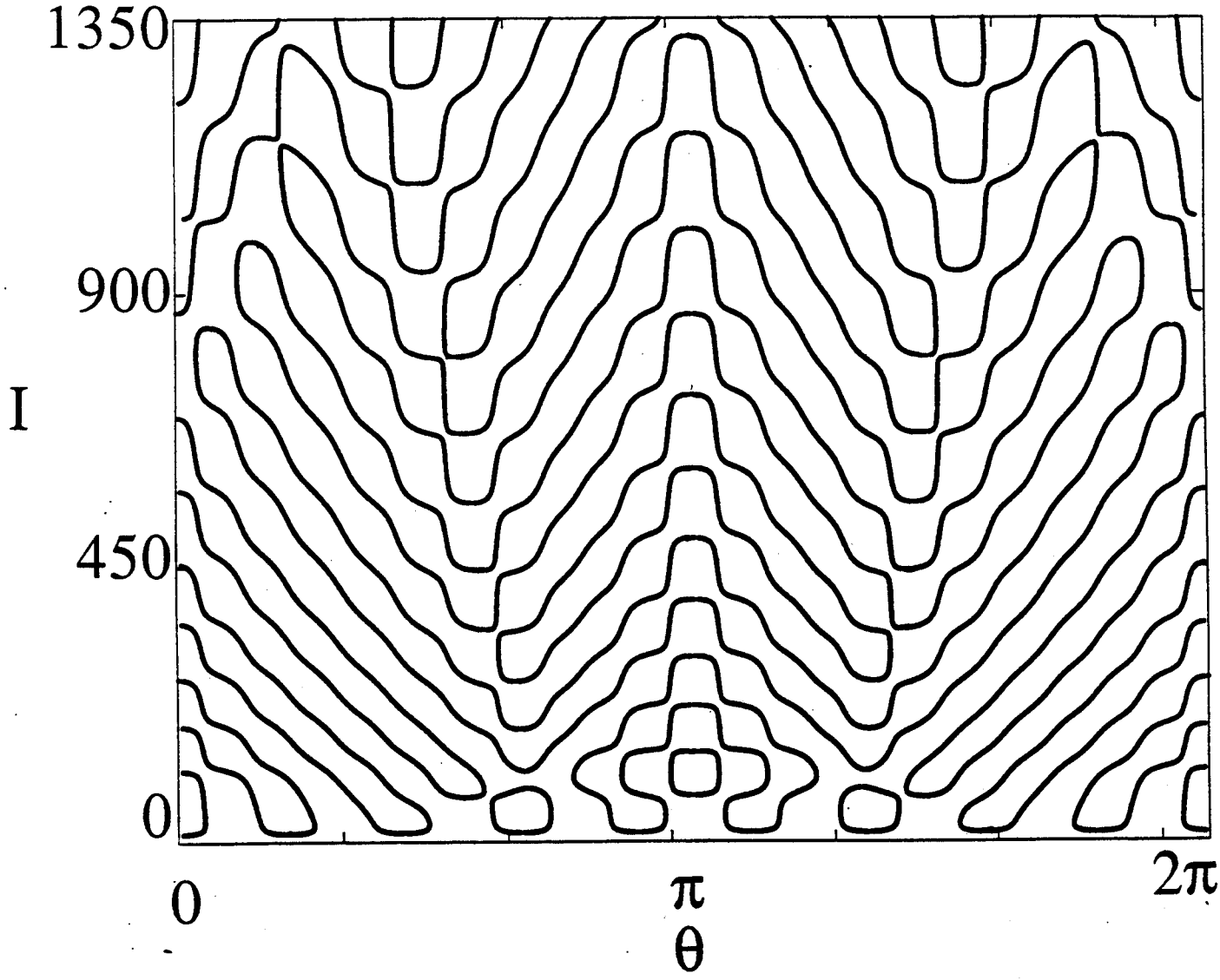

Figure 32

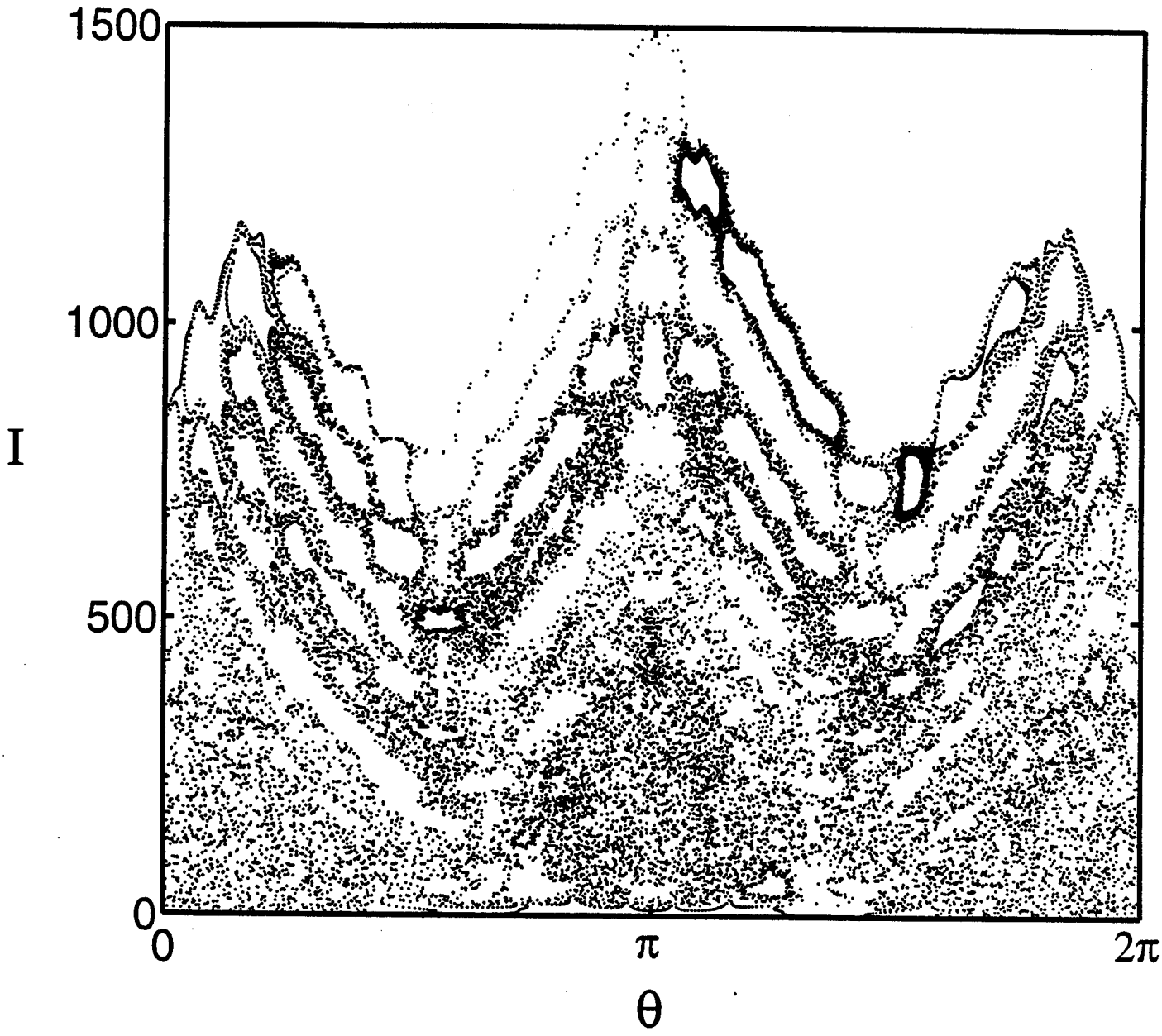

Figure 33

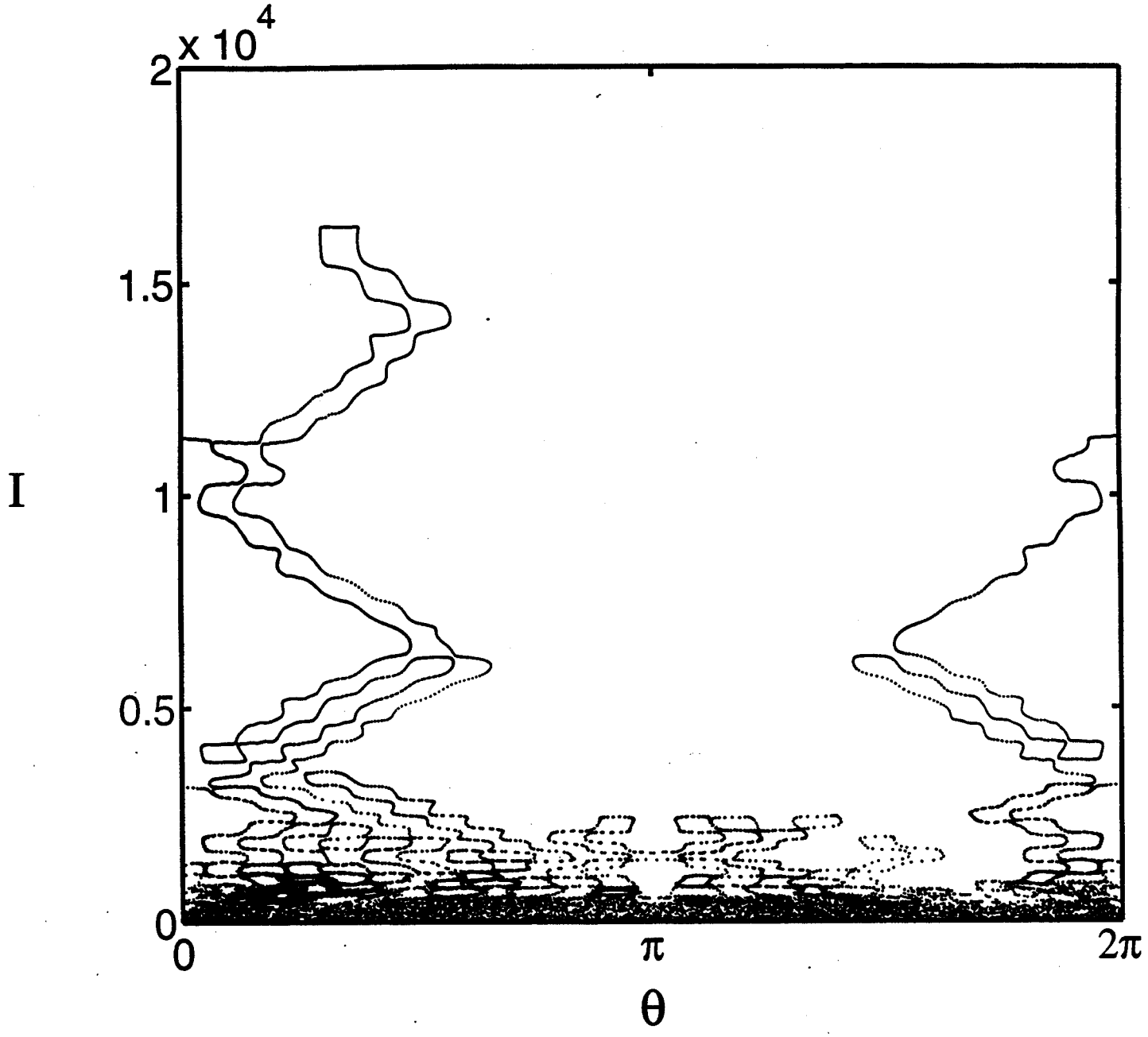

Figure 34

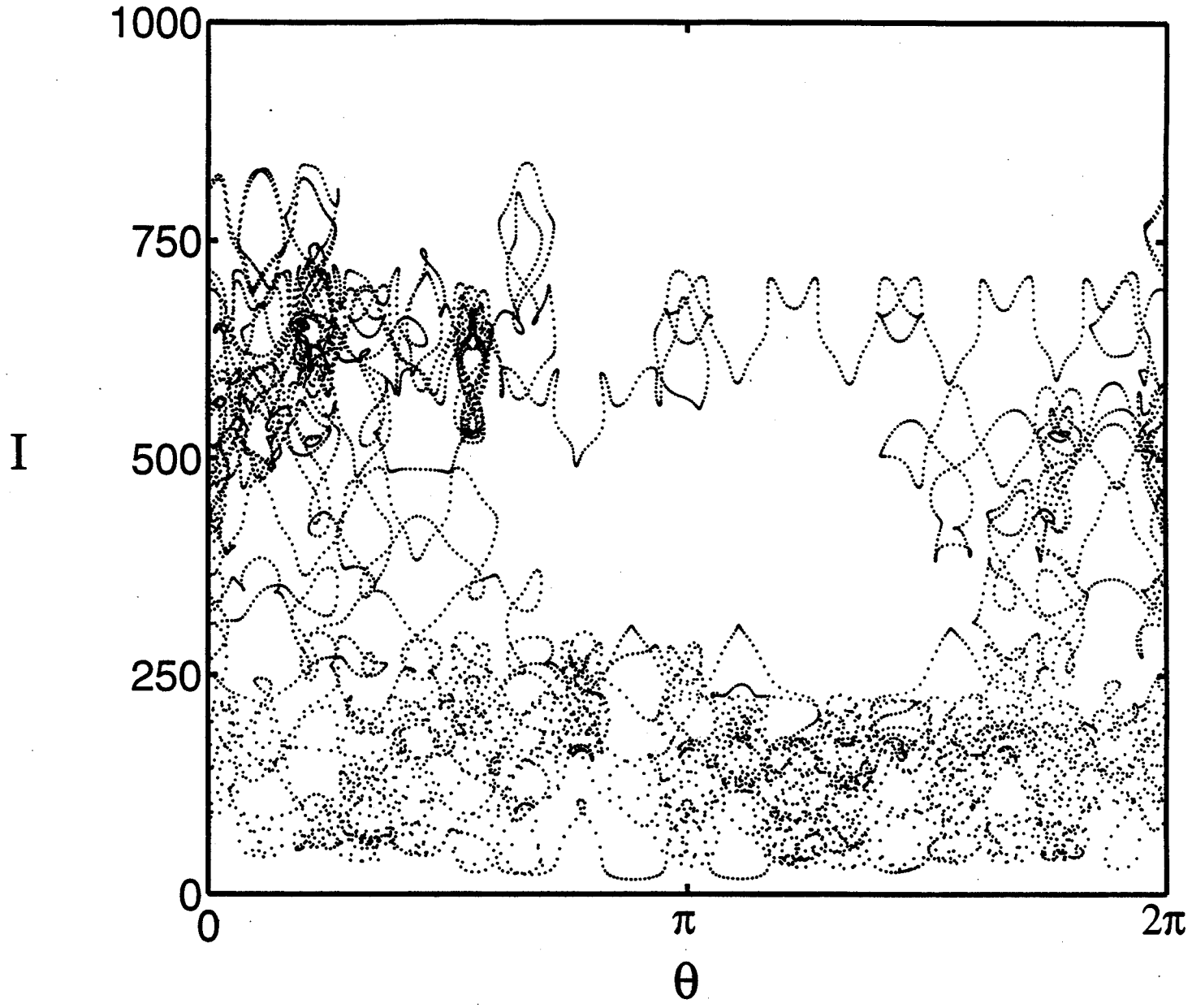

Figure 35

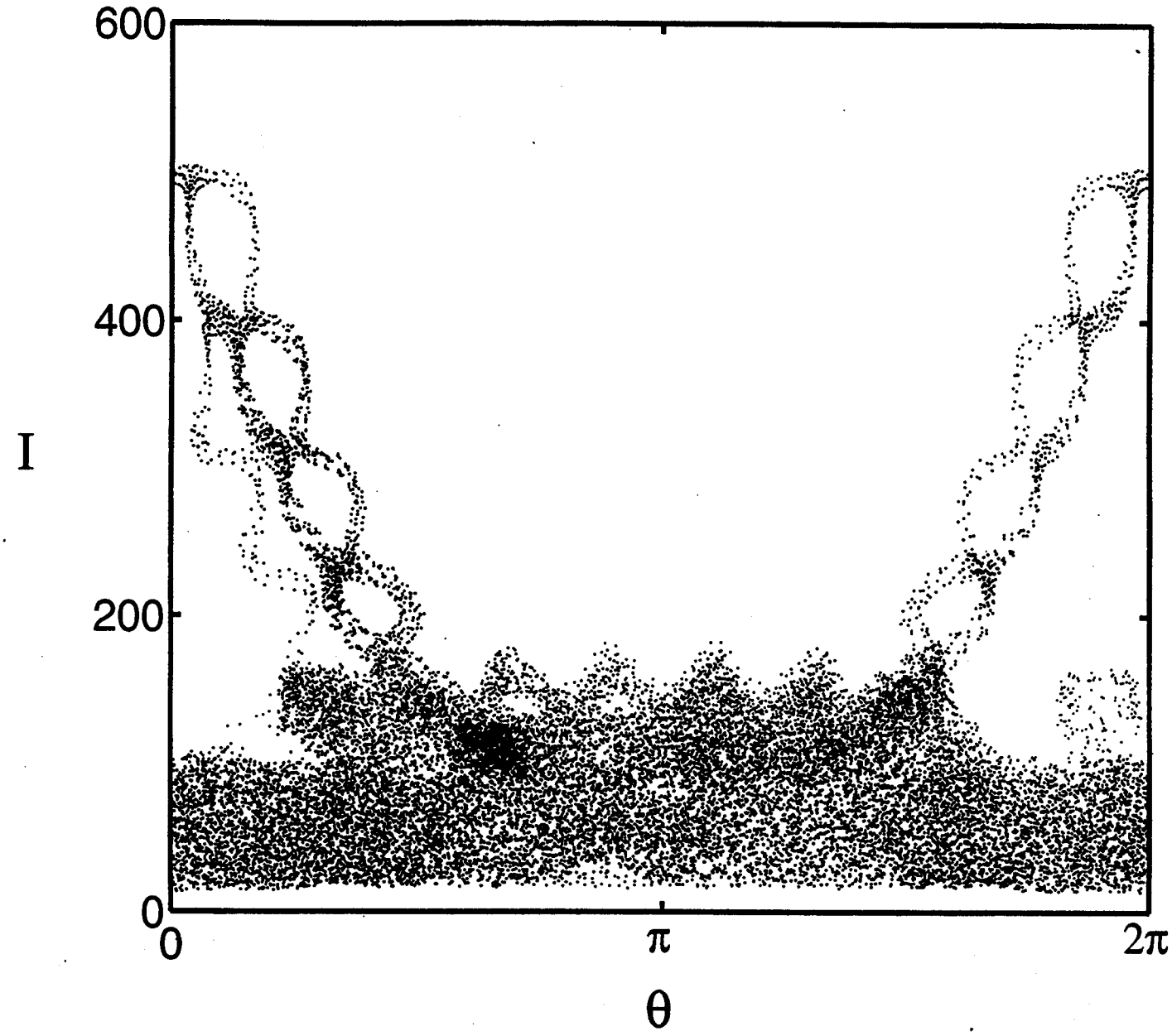

Figure 36

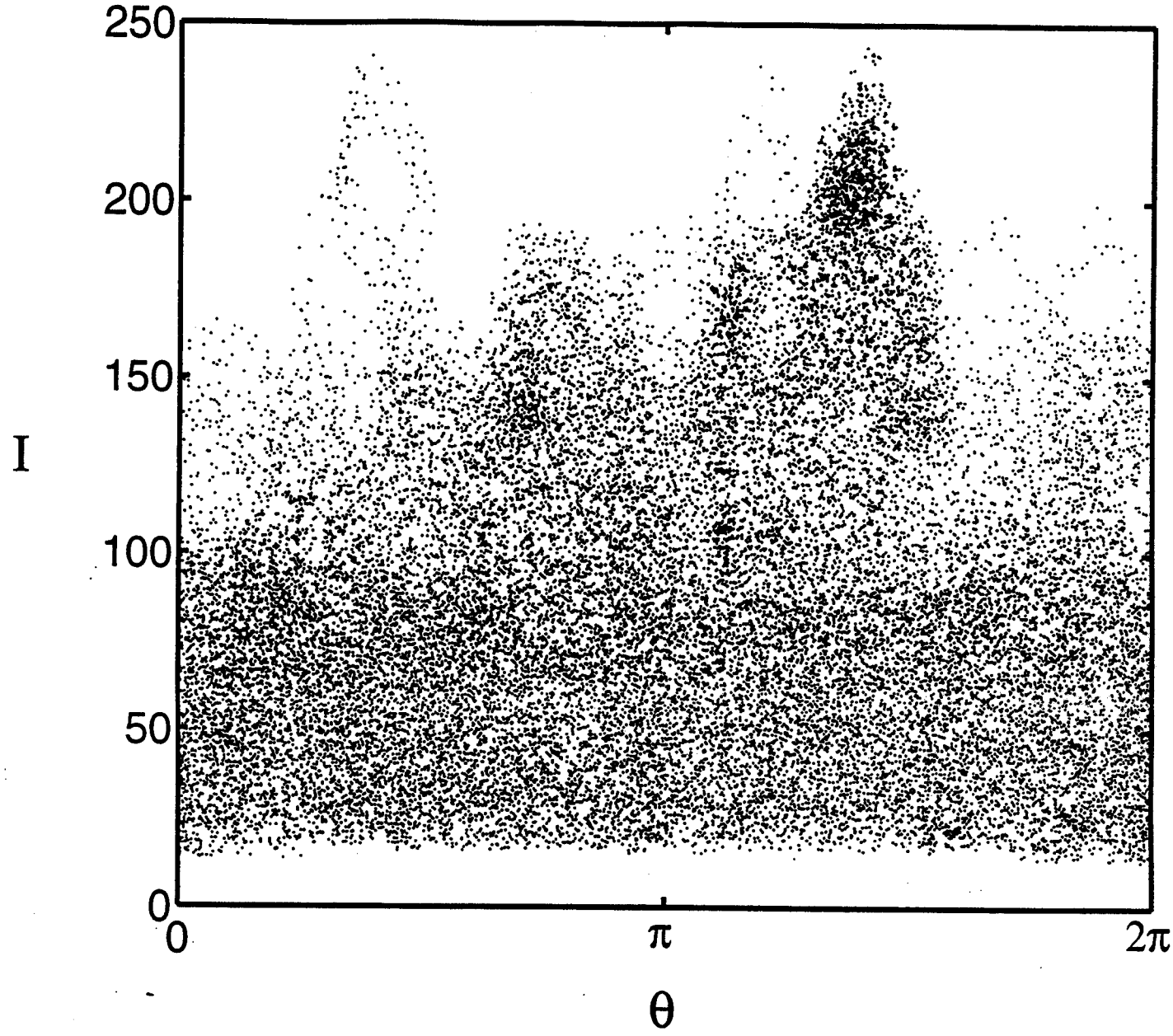

Figure 37